Initiation of cavitation during drawing of crystalline polymers.

Artur Różański
PhD Thesis
September 2010

Supervisor: Prof. dr hab. Andrzej Gałęski

Centre of Molecular and Macromolucular Studies
Polish Academy of Sciences
Department of Polymer Physics

I would like to acknowledge my supervisor,
Prof. dr hab. Andrzej Gałęski, for his confidence in me,
his helpful advises, for all the opportunities he has given me,
and for all the time, discussion and chats we have sheared.

I would also like to thank my family for the support they
provided me through my entire life and in particular,
I must acknowledge my wife and best friend, Anna,
without whose love, I would not have finished this thesis.

1. Introduction

It is very difficult to imagine the technical future of mankind without the dominant position of polymer materials. Unique qualities of the new polymer materials and constant improvement of the already existing products cause an increased use of these materials. Obviously the possibility of using a material for a given application is derivative of its properties. In the case of construction materials, a given material, regardless of the type of deformation to which the material will be subjected, has to exhibit properties which will fulfill the desired requirements. Apart from the basic parameters, important while choosing a given material (mechanical properties), each material should meet a series of other requirements ascribed to a given application. One of such parameters is retaining stable properties throughout the entire lifetime .. However, in the simplest kind of deformation, tensile drawing, deformation of most crystalline polymer materials is accompanied by a strong whitening of the material, occurring shortly before or just after reaching macroscopic yield point. Studies conducted in order to explain reasons for the observed differences showed that a source of strong scattering of light in such deformed material are voids (cavities) and crazes which appeared during deformation of the material.

The first model to deal with the phenomenon of formation of cavities in a crystalline polymer during its deformation was a “micronecking” model proposed by Peterlin [1-3]. Even though the model explained many phenomena taking place during plastic deformation of polymers, it contained significant inconsistency. . Further research conducted in many laboratories in the world allowed to examine and better understand the mechanisms accompanying deformation of crystalline polymers [4-8]. However, the phenomenon of cavitation was only treated as an effect accompanying deformation process, related to distribution of stresses inside the polymer material, a result of operation of other deformation mechanisms. Moreover, cavitation was frequently treated as a phenomenon which not only does not influence the course of deformation, but even masks the true mechanisms activated during deformation of a crystalline polymer, thereby making it difficult to examine them. Pawlak et al. [9] demonstrated that cavitation of the crystalline polymers is not only responsible material whitening, but also influences the mechanical parameters such as yield stress.

For years the term “cavitation” only referred to the process of ruptures and discontinuities occurring in low molecular weight liquids. The phenomenon of cavitation was observed already at the end of 19^{th} century during examination of propellers, which bore clear signs of erosion caused by

implosion of cavitation bubbles. Long before, that is in 1662 Huygens carried out first experimental observations of negative pressure present in water, which as we know, is the source of cavitation in liquids. An experiment, presented in 1662 and published in a paper [10] in 1672, was repeated many times for water, mercury and other liquids by other researchers [11-14]. The obtained results suggested the possibility of appearance of discontinuities in liquids, but these were the studies by Reynolds [12, 13, 15] at the turn of 19thand 20th century which allowed to better understand the nature of the phenomenon, e.g. an experiment involving forcing a water flow in a glass capillary in which a constriction (Venturi tube) was made. The phenomenon of cavitation in low molecular liquids (especially water because of its ubiquity and importance for man) and the issue of strength of these liquids exposed to negative pressure were the subject of intensive experiments at the beginning of 20th century. Until present, a coherent theory describing the phenomenon, one that would include all the parameters and properties of liquids has not been developed, however, many studies published so far allowed to thoroughly examine and understand the process of cavitation in liquids. The results, present among others in papers [16, 17], demonstrate that cavitation is influenced by the following factors:

- formation of tensile stresses in the liquid (regions of lowered/negative pressure)
- physical and thermodynamic parameters of the liquid
- presence of cavitation nuclei in the form of vapour or gas bubbles and all kinds of solid impurities in the liquid.

Understanding the mechanisms responsible for phenomenon of cavitation in liquids can eliminate or reduce its intensity when it has a negative impact on the durability of materials or functioning of devices, and to intensify the phenomenon when the presence of cavitation is desired. Both the positive and negative aspects of cavitation in liquids of low molecular weight will be discussed further in the following chapter.

If a deformation of a crystalline polymer is accompanied by cavitation, it is localized in the amorphous phase of the material. In some aspects the properties of the amorphous phase (such as folds, chain ends, dangling chains, macromolecules connecting at least two different lamellae and numerous chains not connected with crystals in a permanent way) present in the interlamellar regions inside the spherulites and localized on the interspherulitic boundaries, are similar to the properties of low molecular liquids at the temperature above its glass transition temperature. A significant difference, among others, is the presence of physical constraints in the amorphous phase structure,

reversible chain entanglements and fragments of macromolecules spanning interfacial boundaries of crystallites, which markedly decrease the mobility of macromolecules. Extensive research on cavitation in low molecular weight liquids, conducted for more than 100 years, allowed to learn many aspects accompanying the phenomenon. Thorough analysis of achievements in this field seems vital for proper understanding of the nature of cavitation accompanying deformation of crystalline polymers. Therefore, further in the thesis the state of knowledge concerning negative pressure and the phenomenon of cavitation in low molecular liquids will be discussed, together with the results of studies on cavitation occurring during deformation of crystalline polymers obtained so far.

2. State of knowledge

2.1. Cavitation in low molecular weight liquid.

It is known that any two parameters, e.g. pressure and volume determine equilibrium state of a body, and that the third parameter, in this case temperature, can be determined on the basis of an equation of state. There are, however, certain well-defined values of the mentioned parameters for

which the examined system remaining in a state of thermodynamic equilibrium, consists of several homogeneous parts - phases. In the case of ideal gas Clausius-Clapeyron equation is used for description of phase equilibrium:

$$pV=RT \tag{2.1}$$

where *p* is pressure, *V* volume, *T* absolute temperature and *R* a universal gas constant. In the case of real substances most commonly used is the van der Waals equation in the form:

$$(p+a^2/V_m^2)(V_m-b)=RT \tag{2.2}$$

in which the coefficient *a* is a parameter taking into account interaction between gas molecules and the coefficient *b* is characterized by the finite size of particles. The parameters of state bound by the van der Waals equation, are interrelated as presented in Figure 1. For the selected temperatures one obtains relations between pressure and volume as shown in Figure 2.

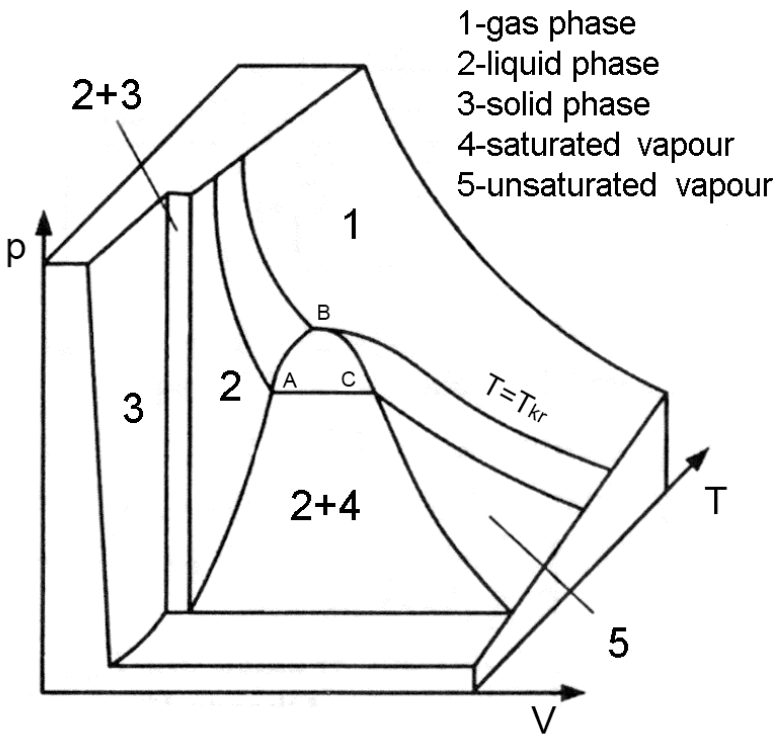

Fig.1. Relations between the parameters of state (*V, T, p*) on the basis of van der Waals equation [18].

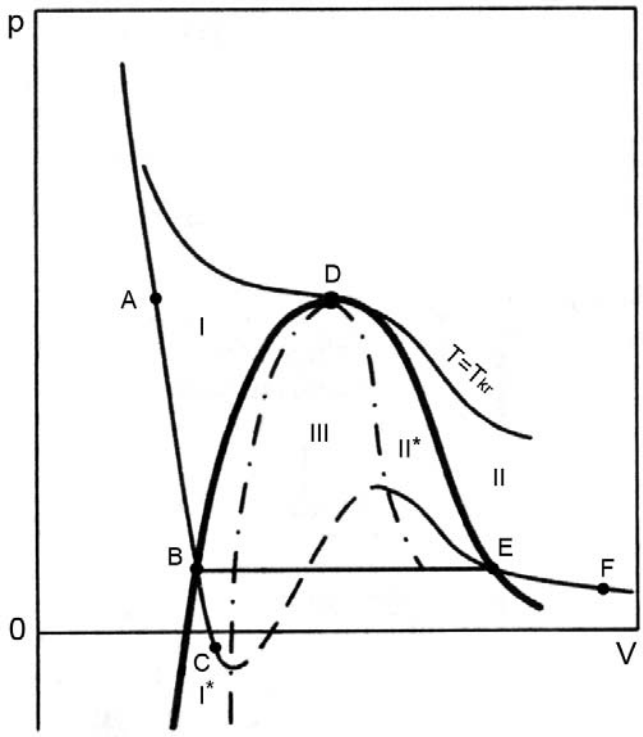

Fig. 2. Van der Waals isotherms: I- stable liquid phase, II- stable vapour, I^*- metastable liquid, II^*- superheated vapour, III- area of instability of phase states [18].

Below the critical temperature the shape of the isotherm indicates, both for liquid and vapour, the possibility of occurrence of metastable phase states. The critical temperature is therefore a limit above which isotherms do not exhibit extrema and there are no areas of metastability. If a liquid of given thermodynamic parameters (point A) is subjected to tensile forces, without changing the temperature of the system, changes in the liquid can be followed along the isotherm (on AB segment). Further lowering of pressure (below point B) may lead to formation of unstable phase states in the system. If the liquid contains a sufficient number of cavitation nuclei (gas or vapour bubbles, impurities) lowering pressure leads to appearance of an unstable phase (of vapour) in the system (point F). Phase transition for such a liquid is not expressed with an isotherm, but takes place along the BE segment. However, if the liquid is chemically homogeneous, lowering pressure in the system is accompanied by changes expressed by an isotherm (BC segment). In the point C the liquid is called ”liquid under tension” and the difference in pressure between points B and C is equal to the strength of the liquid.

For years attempts have been made to present models that would describe phenomena taking place in liquids (especially in water) subjected to tensile stresses, and perhaps more importantly, ones that would be able to satisfactorily estimate the maximum strength of these liquids. Initially attempts

were made to estimate the strength of water on the basis of van der Waals and Berthelot equation. Strength of water determined by Benson and Gerjuoya, obtained on the basis of the above-mentioned equations were: -99,6 MPa and -480 MPa respectively [19]. Reliability of the obtained results has been questioned since coefficients of thermal expansion and compressibility of water estimated on the basis of these data markedly differed from the experimental data. However, the strength of water determined basing on the theory of homogeneous nucleation should reach the value of -140 MPa [20]. According to Speedy [21] the strength of water at the temperature 35^{o}C should reach up to -200 MPa. Most of the models according to which the strength of water was determined assumed chemical homogeneity of the liquid.

If the liquid subjected to tensile stress was a chemically homogenous substance, then cavitation would be a completely unknown phenomenon with no practical use. In such liquids, devoid of any impurities, liquid-gas phase transition being a result of tensile stress would be virtually impossible, since it would require an application of stress reaching up to hundreds of megapascals. For such liquids a source of cavitation could only be voids between molecules of the liquid, transiently generated as a result thermal movements. Cavitation occurring under such conditions is defined as homogeneously nucleated. Fundamentals of the theory of homogeneous nucleation of cavitation (discussed below) were presented by Frenkel [20].

In a chemically homogeneous liquid surface tension σ operates as a result of intermolecular interactions, which prevents formation of voids. Pressure present in the liquid, p, outside the bubble of radius R, is connected with pressure inside the bubble, p_B, in a following relation:

$$p_B - p = 2\sigma/R \tag{2.3}$$

If the temperature of the system is uniform and only vapour is present inside the bubble, then the pressure p_B is equal to the pressure of saturated vapour, p_V. In order for a bubble to remain stable the pressure in the liquid must be lower than the pressure within it. At the same time, if the pressure in the liquid remains constant, less than $p_V - 2\sigma/R$, the bubble after reaching the critical size, will grow, finally leading to appearance of areas of discontinuity (rupture of liquid). In this case, the strength of the liquid is determined by negative pressure at which cavitation occurs:

$$\Delta p_C = 2\sigma/R_C \tag{2.4}$$

An important parameter is also energy cost connected with formation of a bubble of radius R [22, 23]. Assuming that a bubble is in the state of thermodynamic equilibrium with the surrounding

liquid, energy cost is derivative of two factors: generating a surface of the bubble of radius R ($4\pi R^2\sigma$) in the liquid and formation of free volume ($4/3(\pi R^3 \Delta p)$). Thus, the minimum work necessary to create a vapour bubble is defined by a following equation:

$$W=4\pi R^2\sigma-4/3(\pi R^3\Delta p) \quad (2.5)$$

For a given critical radius $R=R_C$ (Figure 3) the value of energy is highest:

$$W_C=16\pi\sigma^3/3(\Delta p_C)^2 \quad (2.6)$$

Bubbles of a radius smaller than the critical radius require additional cost of free energy for further growth, whereas for those with a radius bigger than R_C, the increase in the size of a bubble is accompanied by a decrease in free energy. Thus, such bubbles can grow.

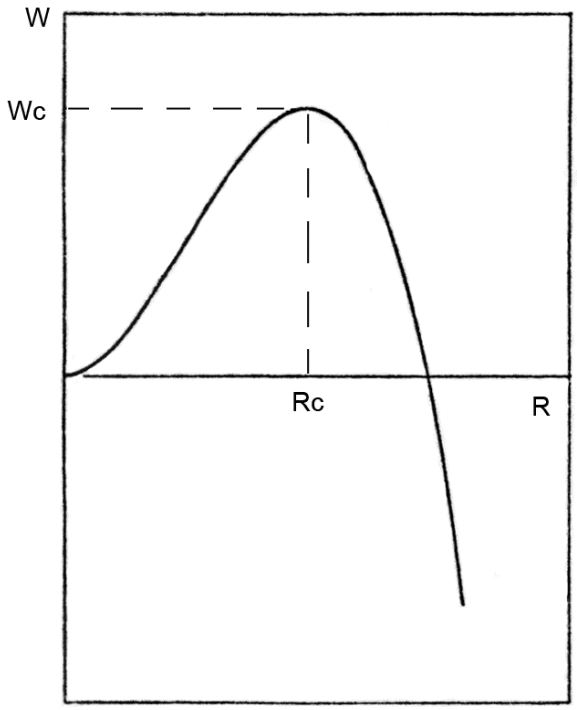

Fig. 3. Work necessary to generate a bubble of size R in the liquid subjected to negative pressure [22].

Vapour bubbles can be formed in a chemically homogenous liquid as a result of local fluctuations of some of the parameters of the molecule system. These fluctuations may lead to deviations of given thermodynamic parameters such as temperature or entropy in relation to mean values of the whole system. In a chemically pure liquid exceeding the energetic barrier, W_C, can thus occur as a result of local thermal movements of a molecule or a group of molecules. However, in order for a bubble of critical size to be formed in a liquid, a whole series of “beneficial” thermal fluctuations

are required at the local level; such a situation occurs very rarely. The theory of homogenous nucleation connects W_C with the kinetic energy of molecules in a relation:

$$G_b=W_C/kT \tag{2.7}$$

where: k is the Boltzmann constant and T is temperature. In the above relation G_B (the Gibbs number) determines the probability of occurrence of homogenous nucleation for a given volume in a finite period of time.

The rate of formation of a bubble in a mole of a liquid under negative pressure conditions Δp can be determined from a relation [17]:

$$dn/dt=(NkT/h)\{exp[-(\Delta f_0^*+W_C)/kT]\}=(NkT/h)\{exp[-(\Delta f_0^*+16\pi\sigma 3/3\Delta p^2)/kT]\} \tag{2.8}$$

where: n denotes the number of molecules, Δf_0^* symbolizes activation energy of molecule movement, N is the number of molecules in a given volume – the Avogadro number. From the above equation negative pressure at which rupture of liquid will occur in a period of time t can be calculated according to a following relation:

$$p = -\{(16\pi/3)\sigma^3/[kTln(NkTt/h)-\Delta f^*]\}^{1/2} \tag{2.9}$$

Fisher [22] determined theoretical strength of a number of liquids on the basis of the above equation. For water, mercury, ethanol and diethyl ether the values were -132 MPa, -2230 MPa, -2.3 MPa and -13.8 MPa, respectively.

Attempts were also made to relate the nucleation rate, J, defined as a number of nuclei formed in a volume unit in a given period of time, with the G_b parameter [17]. Generally, the relation can be expressed in the following form:

$$J=J_0e^{-Gb} \tag{2.10}$$

where: J_0 is a proportionality parameter. In a commonly accepted form, proposed by Blender and Katz [24] it assumes the following form:

$$J_0=N(2\sigma/\pi m)^{1/2} \tag{2.11}$$

where: N denotes the number of molecules per volume unit and m the mass of a molecule.

If one wanted to determine tensile strength of water according to (2.3) relation, assuming the typical value of surface tension for this liquid and the possibility of generating a bubble of critical radius equal to half of the distance between the molecules (ok. 10^{-10}m), one would obtain a result around -1400MPa. However, it is known that liquids not subjected to the process of purification contain a huge number of cavitation nuclei, in the form of vapour or gas microbubbles and all kinds of solid impurities

whose presence substantially decreases the liquid's ability to transfer tensile stresses. For such liquids, subjected to negative pressure, the process of cavitation is of heterogenous nature.

The reasons for presence of gas bubbles in liquids are quite natural. Dissolved gas, usually coming from the atmosphere, can be present in a liquid in the form of single molecules and in some conditions, especially at higher levels of saturation of liquid with gas, it can form groups of molecules finally emitted in the form of gas bubbles. Microbubbles present in the liquid measuring between 0.1-10 μm may form cavitation nuclei, which substantially decreases strength of the liquid.

The second group of cavitation nuclei in liquids are vapour bubbles. In ambient conditions the presence of such bubbles can be explained e.g. by the influence of cosmic radiation [26]. Collisions between molecules with high energy cosmic radiation and molecules of a liquid can cause emission of a locally significant amount of heat, which leads to formation of vapour bubbles.

Stress necessary for generating cavitation in the liquid is equal to tensile strength in the given conditions (for a defined concentration of undissolved gases and impurities). In the case of water, whose molecule is of dipolar structure, a number of its physical parameters (density, viscosity or surface tension) also strongly depend on temperature [25]. It turns out that water achieves the highest density at the temperature of around 4^{o}C, whereas viscosity decreases with its increase, especially around room temperature. Stability of cavitation nuclei in the form of gas bubbles is significantly influenced by surface tension. This parameter is also strongly dependent on temperature – it decreases as the temperature increases and reaches value close to zero around the critical point. By influencing a number of physical parameters, temperature strongly determines strength of liquid subjected to tensile stresses.

Fig. 4 presents the cavitation strength of water (Δp_C) in relation to temperature and initial radius R_0 of a bubble which is a cavitation nuclei [26]. The analysis of the presented relations shows that water devoid of bubbles which could become a cavitation nuclei, especially at the temperature close to zero, exhibits very strong ability to transfer tensile stresses. Introducing to the system bubbles with a bigger initial radius significantly decreases strength of the liquid. In the case of real liquids the bubble's radius usually falls in the range 10^{-7}-10^{-6} m, which leads to a decrease in strength of water to the level of around -1 MPa.

Cavitation can therefore be heterogenously nucleated on gas or vapour bubbles. However, the presence of freely floating stable bubbles seems highly improbable. They should either increase in size or dissolve [27, 28]. Therefore bubbles in order to nucleate cavitation need to be appropriately stabilized.

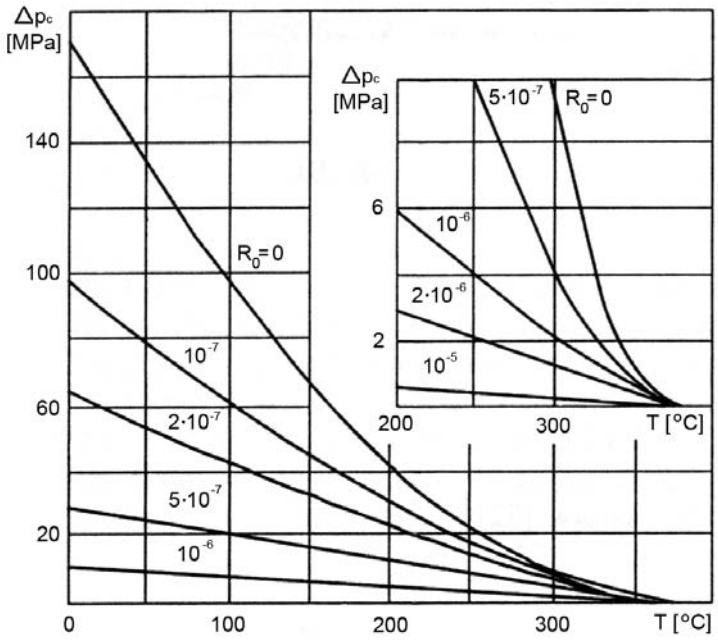

Fig. 4. Cavitation strength of water as a function of temperature and initial radius of a vapour bubble in cm [26].

An interesting mechanism of stabilization of cavitation nuclei described below was proposed by Fax and Herzfeld [29], later also discussed by Yount [30]. Bubbles filled both with water and gas can be additionally surrounded by monomolecular layer of organic substance when such impurities are present in the analyzed liquid. The layer, resembling a skin, may have a stabilizing effect on the bubble, creating a barrier for the gas/vapour filling the bubble. According to Yount formation of such bubbles is a natural phenomenon, however, it is assumed that influence of such objects on heterogenous cavitation in liquids is considerably small.

Stability of bubbles can be effectively enhanced in the presence of solid impurities present in the liquid even after its precise purification. Depending on the nature of the surface (wettability) of such impurities, bubbles formed at the liquid/solid phase boundary can assume shapes presented in Figure 5 [17].

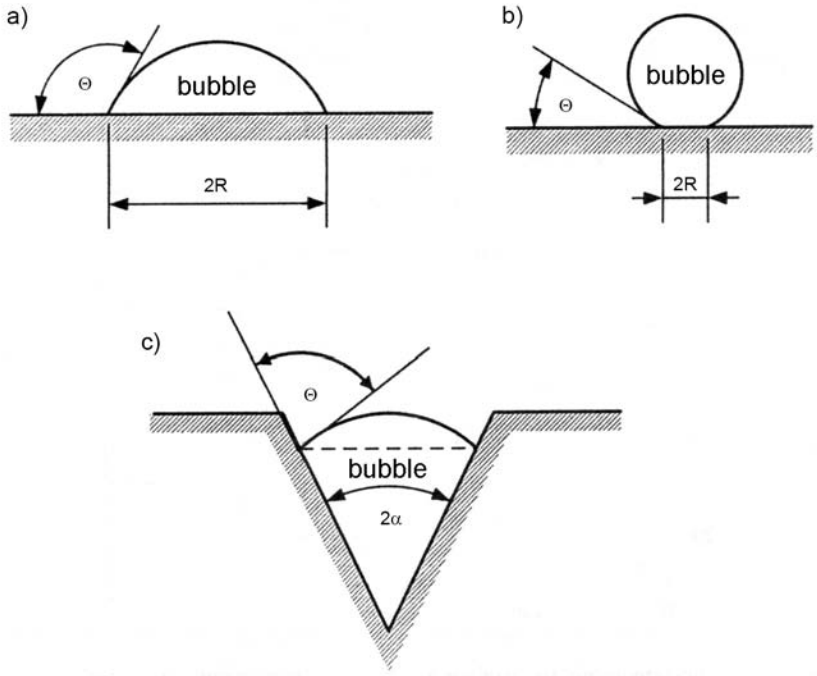

Fig. 5. Various modes of heterogeneous nucleation: a) flat hydrophobic surface; b) flat hydrophilic surface; c) a conical cavity [17] that can originate from a scratch.

In the case of homogenous nucleation bubbles of radius *R* increasing in volume lead to a rupture of liquid, when the pressure of the liquid falls below the critical value p_V-$2\sigma/R$. In such a case strength of the liquid is equal to the expression: $2\sigma/R$. The presence of solid impurities allows bubbles to be generated at the interfacial surface. Then in order to calculate the strength of the liquid it is also necessary to take into account the angle between the surface of the impurity and the surface of the bubble (θ):

$$\Delta p = 2\sigma \sin\theta / R \qquad (2.12)$$

In this relation *R* is a radius of the bubble determined as presented in the Fig. 5.

The presence of a surface of hydrophobic properties in the liquid (water) causes a substantial decrease in the strength of the liquid. The decrease intensifies with an increase in angle θ (when $\theta \rightarrow \pi$). Strength of the liquid containing solid impurities, whose surfaces exhibit hydrophilic properties, is close to strength of the liquid whose cavitation is homogenously nucleated. This results from comparable size of bubbles being formed in both systems.

Apart from smooth surfaces one should also assume the presence of other geometries. In order to illustrate the influence of geometry of the surface on the strength of the liquid the presence of conical cavities is usually assumed (Fig.4). If a half-angle at the top of the cavity is denoted as α, the strength of the liquid reaches the minimum value when a relation $\theta=\alpha+\pi/2$ is fulfilled. Additionally, when a condition $\theta>\alpha+\pi/2$ is fulfilled, a change in the meniscus curve makes the gas bubble generated in such a cavity highly resistant to pressure exerted by the liquid. A hypothesis, first

formulated by Harvey [31], assumes the existence of such particularly stable nuclei, which would be ideal candidates for initiating cavitation if the pressure in the liquid lowered.

Certainly some areas on the surface of the solid impurity of specific geometry are more “predisposed” to generating a bubble. This is especially visible during heating water in a vessel. Just before reaching the boiling point microbubbles appear in some areas on the walls of the vessel. Further increase in the temperature of the system causes “emission to liquid” of macroscopic bubbles from these specific areas.

Interesting results have been presented in the papers [32, 33]. The authors of these publications used acoustic waves in order to generate bubbles on the surface of a silicone wafer with hydrophobic properties. On the smooth surface of the wafer (roughness less than 2 nm) freshly immersed in water, the bubbles occurred under negative pressure reaching -4 MPa. However, cavitation was not observed when the substrate just before being immersed in water has been coated with a thin layer of ethanol. The observed differences resulted from a much larger amount of gas trapped in the cavities of the surface when the wafer, just before being immersed in water, was not properly protected. Moreover, the decrease in the intensity of cavitation with time (gas diffusion) and with the number of measurement cycles (reduction of the amount of gas in traps in subsequent test cycles) was observed.

Theoretical discussion on the phenomenon of cavitation in low molecular liquids and the obtained values of strength of the liquid, calculated on the basis of the above mentioned assumptions, certainly required confrontation with experimental data.

The oldest measurement method of the strength of the liquid was proposed by Bertholet in 1850 [34]. A glass one-side closed capillary is filled with the examined liquid and then its second end is sealed. Such prepared system is heated until the liquid tightly fills the entire volume of the capillary (as a result of thermal expansion). During cooling of the capillary, when the temperature is lowered to appropriate level, negative pressure is generated in the liquid. Further cooling of the capillary leads to rupture of liquid and formation of a bubble (as before heating). Knowledge of coefficients of thermal expansion (α_p) and thermal compressibility (χ_T) of the liquid as well as the experimentally determined temperatures at which dissolution of the bubble (T_d) and rupture of the liquid took place allowed to determine negative pressure. Bertholet, on the basis of a change in the volume of the liquid (ΔV)

which occurred after its rupture, calculated the value of negative pressure (P_c) generated in the capillary during the experiment at the level of around -5 MPa according to the following relation:

$$P_c = \Delta V / \chi_T \qquad (2.13)$$

Attempts have also been made to assess P_c on the basis of the determined values of T_d and T_c using the relation:

$$\Delta p = P_d - P_c = \int_{T_c}^{T_d} \frac{\alpha_p}{\chi_T} dT \qquad (2.14)$$

where P_d is pressure in the capillary at the temperature T_d. Very frequently the value of P_d has been neglected. Using the equation (2.14) and neglecting P_d unit Dixon achieved the value of -16 MPa at the temperature of 72.9^{o}C [35] and Vincent -15.9 MPa at 54^{o}C [36]. The assumption concerning the possibility of omission of P_d unit has been criticized. The results presented in the papers [37-40] showed that just before the bubble dissolves, high pressure, whose values should be taken into account, is generated in the capillary. Correct values should therefore be less negative than those presented by Dixon or Vincent. A few groups obtained results of measurements of strength of water (-4,2 MPa [38], -5 MPa [39], -2 MPa [40]) assuming the non-zero value of the T_d, which makes it necessary to include in the relation pressure generated during heating the liquid in a capillary. The presented results of negative pressure measurements exhibited a significant scatter of results, not only for different capillaries (i.e. material from which the capillary was made of) but also in relation to subsequent measurements performed for the same capillary.

A simple capillary used by Bertholet was replaced with a capillary in the shape of helix (Fig. 6) by Mayer in 1911 [41]. A mirror was placed at the end of the capillary, whose small changes in position supplied information about the changes of pressure in the test capillary. Settings of the mirror were properly calibrated before measurements. The maximum value of tensile stresses for water determined by Meyer was -3.4 MPa.

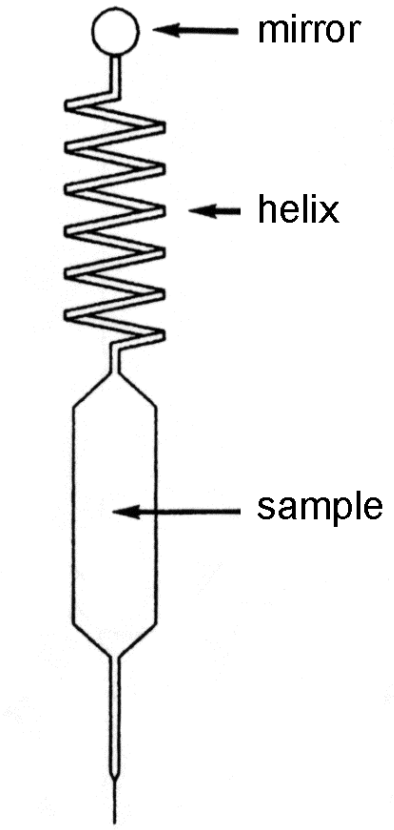

Fig. 6. Schematic of the apparatus used by Meyer for measuring negative pressure in liquids [41].

An interesting method of measurement of strength of liquid was proposed by Reynolds in 1882 [42]. A specially shaped tube was filled with the examined liquid (Fig. 7). Next the capillary was brought to rotation in a horizontal plane, smoothly changing rotational speed up to rupture of the liquid as a result of centrifugal force.

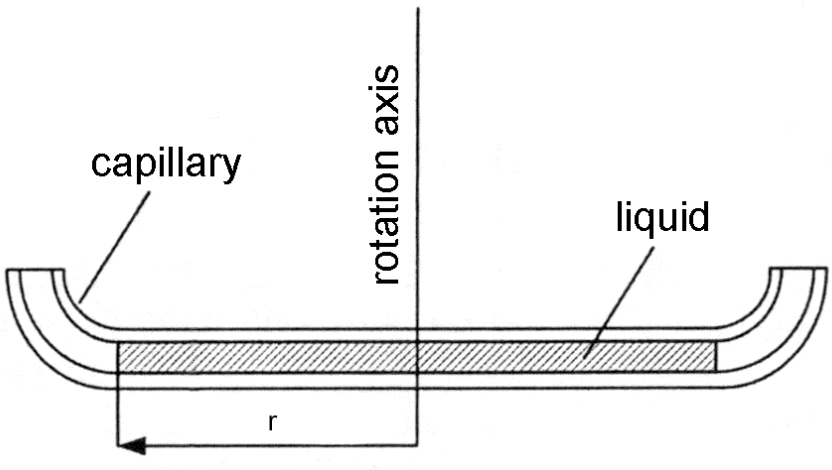

Fig. 7. Capillary for determination of tensile stresses using Reynolds method.

Knowing the density of the examined liquid -*d*- and the experimentally determined parameters: *r* – distance from meniscus to rotation axis, *ω* – angular velocity registered at the time of rupture of the liquid, one could assess the strength of the liquid according to the following relation:

$$p=p_o-1/2(d\omega^2r^2) \quad (2.15)$$

A substantial number of studies on strength of liquids, using the method described in the previous paragraph, were conducted by Briggs [43, 44]. Apart from water also selected organic liquids were of interest to him. In order to minimize the amount of air in the examined liquids, they were subjected to boiling out, up to evaporation of around 25% of the initial volume. The liquids were directly introduced from a vessel into a test capillary with the use of a trap. Additionally, one ensured a few minute flow of the selected liquids through a capillary. Extensive research allowed to determine the maximum strength of the liquids and to assess the temperature at which the strength achieves the biggest value (-27.5 MPa at 8^oC for water, -28.8 MPa at 23^oC for acetic acid, -15 MPa at 19^oC for benzene, -30 MPa at 0^oC for aniline, -27.6 MPa for tetrachloromethane, -31.7 MPa for chloroform).

The determined values of negative pressure at which the cavitation process took place in water, obtained on the basis of measurement methods presented above, are considerably lower than those predicted by a theory of homogeneous nucleation (-140 MPa) [20] or suggested by Speedy (-200 MPa) [21]. Only a significant reduction in the volume of the examined liquid allowed to obtain strength values similar to those theoretically predicted. Decreasing the volume of the liquid reduces the probability of occurrence in the examined sample nuclei capable of nucleating the cavitation process. In this case, the experimental conditions are similar to those provided by a theory of homogeneous nucleation.

In 1967 Roedder published results of studies on microscopic inclusions (in the range 10-100 μm) of water naturally occurring in some minerals [45]. The data obtained showed that the ice trapped in these inclusions melts at the temperature of 6.5℃, which would indicate the presence of pressure reaching -95 MPa. Also the results of negative pressure measurements presented by Apfel and Smith [46], which concerned small amounts of diethyl ether, were similar to those provided by the theory. The idea of experiment was very similar to the method used by Briggs. Using a special capillary allowed to examine small volumes of the liquid -0.02ml. During experiments a large scatter of stress results were observed, at which discontinuities of a column of liquid appeared, however a part of the

obtained data was only about 10% lower than the values provided by a theory of homogeneous nucleation of cavitation.

Angell and his team studied water microinclusions trapped in synthetic quartz, fluorite and calcite crystals [47] using the Berthelot method [34]. Specially prepared crystals of these minerals were placed in a capillary containing a given amount of ultra-pure water. The whole has been subjected to treatment in an autoclave. Changes in the crystal structure, taking place in a reactor caused trapping of water in the inclusions (Fig. 8), whose parameters depended on the temperature and pressure applied. Analogically to the already discussed Bertholet method, disappearance temperature of the bubble (T_d) during heating of the system and formation of the bubble (T_c) during its cooling were determined using microscopic methods. In order to determine the value of P_c the authors of the experiment used for extrapolation the Haar-Gallagher-Kell equation of state [48] (HGK equation of state is a multiparameter relation obtained as a result of matching a number of precisely determined parameters of a liquid; qualitatively the equation is similar to the equation of state proposed by Speedy [21], however, it significantly differs quantitatively; the estimated strength of water calculated according to the HGK equation is highest at the temperature of 60^oC and is equal to -160 MPa). Proper extrapolation allowed to determine the value of limiting pressure (-140 MPa at the temperature of 40^oC) for stability of water in microinclusions. Strength of water determined by Angell is currently the highest experimentally obtained value for this liquid.

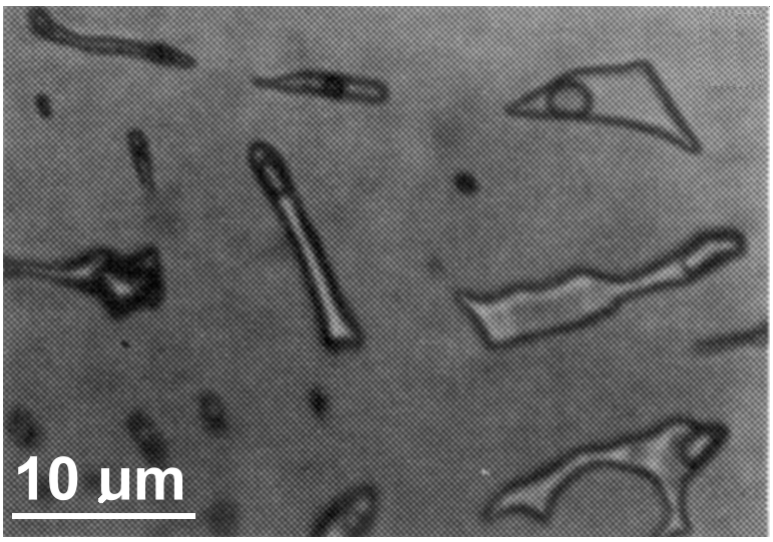

Fig. 8. Microinclusions of water generated in quartz [47].

Such great interest in the subject, whose review has been presented above, resulted from many practical aspects (both positive and negative) accompanying the occurrence of negative pressure and the phenomenon of cavitation in liquids. In most cases formation of cavitation bubbles is not a negative process. These are the phenomena accompanying the implosion of bubbles that bring about adverse effects. As a result of collapse of bubbles microjets appear [60-64] flowing with a speed of about 100 m/s [72] and leading to an increase in the local pressure on the material surface, up to the value of 100-1000 MPa [72]. Analysis of the relation (2.4) allows to understand reasons for sudden pressure impulses accompanying collapse of cavitation bubbles. When a radius of cavitation bubble suddenly decreases, which takes place during collapse of such a bubble (approaches zero), pressure in the implosion area violently increases (approaches infinity). Additional consequence is an intense increase in temperature, which can locally reach thousands degrees, and light emission known as sonoluminescence [73, 74]. Cavitation is also accompanied by acoustic effect [75-78].

In trees transport of water and nutrients to the higher located parts of a plant takes place through a complex system of channels. According to the law of hydrostatics a pressure drop in a water column of 10.2 meters is 0.1 MPa. Therefore, in xylem of trees, particularly the high ones, negative pressure can appear, which is an important part of the complex transport mechanism of nutrients enabling proper functioning of a plant [49-51]. Negative pressure generated in channels may occasionally lead to cavitation of the transported sap, which in turn leads to disruption of a flow continuity and prevents proper nutrition of the part of the plant. Complex architecture of the plant tissue minimizes negative effects accompanying cavitation in xylem and the developed mechanism enable re-filling and restoration of channels. An interesting example of the use of the cavitation process in nature has been presented in the papers [52, 53]. Some species of shrimps developed a special organ, whose rapid opening and closure causes occurrence of cavitation. The authors of the cited papers believe that these animals use cavitation for the purpose of communication and to paralize their victims.

In recent years research has also been conducted on the application of the phenomenon of cavitation in the selected areas of medicine. Although ultrasounds are widely used in medicine, there is a long standing debate on their negative influence on human body [54]. Absorption of sound waves can lead to local changes in the temperature of tissues (this is actually used to destroy tumors) and formation of cavities which cause uncontrollable changes also in the healthy cells. It is believed that

imploding cavitation bubbles generated by ultrasounds increase the effectiveness of destruction of unwanted tissues and fragmentation of stones (e.g. kidney or peevish) formed in human organs.

When a cold liquid "a" of a boiling point T comes into contact with a liquid whose temperature is higher than T, then local superheating of the liquid "a" appears on the contact boundary. An effect of such situation is occurrence of cavitation on the contact boundary, a strong increase in the volume as a result of intense evaporation of the liquid and violent explosion of the system [55]. Such phenomenon could be used to improve efficiency of fuel combustion in engines [56-58]. A special mixture of fuel and water in the presence of surfactants forms an emulsion, whose combustion is accompanied by microexplosions. One of the emulsion components undergoes superheating, which is accompanied by intensive cavitation resulting in strong spraying of the second component in a carburetor. Intensive atomizing of fuel improves its combustion efficiency, reduces the formation of soot, particulate matter, unburned hydrocarbons and carbon monoxide.

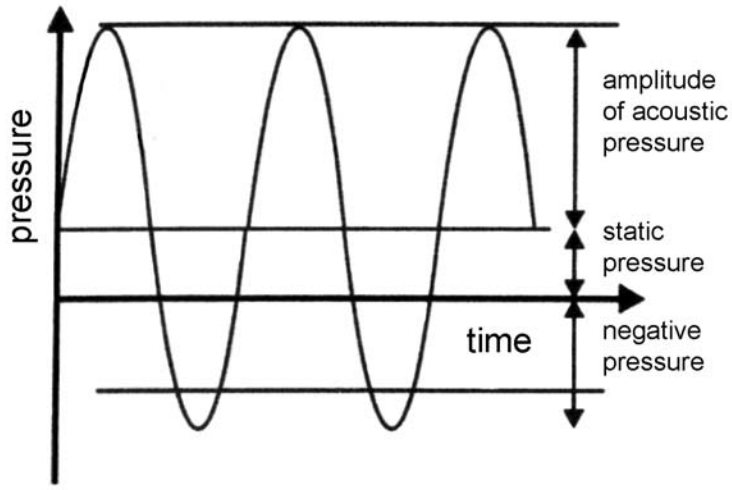

Fig. 9. Pressure distribution occurring as a result of influence of acoustic waves [59].

Implosion of cavitation bubbles is usually accompanied by a strong local temperature increase and a sudden pressure impulse. Such violent phenomena accompanying the process of collapsing bubbles found application in cleaning surfaces of solid materials. With the use of a stream of ultrasounds cavitations are generated in a special tank. Introduction of a sound wave into the liquid leads to creation of tensile stresses in the liquid. Acoustic wave generates distribution of pressure in the liquid, which is the sum of static and oscillating pressure. If an amplitude of acoustic pressure is bigger than the static pressure in the liquid, negative pressure is generated, whose presence finally leads to formation of cavitation bubbles. Bubbles imploding by the surface of the purified material

generate microjets of the liquid [60-64], capable of removing even tiny impurities located in the cavities of the material.

Also the influence of ultrasounds and the accompanying cavitation on the course of chemical reactions has been investigated for years (sonochemistry) [65-68]. It turned out that reactivity of both solid substrates and catalysts can be enhanced as a result of effects accompanying the implosion of cavitation bubbles (cleaning surfaces of reactants, more efficient transport to/from the surface of the reactant/products) that affects the speed, selectivity and efficiency of chemical reactions and sometimes also the character of the obtained product. Even in the case of homogeneous liquids the phenomenon of cavitation can bring about chemical effect. High temperature and pressure accompanying the collapse of cavitation bubbles can affect formation of highly reactive radicals [69]. One of the interesting examples of application of sonochemistry in synthesis are studies presented by Shchukin. The paper [70] presented the method of synthesis of nanoparticles and microspheres of potential application in medicine.

Many research centres also conduct studies on the use of cavitation for water disinfection [65]. Cavitation in combination with ozone or chlorine may increase efficiency of the treatment process by destroying microorganisms and organic pollutants present in the purified liquid.

In the above paragraphs I have presented selected examples of how man makes practical use of the phenomenon of cavitation. Frequently, however, it is an undesirable phenomenon, accompanied by changes in the characteristics of work/durability of devices or destruction of surfaces of materials exposed to cavitation. Destruction of such surfaces, referred to as cavitation erosion, was observed already at the end of 19^{th} century. Probably the first paper to deal with the effects of cavitation erosion was published in 1912 [71] and concerned destruction of surfaces of ship propellers. Cavitation around ship propellers was also of interest to the navy. Implosion of cavitation bubbles was a factor enabling detection of submarines, especially during World War II and shortly after its end in the Cold War period. The remedy against detection was deeper submersion of a ship in order to overwhelm the negative pressure caused by propellers by positive hydrostatic pressure. It was also found that the cavitation in ocean water depends on the period of a year: in spring or summer the plankton causes easy nucleation of cavitation around ship propellers while in winter submarines can travel on shallow waters undetected because of the relative lack of cavitation nuclei [79].

Nowadays the hydrodynamic theory of cavitation erosion is adopted, whose mechanism is explained by implosion of cavitation bubbles. Although collapse of cavitation bubbles occurs in a fraction of a microsecond extreme conditions in the implosion zone (described above) are sufficient to cause defects virtually in most materials. The degree of cavitation erosion depends not only on the properties of the material, but is also derivative of physical and chemical properties of the liquid and intensity of the cavitation process.

2.1.1. References

[1] Peterlin, A. *Kolloid-Z Z. Polym.*, **1969**, *233*, 857.

[2] Peterlin, A. *J. Appl. Phys.*, **1977**, *48*, 4099-4108.

[3] Peterlin, A. *J. Mater. Sci.*, **1971**, *6*, 490-508.

[4] Bowden, P. B.; Young, R. J. *J. Mater. Sci.*, **1974**, *9*, 2034-2051.

[5] Haudin, J. M. In *Plastic deformation of Amorphous and Semicrystalline Materials*, B. Escaig; C. G'Sell, eds.; Les Editeurs de Physique: Paris, **1982**, pp. 291-311.

[6] Lin, L.; Argon, A. S. *J. Mater. Sci.*, **1994**, *29*, 294-323.

[7] Galeski, A. *Prog. Polym. Sci.*, **2003**, *28*, 1643-1699.

[8] Oleinik, E. F. *Polym. Sci. Ser. C.*, **2003**, *45*, 17-117.

[9] Pawlak, A.; Galeski, A. *Macromolecules,* **2005**, 38, 9688-9697.

[10] Huygens, C. tłumaczenie angielskie *Phil. Trans.* **1672**, 7,5027-5030.

[11] Donny, F. *Ann. Chim. Phys.* **1846**, 16, 167-190.

[12] Reynolds, O. In *Scientific Papers on Mechanical and Physical Subject,* Cambridge Univ. Press, **1900-1903**, I, 231-243.

[13] Reynolds, O. In *Scientific Papers on Mechanical and Physical Subject,* Cambridge Univ. Press, **1900-1903**, I, 394-398.

[14] Hayward, A. T. J. *J. Phys. D*. **1970**, 3, 574-579.

[15] Reynolds, O. In *Scientific Papers on Mechanical and Physical Subject,* Cambridge Univ. Press, **1900-1903**, II, 578-587.

[16] Apfel, R. E. *Scientific American,* **1972**, 57-58.

[17] Brennen, Ch.E., "Cavitation and bubbles dynamics", Oxford University Press, **1995**.

[18] Ingarden, R. S.; Jamiołkowski, A.; Mrugała, R., "Fizyka statystyczna i termodynamika", PWN, Warszawa, **1990**.

[19] Benson, S.W., Gerjuoy E., *J.Chem.Phys*, **1949**, 17, 914.

[20] Frenkel, J., "Kinetic Theory of Liquids", The Clarendon Press, Oxford, **1946**.

[21] Speedy, R.J., *J.Phys.Chem.*, **1982**, 86, 982.

[22] Fisher, J.C., *J. Appl. Phys*., **1948**, 19, 1062 .

[23] Fisher, J.C., Hollomon, J.H., Turnbull, D., *J.App.Phys.*, **1948**, 19, 775.

[24] Blander, M., Katz, J. L., *AIChE Journal,* **1975**, 21, No. 5, 833-848

[25] Kowal, A. L.; Świderska-Bróż, M., "Oczyszczanie wody", PWN, Warszawa, **1997**.

[26] Akulichev, V. A., "Cavitation in Criogenic and Boiling Liquids", Nauka, Moskwa, **1978**.

[27] Liebermann, L., *J. Appl. Phys.*, **1957**, 28, 205-211.

[28] Epstein, P. S.; Plesset, M. S., *J. Chem. Phys.,* **1950**, 18, 1505-1509.

[29] Fox, F. E.; Herzfeld, K. F., *J. Acoust. Soc. Am.,* **1954**, 26, 984-989.

[30] Yount, D. E.; Gillary, E. Q.; Hoffman, D. C., *J. Acoust. Soc. Am.,* **1984**, 76, 1511-1521.

[31] Harvey E.N., McElroy W.M., Whiteley, A. H., *J.Appl.Phys.*,**1947**, 18, 1620.

[32] Bremond, N.; Arora, M.; Ohl, C. -D.; Lohse, D., *J. Phys.:Condens. Matter,* **2005**, 17, 3603-3608.

[33] Bremond, N.; Arora, M.; Ohl, C. -D.; Lohse, D., *Phys. Rev. Lett.,* **2006**, 96, 224501, 1-4.

[34] Berthelot, M., *Ann. Chim. Phys.,* **1850**, 30, 232-237.

[35] Dixon, H. H., *Sci. Proc. Roy. Dublin Soc.,* **1909**, 12, 60-65.

[36] Vincent, R. S., *Proc. Roy. Soc.,* **1941**, 53, 126-140.

[37] Temperley, H. N. V.; Chambers, L. G., *Proc. Phys. Soc.,* **1946**, 58, 420-436.

[38] Temperley, H. N. V., *Proc. Phys. Soc.,* **1946**, 58, 436-443.

[39] Lewis, G. M., *Proc. Phys. Soc.,***1961**, 78, 133-144.

[40] Rees, E. P.; Trevena, D. H., *Brit. J. Appl. Phys.* **1966**, 17, 671-674.

[41] Meyer, J., "Zur Kenntnis des negativen Drucken in Flussigkeiten", Abhandl. d. Deutsch. Bunsen-Gessellschaft, **1911**, 6, 1-53.

[42] Reynolds, O. *Mem. Manchester Lit. Phil. Soc.,* **1882**, 7, 3rd series, 1.

[43] Briggs, L.J., *J.Appl.Phys.*, **1950**, 21, 721.

[44] Briggs, L.J., *J.Chem. Phys.*, **1951**, 19, 970.

[45] Roedder, E., *Science,* **1967**, 155, 1413-1417.

[46] Apfel R., Smith M., *J.Appl.Phys.*, **1977**, 48, 2077.

[47] Zheng, Q.; Durben, D.J.; Wolf, G.H.; Angell, C.A., *Science*, **1991**, 254, 829.

[48] Haar, L.; Gallagher, J.; Kell, G.S., "National Bureau of Standards-National Research Coucil Steam Tables", McGraw-Hill, New York, 1985.

[49] Tyree, M. T.; Zimmermann, M. H., "Xylem Structure and the Ascent of Sap", Springer-Verlag, Berlin, Heidelberg, New York, **2002**.

[50] Cochard, H., *C. R. Physique,* **2006**, 7,

[51] Steudle, E., *Nature*, **1995**, 378, 66.

[52] Versluis, M.; Schmitz, B.; von der Heydt, A.; Lohse, *Science,* **2000**, 289, 2114–2117.

[53] Patek, S.N.; Korff, W.L.; Caldwell, R.L., *Nature* **2004**, 428, 819–820.

[54] Leighton, T.G., The Acoustic Bubble, Academic Press, London, **1994**.

[55] Reid, R.C., *Amer. Sci.* **1976**, 64, 146–156.

[56] Kadota, T.; Yamasaki, H., *Prog. Energy Comb. Sci.* **2002**, 28, 385–404.

[57] Armas, O.; Ballesteros, R.; Martos, F.J.; Agudelo, J.R., *Fuel*, **2005**, 84, 1011–1018.

[58] Lin, C.-Y.; Chen, L.-W., *Fuel* **2006**, 85, 593–600.

[59] Leighton, T.G., "The Acoustic Bubble", Academic Press, London, **1994**.

[60] Naude C.F.; Ellis, A.T.; *ASME. J.Basic Eng*., **1961**, 83, 648.

[61] Benjamin, T.B.; Ellis, A.T., *Phil.Trans.Roy.Soc.*, Ser.A, **1966**, 260, 221.

[62] Lauterborn, W.; Bolle, H., *J.Fluid Mech.*, **1975**, 72, 391.

[63] Frost, D.; Sturtevant, B., *ASME J.Heat Transfer*, **1986**, 108, 336.

[64] Tomita, Y.; Shima, A.; *Acustica*, No.3 **1990**, 71, 161.

[65] Mason, T.J.; Lorimer, J.P., " Applied Sonochemistry", Wiley–VCH, Weinheim, **2002**.

[66] Cravotto, G.; Cintas, P., *Chem. Soc. Rev.,* **2006**, 35, 180–196.

[67] Lickiss, P.H.; McGrath V.E., *Chem. in Brit.*, **1996**, March, 47.

[68] Gutierrez, M.; Henglein, A.; *J.Phys.Chem.*, **1987**, 91, 6687.

[69] Sehgal, C.; Sutherland, R.G.; Verrall, R.E., J.Phys.Chem., **1982**, 86, 2982.

[70] Shchukin, D.G.; Möhwald, H., *Phys. Chem.* **2006**, 8, 3496–3506.

[71] Silberrard, D., *Engineering,* **1912**, 33-35.

[72] Vogel, A; Lauterborn, W; Timm, R, *j. Fluid Mech.,* **1989**, 206, 299-338.

[73] Putterman, S., *Physics World*, **1998**, 11, 38.

[74] Sehgal, C.; Sutherland, R.G.; Verrall, R.E., *J.Phys.Chem.*, **1980**, 84, 388.

[75] Ceccio, S.L.; Brennen, C.E., *J.Fluid Mech.*, **1991**, 233, 633.

[76] Kimoto H., International ASME Symposium on Cavitation Res. Facilities and Techniques, FED 57, **1987**, 217.

[77] Lush P.A.; Angell B., *ASME., J.Fluids Eng.*, **1984**, 106, 347.

[78] Shima, A.; Takayama, K.; Tomita, Y.; Miura, N., *Acustica*, **1981**, 48, 293.

2.2. Cavitation in polymers.

In the case of macromolecular materials the phenomenon of cavitation has been observed during crystallization (from a melt) of selected crystalline polymers (Fig. 9a) [1-10] and mechanical deformation (tensile drawing) [11-23] of given materials (Fig. 9b). As in the case of liquids of low molecular weight, the driving force of the phenomenon is negative pressure generated in the material. During crystallization negative pressure is generated in the areas tightly surrounded by the growing spherulites and this is where cavitation bubbles are mainly observed. During deformation of the material cavities can also be generated in the interspherulitic regions, although in the interlamellar regions, inside the spherulites, the phenomenon is more intense and takes place at a much earlier stage of deformation.

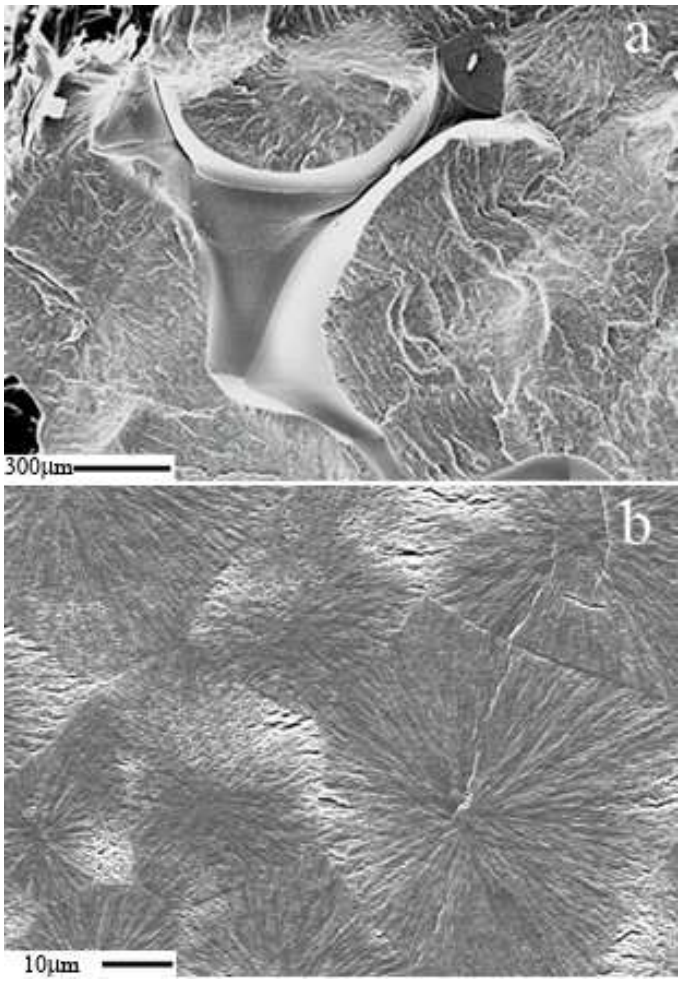

Fig. 9. Phenomenon of cavitation in polypropylene: a) during crystallization from a melt [3], b) during tensile drawing [24].

2.2.1. Cavitation during polymer crystallization.

As it is known, final properties of a polymer material are derivative not only of the chemical structure of a chain but also of supermolecular structure which is formed during solidification of the material. In contrast to compounds of small molecular weights, both inorganic (e.g. salt) and organic (e.g. sugar), polymers crystallize (from molten state) not in the form of monocrystals but in the form of polycrystalline aggregates - spherulites (Figure 10). Spherulites are not "pure" crystals, since they consist of crystalline as well as amorphous regions. Formation of spherulitic structure during cooling of a polymer melt is a two-stage process. In the first stage spherulite nucleation occurs – primary nucleation. Creation of a thermodynamically stable crystal, a nucleus, enables further growth of a spherulite in the radial direction, which takes place through formation of secondary nuclei on the surface of an already existing crystal (second stage).

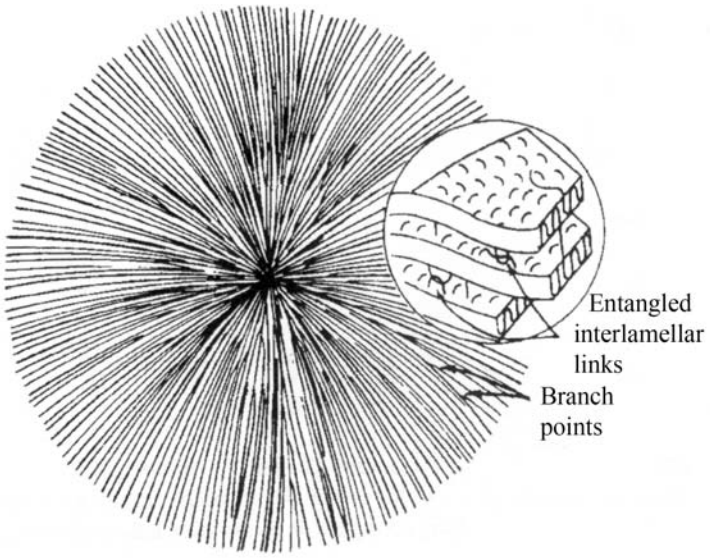

Fig. 10. Schematic of the spherulite structure [25].

Macromolecules are incorporated into the structure of a growing spherulite (creating crystalline regions as well as areas lacking organization - amorphous phase), which leads to its increase in size. In isothermal conditions growth of a spherulite runs uninterrupted until it comes into contact with adjacent spherulites. The boundaries of the impinging spherulites cause formation of regions in which the polymer, still in the molten state, is effectively separated from the rest of a melt (Figure 11a). Crystallization process of polymers is usually accompanied by a decrease in specific volume (literature data [26] indicate that for most polymers specific volume of crystalline phase is smaller by a dozen or so percent than the volume occupied by a melt: about 6.6% for polyethylene, 8.8% for isotactic

polypropylene and 16.0% for poly(methylene oxide)). Therefore, a change in specific volume accompanying the crystallization process requires a constant inflow of new portions of the molten polymer. However, polymer crystallization in the already mentioned regions, tightly cut off from the rest of a melt, is not accompanied by volume compensation. Further course of the solidification process of a polymer is thus accompanied by the buildup of negative pressure in a melt. When negative pressure generated through crystallization reaches the value of the strength of a melt, as in the case of liquids of low molecular weight, the phenomenon of cavitation occurs. Cavitation bubbles being formed relax the generated pressure. Further stages of crystallization lead to an increase in size of the generated bubbles, which will constitute an integral part of the structure of the fully solidified material (Figure 11b). Both local stresses and cavitation bubbles weaken the polymer materials. Therefore, such interspherulitic regions are referred to as "weak spots".

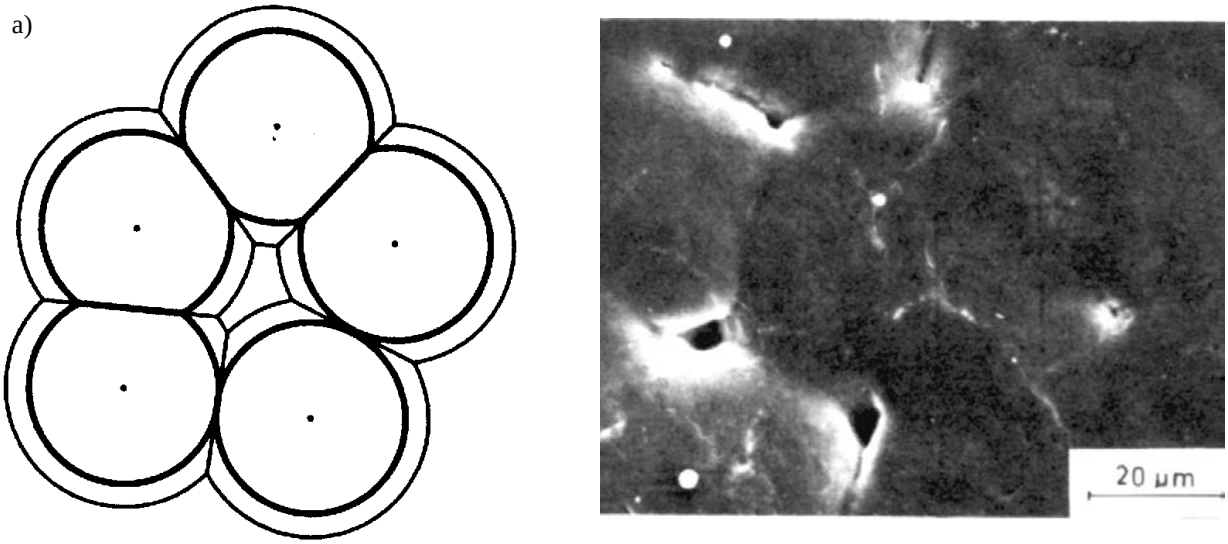

Fig. 11. "Weak spots" in a polymer film: a) diagram presenting formation of a "weak spot"; b) SEM microphotography of poly(methylene oxide) film - free surface [1].

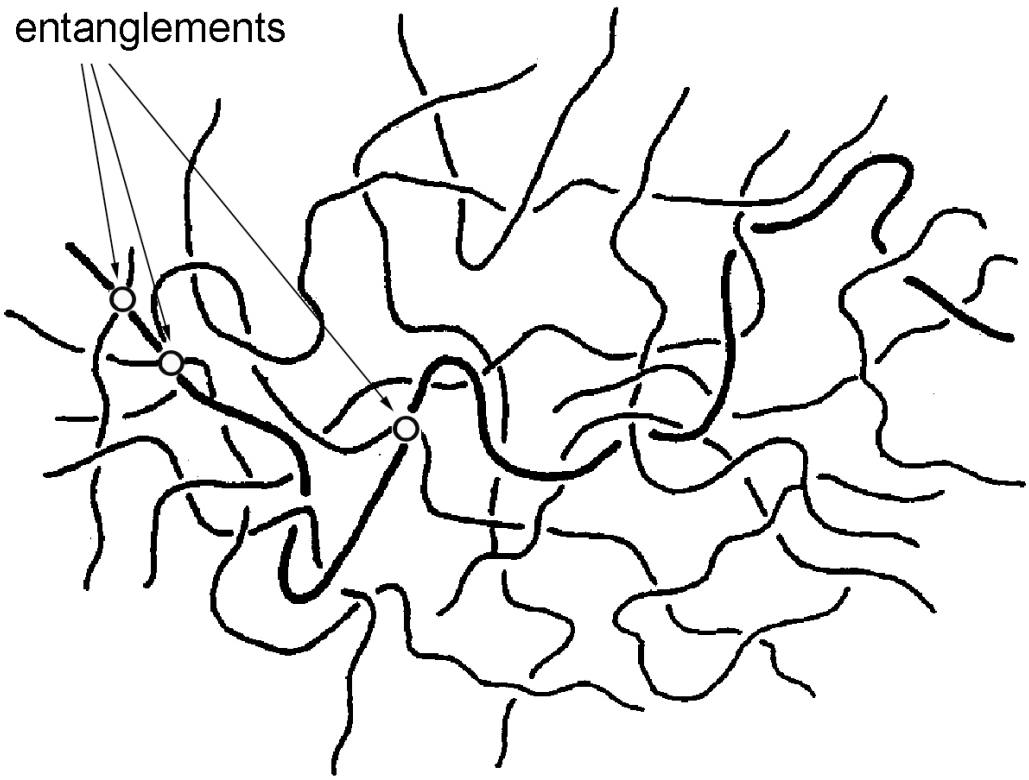

Fig. 12. Entanglement of macromolecules in a polymer melt.

As in the case of liquids of low molecular weight, it is possible to determine negative pressure (of strength of a melt) generated in the interspherulite regions during cavitation process. The parameter is determined on the basis of change in the melting temperature of a spherulite, which increases with occurrence of stresses in the melt. Negative pressure causes local change in supercooling, lowering equilibrium melting temperature, T_m^o, whose consequence is a decrease in the spherulite's growth rate. Measurement of change in the melting temperature of a spherulite in the "weak spot" region, ΔT_m, allows to determine the local supercooling change, equal to a decrease in the equilibrium melting temperature. From the empirical extrapolation of the relation between T_m^o and p [27-31], plotted for positive pressure, to negative values of p, it is possible to calculate negative pressure generated during solidification of the material. This method has been used to determine the value of strength of a melt for a number of polymers [32], such as polypropylene (-20 MPa), high density polyethylene (-10 MPa), poly(methylene oxide) (-10 MPa), poly(ethylene adipate) (-12 MPa), poly(ethylene oxide) (-6 MPa). Such high values of strength of a polymer melt, obtained without using special purification procedure, as in the case of liquids of low molecular weight, and performed for untreated material result probably from numerous entanglements naturally occurring in the molten material (Figure 12). The presence of additional ties, placed on macromolecules by other

macromolecules, ensures high cohesion of the material, which results in a high strength of a polymer melt.

Interesting results were presented in the paper by Nowacki [10], who studied cavitation accompanying crystallization of poly(methylene oxide) and its mixtures with talc and chalk (native and modified with calcium stearate). Negative pressure created in a melt, in the interspherulitic regions, was calculated on the basis of change in the spherulites' growth rate. The presence of chalk modified with calcium stearate drastically decreased strength of a polymer melt, while the unmodified chalk did not produce such an effect. Furthermore, one noted the influence of the content of the filler and the size of its grains on the observed changes in the strength of a melt. The presented results showed that the phenomenon of triggering the cavitation during solidification of the material is of nucleation nature, similarly to low-molecular liquids. The presence of particles with poor adhesion to a polymer thus creates a similar effect as in the case of solid contaminants in liquids of low molecular weight.

2.2.2. Cavitation during polymer deformation.

As it has already been mentioned polymers are a very important and strongly developing class of materials, also engineering materials. Many of them are crystalline polymers. Knowing and understanding basic mechanisms of plastic deformation of such materials is essential to fully exploit the possibilities offered by those macromolecular materials. In the case of polymers in glassy state, due to a relatively simple structure of such materials, research conducted in the last three decades allowed to understand a number of aspects accompanying their deformation. Despite numerous studies being carried out in many research centres [35-39], the mechanisms of plastic deformation of crystalline polymers due to complex, hierarchical architecture of such materials still require a more detailed research. In order to fully understand the nature of deformation of crystalline polymers three basic levels of the material microstructure need to be considered [40]:

- a range of 0,2-2 nm corresponding to interactions between neighbouring segments of a chain both in crystalline and amorphous phase (Figure 13a)
- a range of 10-30 nm representing thickness of crystalline lamellae and amorphous layers between adjacent lamellae (Figure 13b)
- a range of 0.5-100 μm corresponding to the size of supermolecular structures such as spherulites creating complex systems of crystalline lamellae and regions lacking organization (Figure 13c).

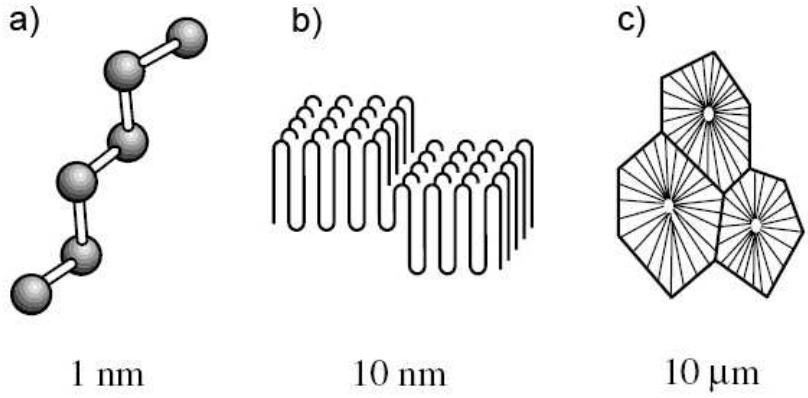

Fig. 13. Levels of structure of crystalline polymer [40]: a) macromolecule's fragment; b) lamellar chain; c) spherulitic structure.

Therefore, the description of plastic deformation of crystalline polymers of a spherulitic morphology is incredibly complex and requires consideration of a number of phenomena accompanying deformation of such a material at given structural levels.

Deformation of a crystalline polymer is a process which should include the presence of crystalline lamellae as well as amorphous layers lacking organization. It is assumed that at temperatures in which amorphous phase exhibits rubber-like properties, it is in the interlamellar regions that the initial stage of polymer deformation takes place. This results, among others, from data presented in the paper [41], whose authors demonstrated that stress required to initiate deformation of amorphous phase constitutes from 2 to 10% of the value of stress needed to activate the mechanisms of crystalline phase deformation.

Studies conducted by Bartczak at al. [42-44] also confirm the observed dependencies. Furthermore, as has been mentioned at the beginning, if the deformation of a polymer is accompanied by cavitation, it is in the amorphous phase of the material that cavities being formed during deformation are located. Understanding the phenomena taking place in the early stages of deformation in the interlamellar layers of spherulites seems vital for understanding the nature of formation of cavities in polymers in which such a process takes place.

It is currently believed that deformation of amorphous phase takes place according to three basic mechanisms, schematically presented in Fig. 14 [37, 39].

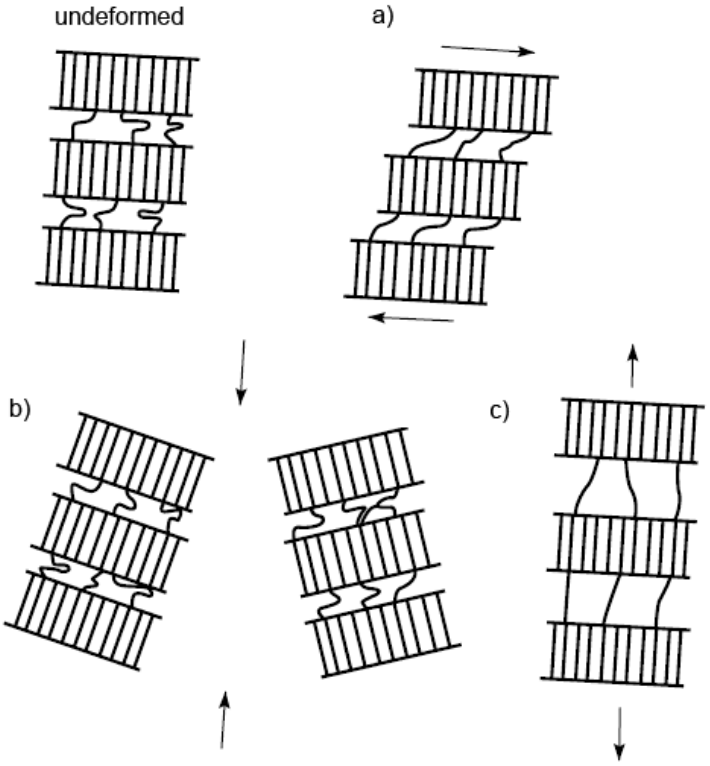

Fig. 14. Models of deformation in amorphous regions [39]: a) interlamellar slips; b) stack rotation; c) interlamellar separation.

Interlamellar slips (Figure 14a) [45-47] are realized as a result of simple shear of amorphous layers between lamellae taking place parallel to lamellar surfaces. This deformation mechanism is believed to be relatively easily activated in the early stages of deformation when amorphous phase exhibits rubber-like properties [39]. The mechanism is inactive when deformation takes place below glass transition temperature of amorphous phase. Lack of interlamellar slips, accounts, among others, for a high increase in the elastic modulus of the deformed material below Tg of the material. Almost complete reversibility of this type of deformation has also been observed, which was explained by elastic properties of amorphous phase or significant residual stresses in the undeformed material [45, 46]. The author of the paper [48] observed a complete reversibility of interlamellar slips up to deformation $e<0.6$. According to Keller [45] some irreversibility of interlamellar slips can be attributed to the processes of breaking of chains (which reduce residual stress), or pulling out of macromolecules from lamellae (increasing frictional forces between surfaces of the moving lamellae). Furthermore, the authors of the papers [45, 49] on the basis of wide and small- angle scattering measurements (WAXS and SAXS) suggested that interlamellar slips “compete” with one of the deformation mechanisms of

crystalline phase, i.e. crystallographic slips. Interlamellar slips cause crystalline lamellae to rotate around the direction of deformation, while crystallographic slips cause the chain to rotate.

The second mechanism accompanying deformation of amorphous phase, schematically presented in Fig. 14 b, is lamella-stack rotation. This type of deformation activated through shear of the material requires cooperative movements of amorphous phase and crystallites. In order for such a mechanism to be activated stack of lamellae have to be surrounded by a relatively easily deformable amorphous phase. Such deformation mechanism was first observed by Groves and Hirsch [50]. The results of small-angle X-ray scattering in combination with data obtained for wide-angle scattering presented in the paper [47] allowed to distinguish this mechanism from those accompanying the process of material deformation. Direct observations of rotation of stacks of lamellae using high resolution scanning electron microscopy have been presented in the article [51]. The author of mentioned paper proved that stacks of lamellae, consisting of three to ten crystallites, move cooperatively under the influence of stress.

The last type of deformation of amorphous phase, particularly important for the phenomenon of cavitation, is interlamellar separation (Fig. 14c) [45, 47, 52-54]. The paper which presents the mechanism of interlamellar slips [45], on the basis of SAXS measurements also notes a change in the value of a long period, which could not be accounted for by the presence of crystallographic slips. The proposed mechanism involving a change of distance between the adjacent lamellae, parallel to one other, when the direction of stress is perpendicular to their surface, satisfactorily explained the observed changes. This type of deformation and the ability to activate this mechanism strongly depend on the material structure, particularly on the number and the distribution of active, taut tie molecules between the lamellae and the lateral dimension of the lamellar crystals. Lamellar separation in the volume of a sample must be accompanied by either "flowing in" of the material into the opening gaps between lamellae or an intensive process of a decrease in density of the deformed material, e.g. occurrence of cavities. Due to limitations resulting from the presence of neighbouring lamellae the first type of contraction seems unlikely since it would require a massive rapture of tie molecules. It is believed that in order to encourage this type of material contraction accompanying lamellae separation, the deformation process should be conducted at elevated temperature, for which the mobility of amorphous phase significantly increases and which additionally facilitates pulling macromolecules out of the crystallites [55]. However, much more frequently, especially for materials

such as polypropylene, high density polyethylene or poly(methylene oxide), that is materials characterized by a relatively high modulus and also capable of substantial plastic deformation, the separation process is accompanied by local changes in density of a sample, whose final result is formation of the material discontinuity – a cavity. Macroscopic effect of this type of contraction is a strong whitening accompanying deformation (uniaxial stretching) of the aforementioned materials.

Spherulites, as mentioned earlier (Figure 10), consist of radially arranged lamellae and amorphous regions. Mechanical response of such complex polycrystalline aggregates is one of the most important issues concerning deformation of materials of this kind of structure. Considering a typical architecture of a spherulite (Figure 10) one should take into account three characteristic regions differing in relative arrangement of lamellae, whose mechanical response under the influence of the applied stress significantly differs (Figure 15). Due to complexity of the problem the research much more frequently focused on the selected spherulite regions listed below:

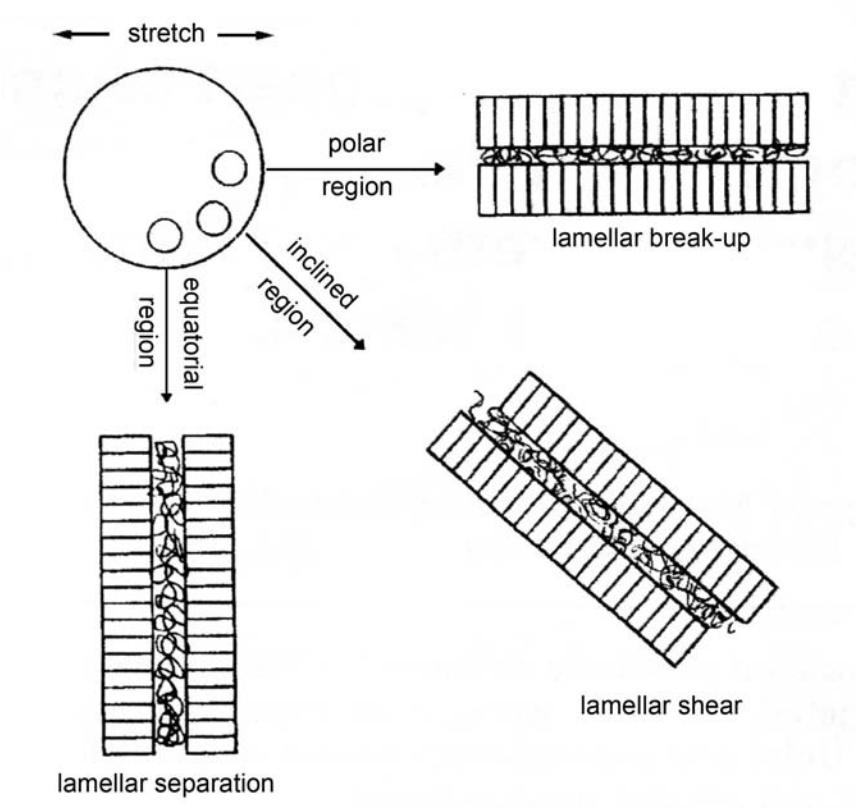

Fig. 15. Scheme of strains acting in various regions of a spherulite during uniaxial stretching.

- Polar region: in this spherulite region most macromolecules are arranged perpendicularly to the direction of deformation. A consequence of such chain arrangement is orientation of lamellar surfaces parallel to the direction of the applied stress. Two most important processes accompanying

deformation of this spherulite region is micronecking (taking place according to mechanism proposed by Peterlin) and formation of microcavities [56, 57]. Consequently, this spherulite region exhibits the highest plastic deformation resistance during uniaxial tension.

- Equatorial region: in this region lamellae are arranged almost perpendicularly to the direction of deformation. Results presented in the papers [37, 38, 58] show that it is the equatorial region that deformation first appears in, which is explained by the presence of easily activated deformation mechanisms of amorphous phase such as lamellar separation and rotation. Research performed for single large polybutene spherulites presented in the paper [59] showed that deformation initiated in the centre of a spherulite (according to theory it is in the centre of a spherulite that stress reaches the highest value [60]) spreads over the equator along the radius.

- Diagonal region: material deformation of this sperulite region takes place intermediately to the above mentioned limiting cases. The process of lamellar separation is observed accompanied by shear of interlamellar amorphous layers. The result of the complex processes taking place in this deformation region is lamellar rotation in the direction of the applied stress and a macroscopic change in the spherulite's shape: sphere-ellipse.

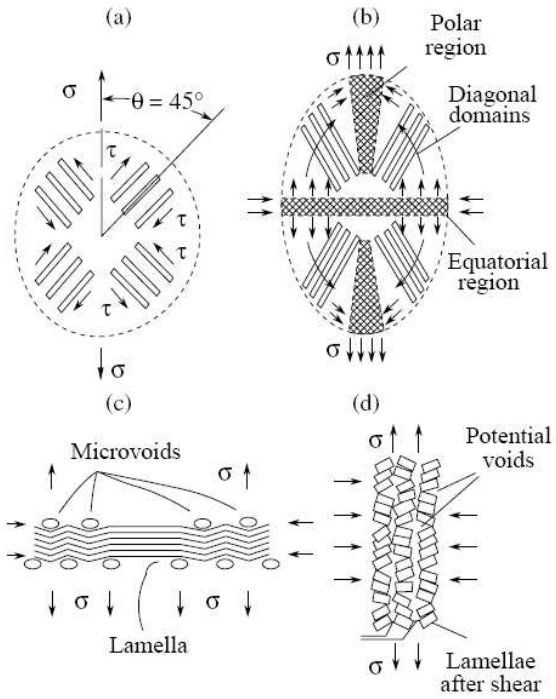

Fig. 16. Stages in the formation of cavities in the spherulite structure during uniaxial deformation [61]: a) crystallites of the diagonal region; b) lamellar rotation in the diagonal region resulting from an increase in tensile and compressive stresses in the equatorial region of a spherulite; c) kinking of

lamellae due to shear instability in the amorphous matrix in equatorial region; d) shear instability due to chain slip in lamellae in polar regions.

Complex changes taking place in the spherulite structure, including changes in distribution of stress in individual regions and the phenomenon of cavitation accompanying deformation process were presented in the paper by Gałęski [61].

Although formation of stresses inside the spherulite structure is a complex phenomenon, it has been observed, on the basis of transmission electron micrographs combined with the process of contrasting samples, that a number of interrelated processes occur preferentially in the selected areas of different lamellar arrangement (Figure 16). Under the influence of the applied stress the lamellae oriented at an angle of approximately 45^{o} to the direction of deformation (diagonal region of a spherulite) are brought to rotation under the influence of intra-and interlamellar slips (Figure 16a). Such a type of deformation and change in the spherulites's shape accompanying deformation process of such structural object results from formation of additional tensile and compressive stresses in equatorial and polar regions (Figure 16b). Under the action of these stresses selected mechanisms of crystal deformation in the equatorial region are blocked due to the specific orientation of packets of lamellae with respect to stresses. As a result, lamellae undergo kinking, which leads to formation of cavities in this spherulite region (Figure 16c). Analogous processes should also take place in the spherulite's polar region. Specific arrangement of crystallites prevents deformation of amorphous phase. Lamellar deformation, analogous to crystallites in the equatorial region, takes place as a result of their limited crystallographic slips and local break-up. Lack of proper contraction of the amorphous phase leads to formation of regions of lower density, whose consequence in further stages of deformation of spherulite's polar region is formation of cavities (rysunek 16d).

An interesting model (Figure 17) presenting subsequent stages of formation, growth and reorganization of voids formed in a linear polyethylene during its deformation was presented by Butler [62]. A precise tool, that is small-angle X-ray scattering technique, allowed to determine at what stage of deformation cavities are created, what is their initial shape and what symmetry changes are observed as a result of activation of subsequent mechanisms of plastic deformation of polyethylene.

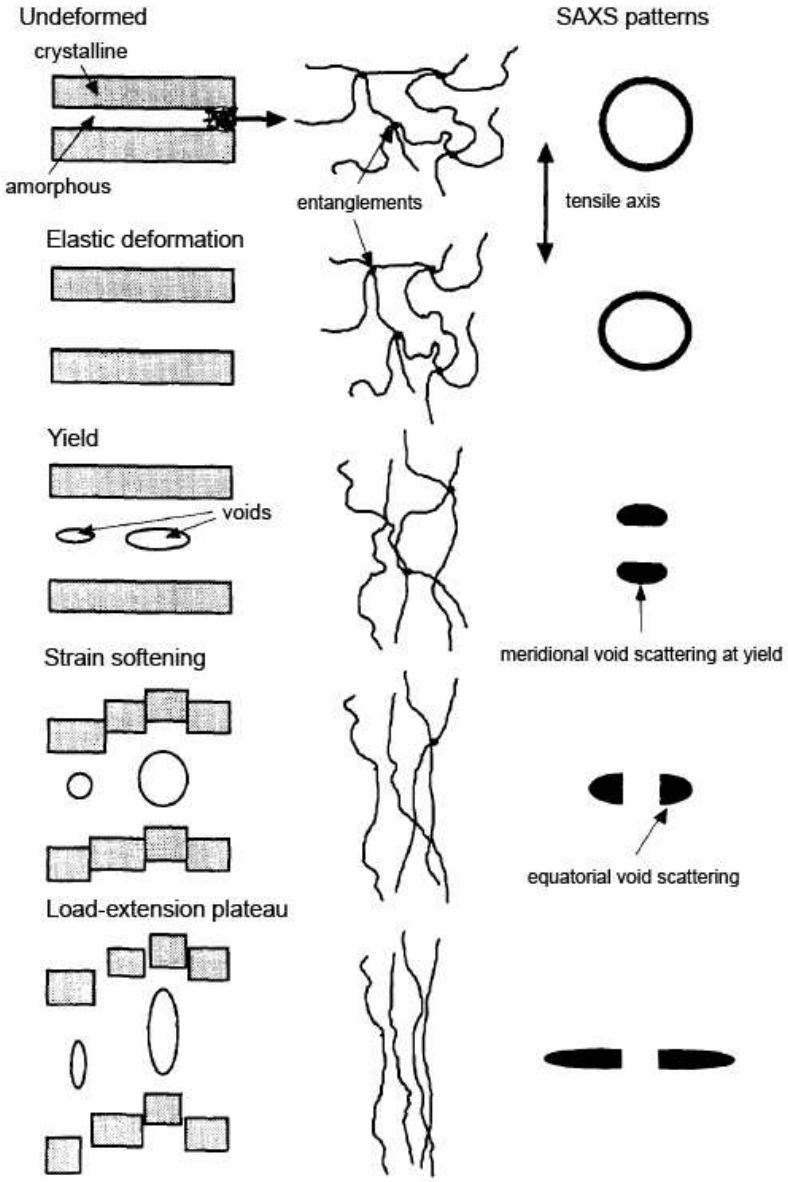

Fig. 17. Schematic of cavity formation and growth in the interlamellar region during deformation of the material [62].

Results presented in the paper [62] and the presented schematic show that first discontinuities in the material appear just before or shortly after reaching the macroscopic yield point. Initially the cavities of ellipsoidal shape are oriented with its long axis perpendicularly to the direction of deformation. Such shape of cavities is forced by the material's lamellar structure. The presence of objects with such parameters is confirmed by a strong signal on a diffractogram in the meridional region (high intensity of signals coming from cavities is a result of significant difference in the electron density of the material and the generated cavities). Change of interlamellar distances and fragmentation of lamellae force a change in the shape of cavities. The phenomenon can be observed on a small angle scattering pattern. It manifests itself in the fading signal in the meridional region and

appearance of strong scattering in the equatorial zone. Further deformation of the material is accompanied by strong extension and thinning of cavities, whose symptom is a long, narrow diffraction signal in the equatorial region of a scattering pattern.

A different approach which explains results obtained from small-angle X-ray scattering measurements was presented in the paper [63]. Zhang suggested the possibility of creation of the second fraction of cavities, oriented parallel to the direction of deformation, as a result of the process of lamellar fragmentation. The signal in the equatorial region may therefore appear not as a result of reorganization of shape but due to formation of another population of cavities in further stages of deformation.

The observed mechanisms of deformation of crystalline polymers appearing during tensile stretching are related to a number of factors such as deformation rate [64-66], temperature of deformation [66, 67], molecular weight [22, 65, 68-70], thermal history [21, 62, 65, 68-70] and orientation of lamellar structure [66]. It turns out that also cavitation accompanying deformation of the material is a phenomenon sensitive to the aforementioned factors. Furthermore, cavitation is a process simultaneously determined by several of the mentioned parameters, therefore, depending on the characteristics of the material and conditions under which the deformation process takes place, each of the mentioned factors plays a more or less important role. Certain factors are so important that they determine the presence or absence of cavitation, others only influence the scope of the phenomenon. Factors that influence the phenomenon of cavitation accompanying deformation process of crystalline polymers will be discussed below.

The main criterion determining the presence of cavitation during plastic deformation is thickness and degree of defectiveness of crystallites in the material. The authors of the paper [20] clearly demonstrated that during plastic deformation there is a kind of "rivalry" between activation of deformation mechanisms of crystalline phase and cavitation occurring in amorphous regions. Deformation of materials with large, strong, well-developed crystals, such as polypropylene, high density polyethylene or poly(methylene oxide), is accompanied by cavity formation, however, in the case of materials of small, strongly defected crystallites such as low density polyethylene, ethylene copolymers, deformation takes place without cavitation. That is because the plastic deformation of crystals is initiated before the stress reaches the resilience of the amorphous phase. On the basis of surface tension and thickness of amorphous regions the authors of the mentioned paper estimated

negative pressure necessary to generate stable cavitations, equivalent to strength of amorphous phase, in the following materials: polypropylene (-13.7 MPa), poly(methylene oxide) (-35.8 MPa), polyethylene of high (-15.1 MPa) and low density (-17.6 MPa). Negative pressure occurring locally at yield point in polypropylene (-20.7 MPa), poly(methylene oxide) (-42 MPa), polyethylene of high (-15.3 MPa) and low density (-4.7 MPa) have also been determined. In the cases where the resistance of amorphous phase is lower than the negative pressure at yield point (PP, HDPE, POM), the applied stress will cause cavitation of amorphous phase prior to activation of deformation mechanisms of crystalline phase. In materials of thinner and softer crystals (LDPE) deformation of crystals will be initiated before stress exceeds strength of the amorphous phase.

Even in the case of the aforementioned polymers, in which the phenomenon of cavitation was observed, thanks to changes at the level of material structure, caused by difference in thermal history during crystallization of the material and after its solidification, one can influence the intensity of the process of cavity formation [21]. Running the crystallization process at a higher temperature (isothermal crystallization) or at a lower cooling rate (non-isothermal crystallization) one obtains materials with thicker crystals, exhibiting higher mechanical strength. Analogous effect can be achieved by running the process of annealing of the already solidified materials, which results in thickening of crystallites and increase in their strength. In materials with higher strength of the crystalline phase, as has been mentioned in the previous paragraph, the cavitation process is more intense as an easier phenomenon.

As has already been mentioned, occurrence of cavitation during deformation of a crystalline polymer is first observed in the spherulite's equatorial region. Specific arrangement of lamellae in that region, whose surfaces are oriented perpendicularly to direction of deformation, facilitates their separation, which results in formation of discontinuity in the material structure. Important factor influencing the phenomenon of cavitation is thus orientation of the material's lamellar structure. The role of this parameter in the process of cavitation has been illustrated in the paper by Pawlak [21]. The subject of study of the mentioned paper were polyethylene injection samples. On the surface of such samples, in contrast to structure outside the area of strong shear and cooling of a melt (core of a sample-Figure18b) arrangement of lamellae is the same as in the spherulite's equatorial region in the material of isotropic structure (Figure 18a). Detailed studies of such a material demonstrated that when deformation takes place perpendicularly to lamellar surfaces, arranged parallel to one another,

cavitation in the surface layer occurs already with deformation from about 0.15%, which is much below the value at which cavitation is observed in isotropic samples, and stress of 2 MPa (first cavities in isotropic samples appear at approximately 10 times higher stress). Specific lamellar arrangement in the material, perpendicular to the direction of deformation, by favouring this type of material response is thus beneficial to the phenomenon of cavitation.

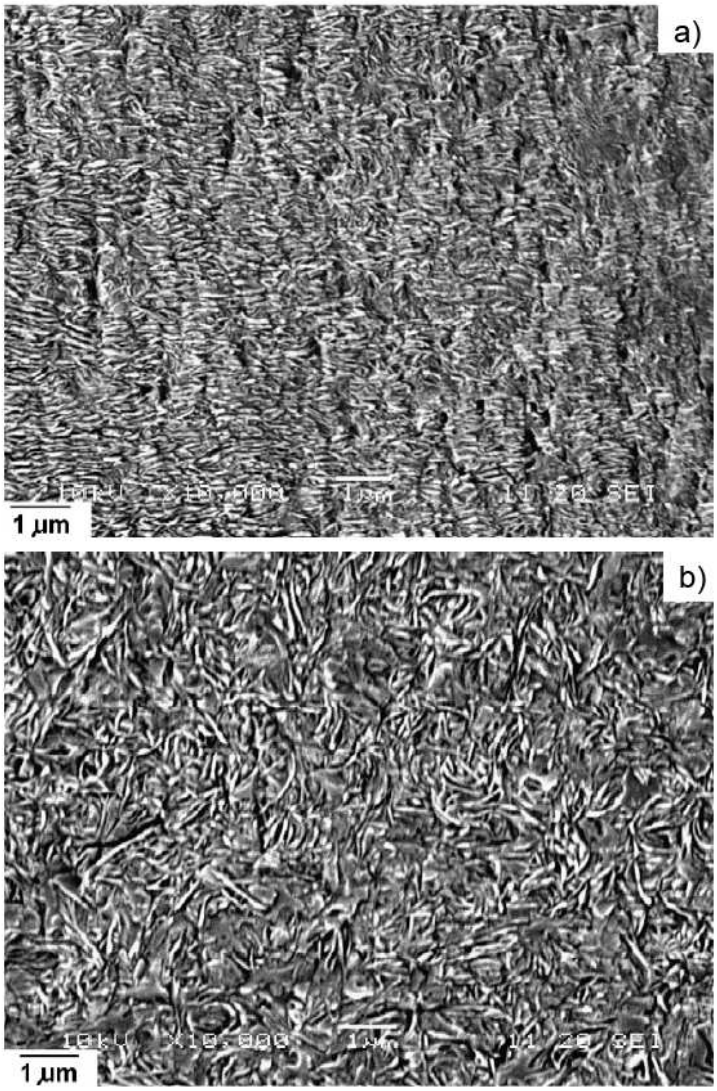

Fig. 18. SEM microphotographs of polyethylene sample : a) skin; b) core of injection molded sample. Details revealed by sectioning and etching with permanganate etchant [21].

Another factor influencing the intensity of cavitation process during deformation of the material is molecular weight of a polymer. Results presented in papers [22, 62] showed that increasing molecular weight of a polymer leads to reduction in the intensity of the cavitation process. The authors explained this effect by a higher number of strongly entangled macromolecules forming amorphous

phase. Macromolecules in the unordered regions of a polymer of a higher mass form a more durable entanglement network, more resistant to tensile stresses.

Apart from parameters related to the material structure, cavitation is also affected by conditions under which deformation of the material is conducted (deformation rate and temperature). The authors of papers [22, 71] proved a strong dependence of cavitation on the deformation rate – an increase in the deformation rate caused an increase in the intensity of cavity formation in the material. The influence of a sample's deformation rate on cavitation is accounted for by changes in the stress values at yield point with a change in deformation rate. When the deformation rate is low, stress at yield point is small enough to activate deformation mechanisms of crystalline phase until the strength of amorphous phase is exceeded. Higher deformation rate corresponds to a change (increase) in the strength of crystals, which results in a higher value of stress initiating plastic deformation. An increase in stress initiating plastic deformation of crystals leads to initiation of cavitation, as an easier phenomenon, when the strength of amorphous phase is exceeded.

Temperature of deformation is also an important parameter. Studies presented in papers [63, 71, 72] show that by running deformation at elevated temperature one can completely eliminate the phenomenon of cavitation. The material cavitating at room temperature deforms without cavitation when ambient temperature is increased. It is believed that the reason for such an effect is lowering stress limit initiating deformation of crystalline phase (crystallographic slips). Before stress exceeds the strength of amorphous phase, deformation mechanisms of crystalline phase will be activated as easier ones.

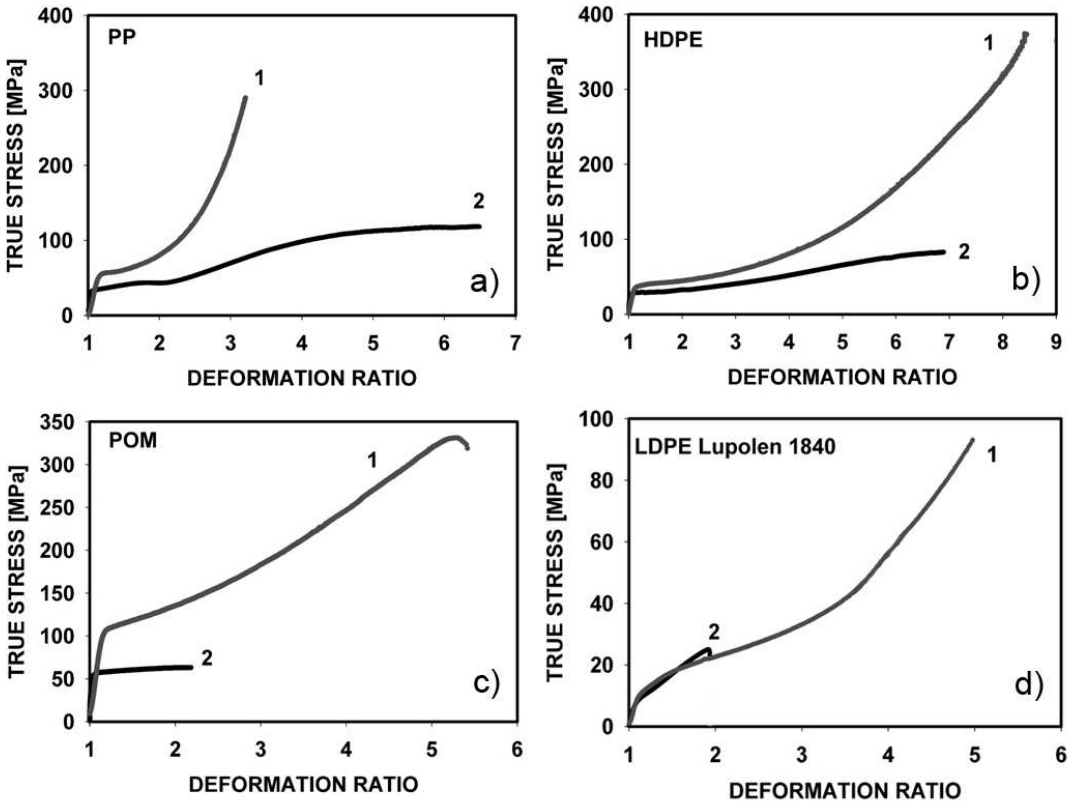

Fig. 19. True stress – true strain curves for selected materials deformed as a result of compression (1) and stretching (2) [20] a) polypropylene; b) high density polyethylene; c) poly(methylene oxide); d) low density polyethylene.

Extensive research on deformation mechanisms of the crystalline polymers, especially in the light of the recent literature data [20], should take into account the presence of cavitation as one of the important phenomena activated during material deformation. The phenomenon of cavitation accompanying deformation of some materials, for years associated with a process only responsible for changes in the material's density and influencing organoleptic properties (whitening of the material), may also be one of the factors influencing and determining mechanical properties of macromolecular materials. The authors of the cited paper showed that for some polymers such as polypropylene, high density polyethylene or poly(methylene oxide) intense cavitation during tensile drawing leads to a decrease in stress and deformation at yield point. The results of tensile drawing have been compared with the results obtained for the compressed samples in a channel die (compression process, which is not accompanied by formation of cavities kinematically corresponds to uniaxial stretching). For the above mentioned polymers differences in mechanical properties were observed (Figure 19a, b, c), which according to the authors of the paper were a result of the presence of cavitation in the stretched samples. For low density polyethylene (Figure 19d), whose stretching is not accompanied by

cavitation, no differences in mechanical properties were observed. The presented paper shows how strongly the phenomenon of cavitation influences mechanical parameters of some of the crystalline polymers.

The literature data presented in the above chapter concerning the phenomenon of cavitation in uniaxially deformed crystalline polymers reveal complexity of the discussed subject. Complex spherulitic structure of the material as well as a number of highly diverse factors influencing cavitation prevents thorough understanding of all the aspects concerning creation of discontinuities in the material. Furthermore, for years the phenomenon of cavitation was an issue of secondary importance, an artifact accompanying polymer deformation. It is the research conducted at the Centre of Molecular and Macromolecular Studies of Polish Academy of Sciences which brought the new quality to the discussed subject, whose result, among others, is this dissertation.

2.2.3. References.

[1] Galeski, A.; Piorkowska, E. *J.Polym. Sci., Polym.Phys.Ed.,* **1983**, 21, 1299-1312.

[2] Galeski, A.; Piorkowska E. *J.Polym. Sci., Polym.Phys.Ed.,* **1983**, 21, 1313.

[3] Galeski, A.; Piorkowska E. w *Liquids Under Negative Pressure.* II. Mathematic, Physics and Chemistry, NATO Science Series, red. Imre, A.R.; Maris, H.J.; Williams, P.R. Kluwer Academic Publishers, London, **2002**, 84, 127.

[4] Galeski, A.; Piorkowska, E.; Koenczoel, L.; Baer E. *J.Polym.Sci:Part B:Polym.Phys.*, **1990**, 28, 1171.

[5] Galeski, A.; Koenczoel, L.; Piorkowska, E.; Baer, E. *Nature*, **1987**, 325, 40.

[6] Monasse, B.; Houdin, J.M. *Coll. Polym.Sci.*, **1985**, 263, 822.

[7] Monasse, B.; Houdin, J.M. *Coll. Polym.Sci.*, **1988**, 266, 679.

[8] Thomann, R.; Wang, C.; Kressler, J.; Mulhaupt, R. *Macromol. Chem.Phys.,* **1996**, 197, 1085.

[9] Nowacki, R.; Kolasinska, I.; Piorkowska. *J.Appl.Polym.Sci.,* **2001**, 79, 2439.

[10] Nowacki, R.; Piorkowska, E. *J.Appl.Polym.Sci.,* **2007**, 105, 1053.

[11] Aboulfaraj, M.; G'Sell, C.; Ulrich, B.; Dahoun, A. *Polymer,* **1995**, 36, 731.

[12] Hiss, R.; Hobeika, S.; Lynn, C.; Strobl, G. *Macromolecules,* **1999**, 32, 4390.

[13] Hughes, D.J.; Mahendrasingam, A.; Oatway, W.B.; Heeley, E.L.; Martin, C.; Fuller, W. *Polymer,* **1997**, 38, 6427.

[14] Duffo, P.; Monasse, B.; Haudin, J.M.; G'Sell, C.; Dahoun, A. *J. Mater. Sci*., **1995**, 30, 701.

[15] Castagnet, S.; Girault, S.; Gacougnolle, J.L.; Dang, P. *Polymer*, **2000**, 41, 7523.

[16] Nathani, H.; Dasari, A.; Misra, R.D.K. *Acta Mater*, **2004,** 52, 3217.

[17] Galeski, A. *Prog. Polym. Sci.* **2003**, 28, 1643.

[18] Zhang, X.C.; Butler, M. F.; Cameron, R.E. *Polymer* **2000**, 41, 3797.

[19] Gencur, S.J.; Rimnac, C.M.; Kurtz, S.M. *Biomaterials*, **2003**, 24, 3947.

[20] Pawlak, A.; Galeski, A. *Macromolecules* **2005,** 38, 9688.

[21] Pawlak, A. *Polymer* **2007,** 48, 1397.

[22] Pawlak A, Galeski A, *Macromolecules*, **2008**, 41, 2839.

[23] Butler, M.F.; Donald, A.M.; Ryan, A.J. *Polymer,* **1997,** 38, 5521.

[24] Różański, A. unpublished data.

[25] Hoffman, J.D.; Davis, G.T.; Lauritzen, J.I. w "Treatise on Solid State Chemistry", Plenum, New York, 1976, vol. 3, 497.

[26] Brandrup, J.; Immergut, E.H.; Grulke, E.A. "Polymer Handbook", John Wiley&Sons, Inc., New York, **1999**, rozdz. 5, 12, 26, 98.

[27] Wunderlich, B. "Macromolecular Physics", Crystal Melting, Academic Press: New York, **1980**, vol. 3, 95.

[28] Karl, V.; Asmussen, F.; Uberreiter, K. *Makromol.Chem*. **1977**, 178, 2037.

[29] Tsujita, Y.; Nose, T.; Hata, T. *Polym. J.* **1974**, 6, 51.

[30] Jenckel, E.; Rinkens, H. Z. *Elektrochem* **1956**, 60, 970.

[31] Leute, U.; Dolhopf, W.; Liska, E. *Coll Polym. Sci.* **1978**, 256, 914.

[32] Pawlak, A.; Piorkowska, E. *J.Appl.Polym.Sci.,* **1999**, 74, 1380.

[33] Perez, J. "Physics and Mechanics of Amorphous Polymers", Balkema: Rotterdam **1998**.

[34] Haward, R. N.; Young, R. J. "The Physics of Glassy Polymers", Chapman & Hall: London, **1997**.

[35] Galeski, A. *Prog. Polym. Sci.*, **2003**, *28*, 1643.

[36] Oleinik, E. F. *Polym. Sci. Ser. C.*, **2003**, *45*, 17.

[37] Lin, L.; Argon, A. S. *J. Mater. Sci.*, **1994**, *29*, 294.

[38] Haudin, J. M. "In Plastic deformation of Amorphous and Semicrystalline Materials", B. Escaig; C. G'Sell, eds.; Les Editeurs de Physique: Paris, **1982**, 291.

[39] Bowden, P. B.; Young, R. J. *J. Mater. Sci.*, **1974**, *9*, 2034.

[40] Schultz, J.M., *Polym. Eng. Sci.*, 1984, 24, 770.

[41] Peterson, J.M.; Lindenmeyer, P.H. *J.Appl.Phys.* **1966**, 37, 4051.

[42] Bartczak, Z.; Cohen, R.E.; Argon, A.S. *Macromolecules*, **1992**, 25, 4692

[43] Bartczak, Z.; Argon, A.S.; Cohen, R.E. *Macromolecules*, **1992**, 25, 5036

[44] Bartczak, Z.; Argon, A.S.; Cohen, R.E. *Polymer*, **1994**, 35, 3427

[45] Pope, D.P.; Keller, A. *J. Polym.Sci., Polym.Phys.Ed*, **1975**, 13, 533.

[46] Young, R.J.; Bowden, P.B.; Ritchie, J.M.; Rider, J.G. *J Mater Sci*, **1973**, 8, 23.

[47] Keller, A.; Pope, D.P. J.Mater.Sci. **1971**, 6, 453.

[48] Bartczak, Z. *Polymer*, **2005**, 46, 10339.

[49] Yamada, M.; Miyasaka, M.; Ishikawa, K. *J.Polym.Sci., Polym.Phys.Ed.*, **1976**, 9, 1083.

[50] Groves, G.W.; Hirsch, P.B. *J.Mater.Sci.,* **1969**, 4, 929.

[51] Tagawa, T. *J.Polym.Sci., Polym.Phys.Ed.,* **1980**, 18, 971.

[52] Kaufman, W.E.; Schultz, J.M. *J.Mater.Sci.*, **1973**, 8, 41.

[53] Quynn, R.G.; Brody, H. *J.Macromol.Sci, Phys.*, **1971**, B5, 721.

[54] Paterman, J.; Schultz, J.M. *J.Mater.Sci*, **1978**, 13, 50.

[55] Bartczak, Z.; Galeski, A.; Argon, A. S.; Cohen, R. E. *Polymer*, **1996**, 37, 3113.

[56] Allan, P.; Bevis, M. *Philos.Mag.*, **1980**, 41, 555.

[57] Allan, P.; Bevis, M. *Philos.Mag.*, **1977**, 35, 405.

[58] Hay, I.L.; Keller, A. *Kolloid Z. Z. Polym.*, 1965, 204, 43.

[59] Weinant, E.; Haudin, J.M.; G'Sell, C. *J. Mater. Sci.,***1980**, 15, 2667.

[60] Wang, T.T. *J.Polym.Sci., Part B:Polym.Phys.,* **1974**, 12, 145.

[61] Galeski, A.; Argon, A.S.; Cohen, R.E. *Macromolecules*,**1988**, 21, 2761.

[62] Butler, M.F.; Donald, A.M.; Ryan, A.J. *Polymer*, **1998**, 39, 39.

[63] Zhang, X. C.; Butler, M. F.; Cameron, R. E. *Polymer,* **2000**, 41, 3797.

[64] Viana, J.C. *Polymer,* **2005**, 46, 11773.

[65] Stern, C.; Frick, A.; Weickert, G. *J.Appl.Polym.Sci.,* **2007**, 103, 519.

[66] Hobeika, S.; Men, Y.; Strobl, G. *Macromolecules*, **2000**, 33, 1827.

[67] Hartmann, B.; Lee, G.F.; Wong, W. *Polym. Eng. Sci.,* 1987, 27, 823.

[68] Capaccio, G.; Ward, I.M. *Polymer,* **1975**, 16, 239.

[69] Capaccio, G.; Chapman, T.J.; Ward, I.M. *Polym.Sci, Polym.Phys.Edn.,* **1976**, 14, 1641.

[70] Fu, Q.; Men, Y.; Strobl, G. *Polymer*, **2003**, 44, 1941.

[71] Liu, Y.; Truss, R.W. *J.Polym.Sci., Part B: Polym.Phys.* **1994**, 32, 2037.

[72] Pawlak, A.; Galeski, A.; Gadzinowska, K. in press.

3. Objective of the paper

Mechanical properties of polymers, which are derivative of a number of factors, i.e. parameters of a single chain and organization of the supermolecular structure, for years have been the subject of extensive research. In order to fully exploit the possibilities offered by macromolecular materials, one has to examine their complex, hierarchical structure. The structure of crystalline polymers, primarily due to the presence of two phases of distinctly different properties, crystalline and amorphous, determines mechanisms activated during deformation of such materials. Examination of mechanisms that control plastic deformation of polymers seems vital to obtain materials which would fulfill the desired, demanding requirements.

In the simplest kind of deformation, tensile drawing, deformation of most crystalline materials is accompanied by formation of cavities, which manifests itself by strong whitening of the material. For years cavitation was regarded as an artifact accompanying deformation of selected materials, having no considerable influence on the course of material deformation. It is the research conducted at the Centre of Molecular and Macromolecular Studies of Polish Academy of Sciences which allowed to understand better many aspects connected with formation of discontinuities in the material and demonstrate that cavitation is actually an important, unignorable phenomenon, which nevertheless frequently masks true mechanisms of deformation. Even though a number of factors influencing the intensity of cavitation are known, such as thickness and orientation of crystals, molecular weight of a polymer, deformation rate and temperature or thickness of interlamellar regions, the nature of nuclei initiating cavitation in polymer materials during their deformation as well as the influence of the physical parameters of amorphous phase on the phenomenon are still not known.

In water cavitation is nucleated by solid, hydrophobic impurities, whose cavities are filled with air. Also during crystallization of polymers from the molten state cavitation is supported by the presence of additives, whose surfaces exhibit weak adhesion to a melt. In both cases cavitation exhibits properties of a heterogenously nucleated process. One of the prime objectives of the paper was to examine the nature of the nucleation of cavities generated during deformation of a polymer. It seems that substances present in polymers, such as stabilizers or low molecular weight fractions (oligomers) can significantly influence the intensity of the cavitation process. In order to determine the role of the mentioned additives in nucleation of cavitation, the material has been subjected to purification and the influence of the mentioned “impurities” on initiation and intensity of the cavitation

process has been examined. The conducted studies should enable to determine if nucleation of cavitation during deformation of polymers takes place in a similar, heterogenous manner as in the case of liquids of low molecular weight or it has a homogeneous character.

Few papers concerning cavities formed in materials under the influence of the applied stress focused on the role of amorphous phase in initiation, growth and reorganization of voids on the subsequent stages of deformation. Thus, complex research aimed at determining the role of amorphous phase in formation of discontinuities during deformation of a number of crystalline polymers has been planned. It is another objective of the dissertation to study the influence of the physical parameters of amorphous phase on the phenomenon of cavitation.

The obtained results will allow to understand better the mechanism of cavity formation during deformation of crystalline polymers and thus enable better control of the phenomenon, e.g. elimination of cavitation where it is undesired.

4. Experimental section

4.1. Materials

Studies presented in the paper have been conducted for a number of crystalline polymers, whose deformation was accompanied by cavitation. The materials used are presented and characterized below:

Polypropylene (1), Novolen 1100H (PP1) (M_w=400kg/mol, M_n=80kg/mol, M_w/M_n=5; manufacturer data), of melt flow index MFI=1.8g/10min (for 230^{o}C, 2.16kg according to ISO 1133), density 0.91 g/cm^3, by BASF.

Polypropylene (2), Borclean HB300BF (PP2) (M_w=608kg/mol, M_n=72kg/mol, M_w/M_n=8.44; manufacturer data), of melt flow index MFI=2.5g/10min (for 230^{o}C, 2.16kg according to ISO 1133), by Borealis.

High density polyethylene, Lupolen 6021D (HDPE) (M_w=182kg/mol, M_n=25kg/mol, M_w/M_n=7.2; manufacturer data), of melt flow index MFI=2.6g/10min (for 190^{o}C, 2.16kg according to ISO 1133), by BASF.

Polyamide 6, Polycaprolactam (PA6) (M_w=35kg/mol; manufacturer data), of relative viscosity 4.1, by Polysciences, Inc.

4.2. Purification

The process of polypropylene (PP1) purification has been performed using the following methods:

- purification using supercritical CO_2 extraction. Extraction was run for 13 hours at the temperature of 60^{o}C under pressure of 200 bar. Very slow decompression of the system was applied to enable slow removal of CO_2 and to avoid changes in the material structure.
- purification using extraction with a non-solvent mixture (hexane, chloroform, ethanol 4/1/1 vol.) in Soxhlet apparatus. Components of the mixture are non-solvents of crystalline phase, however they can permeate into the amorphous regions of polyolefins. Extraction process was run for at least 72 hours. After completion of extraction, the purified material was taken out of the non-solvent mixture and placed in a vacuum drier at the temperature of 50^{o}C in order to remove non-solvents. The non-

solvent mixture, after extraction, was evaporated on a vacuum evaporator, so as to perform quality and quantity assessment of substances extracted from the material.

4.3. Apparatus

Results presented further in the paper were obtained on the basis of a number of research methods and techniques. Measuring equipment used to characterize materials which are the subject of the paper included a testing machine, scanning electron microscope (SEM), small- (SAXS) and wide-angle (WAXS) X-ray diffractometer, differential scanning calorimeter (DSC), dynamic mechanical thermal analyzer (DMTA).

4.3.1. Instruments for plastic deformation tests

Mechanical properties of the materials examined in the paper were assessed using a testing machine (Instron 5582) of load range 0-100kN. Shape of samples was according to ISO 527-2 standard, with 1 mm thickness and 4mm width. The gauge length was 25mm. Tests were performed at room temperature at a standard rate $3{,}3\times10^{-3}s^{-1}$. For selected experiments deformation rates of $6{,}7\times10^{-4}s^{-1}$, $3.3\times10^{-5}s^{-1}$, $3.3\times10^{-4}s^{-1}$ and $3.3\times10^{-2}s^{-1}$ were used. The actual shape of a sample during deformation was recorded using Nikon D50 digital camera. In order to determine the local strain, markers of sputter coated gold located along the entire gauge length at a distance of 1mm form one another, were being placed on surfaces of the samples using an ion sputter coater and a mask obtained with the use of photolithography. Similar measuring technique was used in the papers [1-3]. Local strain was calculated as a change in distance between the markers according to a relation: $(l-l_0)/l_0$, where l_0 is a distance between markers for the undeformed sample and l is a distance between markers for the deformed sample. Volume strain for local strains was determined using the following relation: $V\text{-}V_0/V_0$, where V_0 denotes volume of the undeformed sample. To do so, a small mirror was set up during photographic register of deformation, which directed an image of the sample's thickness to a digital camera. The volume of the sample between markers was determined on the basis of a distance between markers and the thickness of the photographed sample.

Deformation of samples during small-angle synchrotron radiation scattering studies was performed on a specially designed testing machine which enabled tension of samples with a simultaneous register of SAXS scattering patterns (Fig. 21). Symmetrically stretched samples were monitored with the use of a camera, which enabled precise calculation of local strain of the sample on the basis of change in distance between the markers. Tests were performed at room temperature at a standard rate $3.3\times10^{-3}s^{-1}$. For selected experiments deformation rate of $6.7\times10^{-4}s^{-1}$ was used. Deformation was conducted for 6s and next a scattering pattern for a given strain (calculated on the basis of images obtained with a photographic camera, with no tension) was registered. The entire procedure was cyclically repeated up to rupture of the sample.

Fig. 21. Measuring system enabling tensile drawing of samples with simultaneous register of small-angle X-ray scattering patterns (synchrotron, Hasylab, Hamburg, Germany).

4.3.2. Differential Scanning Calorimetry (DSC)

Thermal analysis of the examined materials was conducted using an indium-calibrated DSC apparatus (TA 2920, Thermal Analysis). Samples of total mass of 6-8 mg, were being placed in

aluminum pans and pressed slightly in order to ensure good contact with the DSC cell surface. The data was registered during heating at a constant rate of 10°/min, under nitrogen flow.

The degree of crystallinity of the studied samples was determined according to a formula:

$$X_C = \frac{\Delta H_m}{\Delta H_m^0}$$

where: ΔH_m - is the measured specific heat of melting, ΔH^0_m – is the heat of fusion of the crystal. For polypropylene the value of ΔH^0_m=209J/g has been assumed [4].

4.3.3. Positron Annihilation Lifetime Spectroscopy (PALS)

Positron lifetime spectra measurements were performed using ORTEC „fast-fast" spectrometer [5], equipment of The Section of Application of Nuclear Physics, Institute of Experimental Physics, University of Wroclaw. The resolution of the spectrometer was found to be 270 ps.

In this method positrons emitted by the radioactive source (in this case ^{22}Na) penetrate into two samples surrounding the source, which annihilate after thermalization. In the case of polymers, some positrons create a positronium (hydrogen-like bound state of an electron and a positron) in the free volume regions. A mean lifetime of a triplet positronium (ortho-positronium) is related to the size of the free volume regions in which the atoms of ortho-positronium annihilate. Reconstruction of distribution of positronium lifetimes, on the basis of the measured lifetime spectrum and determination of shape of the free volume regions, enables to determine radius or volume distribution of these areas.

Positron lifetime spectra measurements were performed in air at room temperature. Measurement time for one spectrum was 20min., which corresponds to a total of approx. 1x10^6 counts under the measured spectrum. LIFETIME software was used for the analysis [6].

4.3.4. Infrared thermogrpahy

ThermoVision A320 camera from Flir Systems AB, of resolution 320×240 and thermal sensitivity of 0.08^{o}C with autofocus, in compliance with a software, was used. The software enabled constant monitoring of the temperature distribution in the selected regions of the deformed samples.

4.3.5. Density measurement

To measure the density of the samples a gradient column with a vertical linear liquid density gradient (a mixture of ethanol and water) was used. The gradient column was calibrated with beads**,** whose density in temperature was determined to an accuracy of 0.0001g/cm^3.

4.3.6. Scanning Electron Microscopy (SEM)

The bulk morphology of the samples prior to deformation and samples deformed to selected strains was studied using a scanning electron microscope (SEM, Jeol JSM 5500LV). The internal part of a sample was exposed by cutting with an ultramicrotome (Power Tome XL, Boeckeler Instruments, Inc.) equipped with a diamond knife (Diatome Ltd.). The exposed surfaces were etched for 2 hours at room temperature in a solution composed of $KMnO_4$ (0,7 wt%) dissolved in a mixture of concentrated sulphuric acid, orthophosphoric acid and distilled water in the volume ratio 5/4/1, in accordance with the procedure proposed by Basset [7]. To improve etching, the mixture was placed in an ultrasonic bath running periodically for short time periods during the etching process (for approx. 2 min. every 20min.). After completion of etching, the samples were immersed into four tubes in the following order: with diluted suphuric acid (suphuric acid/water 2/7 vol), perhydrol, distilled water and acetone. Washing was run in the presence of ultrasounds, so as to ensure more efficient transport from/to the surface of impurities/liquids. Dried sample was coated with a fine gold layer (about 20nm) by ion-sputtering (JEOL JFC-1200) and examined with a scanning electron microscope JEOL JSM-5500 LV. Microphotographs were registered in a high vacuum mode at the accelerating voltage of 10kV. Microscopic image was created using secondary electron detector (SEI).

4.3.7. Dynamic Mechanical Analysis (DMTA)

Dynamic mechanical measurements were conducted using DMTA MkIII apparatus (Rheometric Scientific Inc.) in a single cantilever bending mode, at the frequency of 1Hz and the heating rate of 2^o/min, in the temperature range from -100^{o}C to 100^{o}C for polypropylene, from -140^{o}C to 100^{o}C for polyethylene, from –140^{o}C to 200^{o}C for polyamide 6. Samples used for measurements (dimensions 25x10x1mm) had been cut out from non-isothermally crystallized films in the conditions analogous to those used while preparing materials for mechanical and X-ray studies.

4.3.8. Nuclear Magnetic Resonance (NMR)

^{13}C NMR spectra in a liquid phase (deutered chloroform as a solvent) were recorded using Bruker AV 200 apparatus operating at the frequency of 50,33MHz. Chemical shifts of signals given in parts per million (ppm) were measured relative to chloroform (^{13}C 77.00).

4.3.9. Wide-angle X-ray Scattering (WAXS)

Analysis of the crystalline structure of the materials and assessment of the degree of their crystallinity was performed using wide-angle X-ray scattering measurements by means of computer controlled goniometer associated coupled to a sealed-tube source of CuKa radiation (Philips), operating at 50 kV and 30 mA. The Cu Kα line was filtered using electronic filtering and the usual thin Ni filter.

The degree of crystallinity was calculated on the basis of diffractograms registered at a step $2\theta=0.05^{o}$ by means of sufficiently thin diaphragms. Since reflections from the crystalline phase and the amorphous halo frequently overlap each other, it was necessary to separate them. Analysis of diffraction profiles of the examined samples and separation of peaks was performed using WAXSFit software designed by M. Rabiej of the University of Bielsko-Biała (AHT) [8]. The software allows to approximate the shape of the peaks with a linear combination of Gauss and Lorentz or Gauss and Cauchy functions and adjusts their settings and magnitudes to the experimental curve with a “genetic” minimizing algorithm. Such calculated surfaces of peaks, corresponding to given crystallographic planes, and amorphous halo allowed to determine the degree of crystallinity of the sample.

The wide-angle X-ray scattering (WAXS) photo camera was used for observations of lamellae orientation. A source of Cu Kα radiation, operating at 50kV and 35mA, was used. Two-dimensional scattered patterns were recorded by camera equipped with a Kodak imaging plate. The distance between a sample and recording plate was 5cm. Exposure time was approx. 10min. Exposed imaging plates were analyzed with PhosporImager SI system (Molecular Dynamics).

4.3.10. Small-angle X-ray Scattering (SAXS)

The small-angle X-ray scattering technique was used for detection of cavities and for determination of long period. The 0.5 m long Kiessig-type camera was equipped with a tapered capillary collimator combined with additional pinholes (300 μm in diameter) forming the beam, and an

imaging plates as a detector and recording medium (Kodak). The camera was coupled to a X-ray source (sealed-tube, fine point Cu Kα filtered radiation, operating at 50 kV and 40 mA; Philips). The time of collection of the pattern was usually around 3 h. Exposed imaging plates were read with Phosphor Imager SI scanner and ImageQuant software (Molecular Dynamics).

In situ studies with the use of synchrotron radiation, λ=0.1542nm, were performed at A2 beamline in Hasylab (Hamburg, Germany). Two-dimensional scattering patterns were registered with the use of MarCCD 165 detector (Mar Research, Norderstedt, Niemcy) of resolution 2048×2048 pixels. The distance between the sample and the detector was 2513mm. Exposure time was 12s for polyethylene and polypropylene and 30s for polyamide 6.

Long periods were determined from one dimensional sections of 2-D pattern. Background and Lorentz corrections were applied to the curves. Long period was then calculated from position of the maximum of corrected curves using the Bragg law.

5. Results and discussion.

5.1. Modification of the amorphous phase of polypropylene. Purification.

The presence of impurities, both in liquids of low molecular weight and in a melt of the crystallizing material, encourages formation of cavitation bubbles. Stabilizers present in the material (added by manufacturers to improve thermal parameters and material processing) and low molecular weight fractions – oligomers (result of an imperfect process of synthesis) can act as impurities, that is substances that affect the intensity of the cavitation process. The above mentioned substances do not co-crystallize with a polymer and are preferentially located in the amorphous phase of the material. In order to assess their impact on cavitation accompanying tensile drawing, commercial polypropylene (PP1) was subjected to purification using supercritical CO_2 extraction and extraction with a non-solvent mixture (hexane, chloroform, ethanol 4/1/1 volume) in Soxhlet apparatus. Both methods of purification of the amorphous phase led to very similar results, hence only results obtained for the material purified using extraction with the non-solvent mixture will be presented further in the chapter. This type of extraction is used in research on thermal and thermooxidative degradation and stability of polyolefin materials [9, 10] as it does not cause any changes to crystalline phase. The samples in the form appropriate for mechanical and X-ray studies, were cut out from a film, 1mm thick, prepared by compression molding at the temperature of 220^{o}C,

In order to test the efficiency of the applied purification method, an oily liquid extracted from the material (extraction process was run for at least 72 hours, oily residue constituted 0.5-0.9% weight) has been analysed. Fig. 22 presents a ^{13}C spectrum of nuclear magnetic resonance performed for the extracted substance, dissolved in deutereted chloroform. The presented spectrum allowed to identify carbon atoms (marked in the figure) forming a molecule of the material acting as a stabilizer (pentaerythritol tetrakis(3-(3,5-di-tert-butyl-4-hydroxyphenyl)propionate), Irganox 1010) and molecules of propylene oligomers of various size and architecture. Therefore, the applied method allowed to remove molecules of the stabilizer and low molecular weight fractions from the examined material, substances whose presence should influence the intensity of cavitation process.

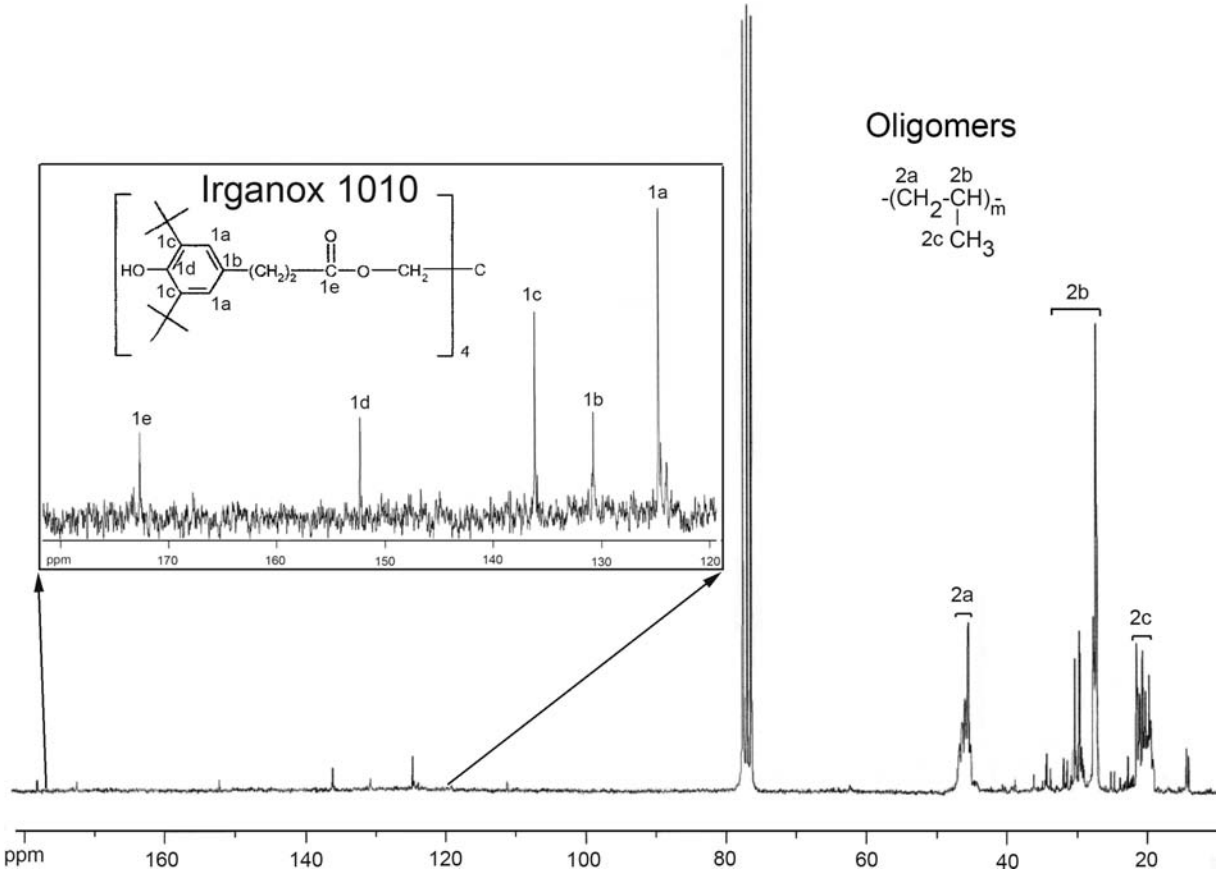

Fig. 22. ^{13}C NMR spectrum of a substance extracted from the examined polypropylene.

In order to assess the influence of the extracted substances (impurities) on cavitation during tensile drawing, purification process should not influence parameters of the crystalline phase of the material.

Hence, using X-ray techniques and differential scanning calorimetry, selected parameters of the crystalline phase of the examined material prior to and after extraction were determined. Once the extraction process has been completed, the samples were being dried at the temperature of 50^{o}C in order to remove the residues of non-solvents. Samples of the reference material were subjected to analogous procedure. Table 1 presents selected parameters of the crystalline phase determined for samples prior to and after the purification process.

Sample	Long period [nm]	Crystallinity degree [%] (DSC)	Crystallinity degree [%] (WAXS)
Reference (RS)	13.3	47.8	46.3
Purified (PS)	13.6	48.0	46.6

Table 1. Parameters of crystalline phase of polypropylene samples prior to and after the purification process.

The presented data indicate lack of substantial changes in the crystalline structure of the material as a result of the extraction process. Therefore, the applied method of material purification allows to obtain a desired effect without markedly influencing other parameters of the material.

In order to assess the influence of the extraction process on parameters of amorphous phase of the material (size of the free volume of amorphous phase) positron-lifetime measurements were performed. The choice of the model for spectra analysis is extremely important. Results presented further in the paper correspond to the model of spectra analysis, which assumes:

- the intensity ratio of anihilating para- and ortho-positronium of 1:3,
- lifetime of annihilating para-positronium, τ_1, of 125 ps,
- the presence of distribution of mean lifetimes corresponding to free annihilation of positrons and annihilation of ortho-positrons by “pick off”. In the analyzed spectrum this corresponds to components of mean values $<\tau_2>$ and $<\tau_3>$, of mean lifetimes τ_2 and τ_3. Distribution of mean lifetimes τ_2 and τ_3 are characterized by dispersion values σ_2 and σ_3. The results of the obtained spectra are presented in Table 2.

Sample	Mean lifetime			σ_2 [ps]	σ_3 [ns]	Component intensity	
	τ_1[ps]	$<\tau_2>$ [ps]	$<\tau_3>$ [ns]			I_1+I_3 [%]	I_2 [%]
Reference sample (RS)	125	357.4±1.6	2.37±0.07	1.9±0.6	0.95±0.09	22.2±0.4	77.8±0.4
Purified sample (PS)	125	371.9±1.2	2.57±0.02	2.2±0.4	0.83±0.04	19.7±0.1	80.3±0.1

Table 2. Results of positron lifetime spectra analysis.

A simple quantum-mechanical model allows to relate a mean lifetime τ_3 with the size of the free volume region. In analysis of the results, as in the case of a model proposed by Tao and Eldrup [11, 12], spherical shape of these regions has been assumed. Basing on the distribution of τ_3 values, volume distributions of the free volume regions, V, were determined as presented in Fig.23.

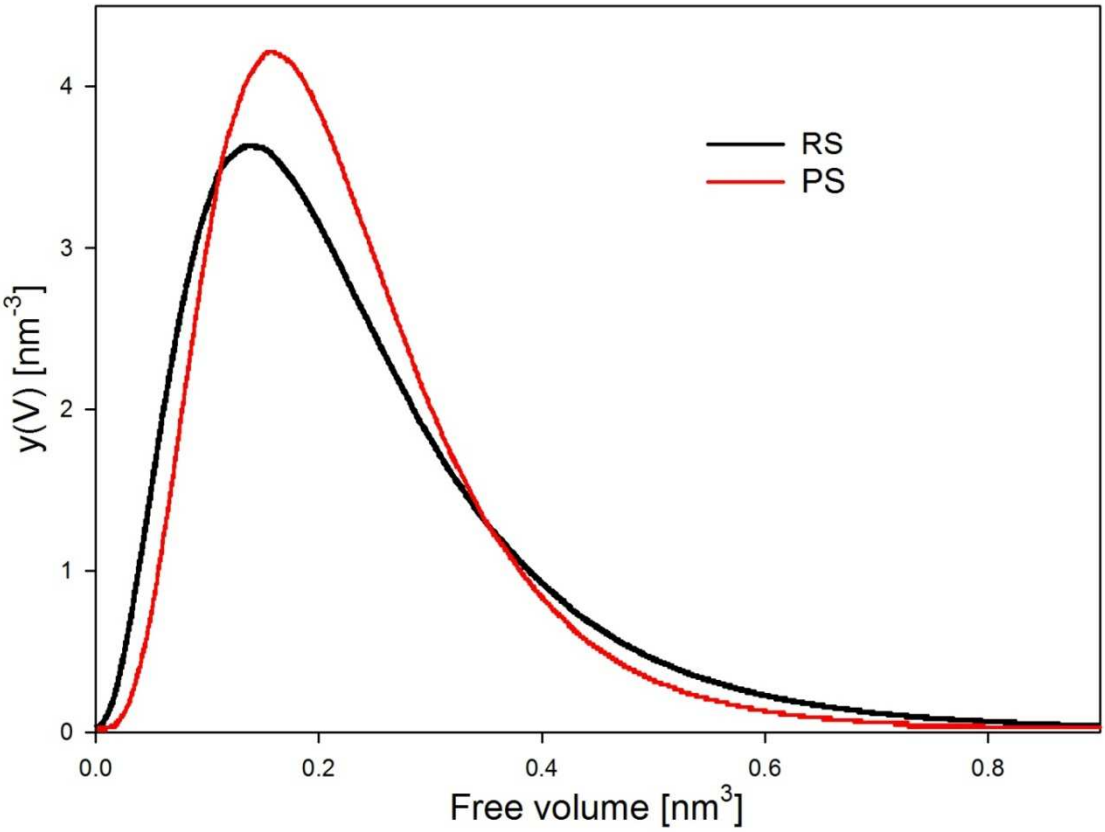

Fig. 23. Size distribution of free volume of the amorphous phase of reference (RS) and purified polypropylene (PS).

Analysis of the presented data clearly indicates an increase in the mean size of the free volume regions in the purified material. Removal, as a result of extraction, of stabilizers and low-molecular weight fractions filling the amorphous part of the material leads to changes in the interlamellar regions, which results in the size increase of empty spaces constituting an integral part of the unordered phase.

In order to assess the influence of the purification process of the material on the phenomenon of cavitation accompanying tensile drawing, *in situ* small-angle X-ray scattering studies using synchrotron radiation were performed. X-ray scattering is much stronger from cavities than from the structural elements of the material due to difference in electron density. SAXS method is therefore a very useful tool for examination of cavitation process in the material. Fig. 24 presents SAXS scattering patterns registered for reference and purified polypropylene deformed at a rate $3.3\times10^{-3}s^{-1}$, up to the local strain of 4.5.

In the case of reference sample (RS) signals indicating formation of cavities in the material, on SAXS scattering patterns, are already observed at the local strain equal to 0.13. The obtained scattering pattern indicates that cavities at this stage of deformation are of ellipsoidal shape and are oriented by their long axis perpendicularly to direction of deformation (signal in the meridional region on a scattering image). Specific arrangement and shape of cavities is forced by the lamellar structure

of the material. On further deformation stages an increase in the intensity of the registered signal is observed in the aforementioned region of a scattering pattern, up to the strain of 0.8. At this stage of deformation a signal in the equatorial region of a scattering pattern is also registered, which indicates the presence of the second population of cavities oriented parallel to the direction of the applied force. Signal appearing in this region of scattering pattern at the cost of intensity in the equatorial region demonstrates that subsequent plastic deformation mechanisms of the material (lamellar fragmentation) activated at this stage of deformation also force reorganization of shape of cavities. Further stages of deformation (>0.8) are accompanied by a substantial decrease in size of cavitation pores perpendicularly to the direction of deformation and their strong orientation towards the direction of deformation. For a local strain equal to 4.5 one observes a decrease in the intensity of signal

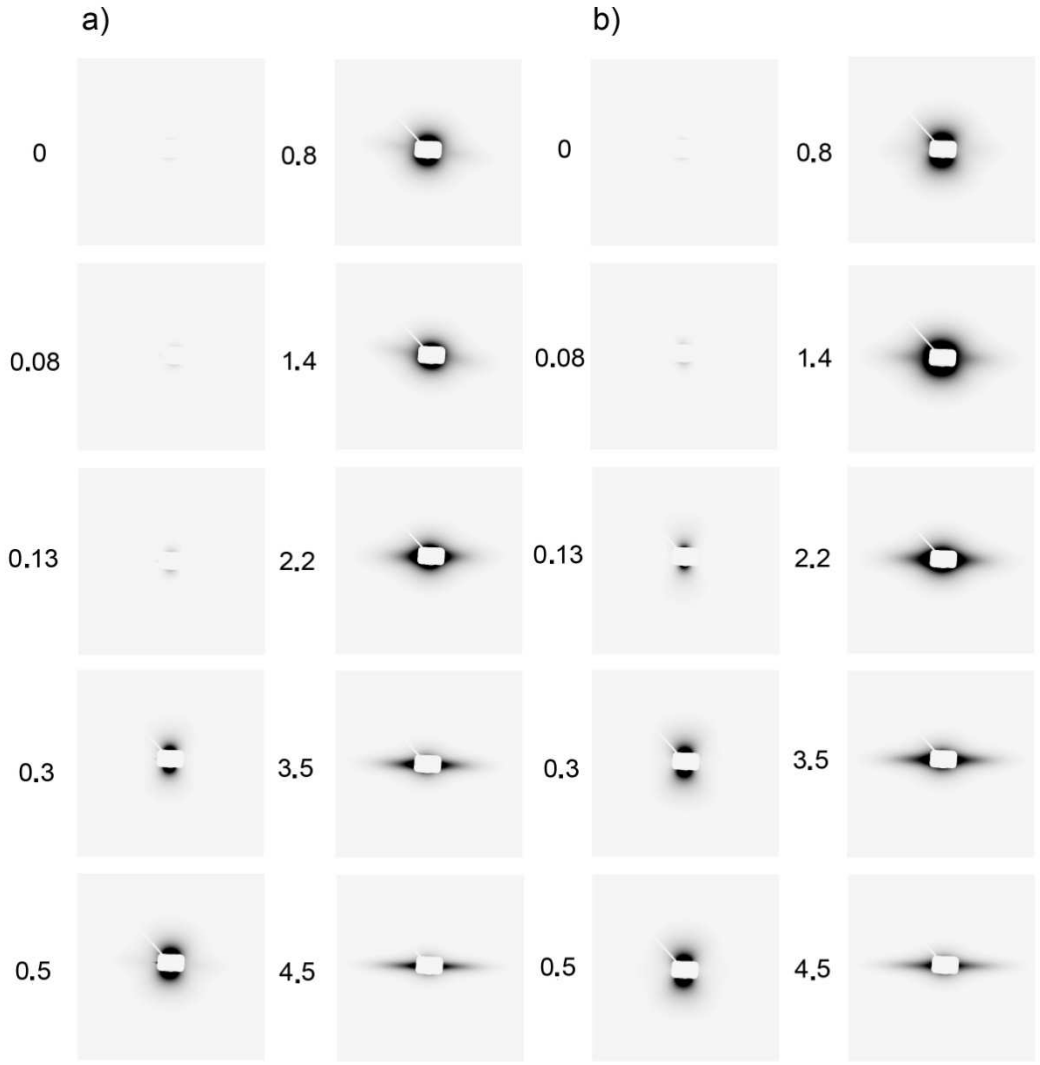

Fig. 24. Small-angle X-ray scattering patterns of a series of polypropylene samples: a) RS; b) PS. Figures correspond to local strain of samples. Deformation rate – $3.3\times10^{-3}s^{-1}$. Direction of deformation – vertical.

coming from cavities. The reason of this effect is that cavities enlarge with deformation and finally most of them scatter x-ray outside of SAXS detection limit.

Deformation of the purified samples is also accompanied by cavitation. It proceeds almost identically as in the case of reference material, however, a significant difference concerns the intensity of scattering signals coming from cavities at subsequent stages of deformation. Analysis of the presented scattering patterns indicates that the intensity of the cavitation process has increased in the purified material. Extraction process, which resulted in the removal of substances capable of nucleating cavitation, not only did not decrease the intensity of cavitation, but produced a reverse effect – an increase in the number of cavitation pores formed during deformation of the material.

Analogous conclusions can be drawn while analyzing volume strain measurements performed for the examined material prior to and after the purification process. Figure 25 presents the relevant data.

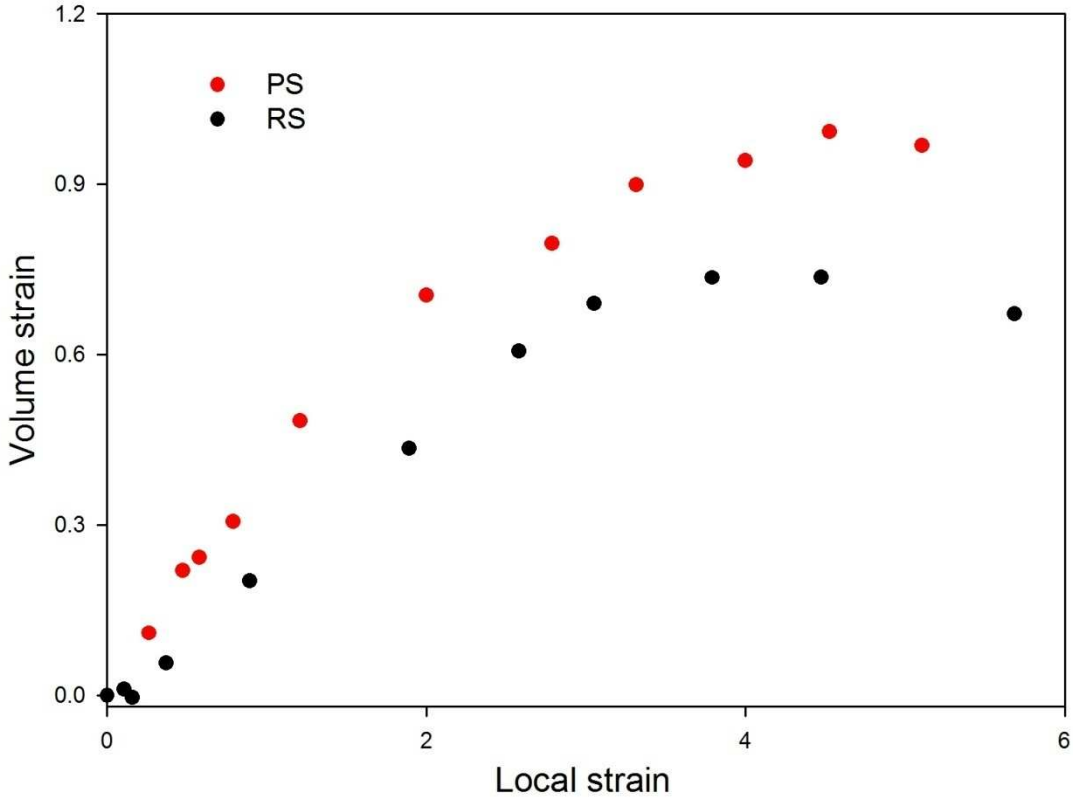

Fig. 25. Volume strain as a function of local strain for reference polypropylene (RS) and purified polypropylene (PS). Deformation rate $3.3\times10^{-3}s^{-1}$.

Deformation of the unmodified polypropylene sample (RS) is accompanied by a strong increase in volume (of around 70%), an effect of discontinuities occurring in the material. The purification process leads to an increase in the intensity of cavitation, whose effect is volume strain

increase, presented in Fig. 25, up to around 95%. Removing stabilizers filling the amorphous phase of the material and low molecular weight fractions results in an increase of approx. 30% in the intensity of cavity formation in the material.

Intensity of cavitation accompanying tensile drawing of crystalline polymers is affected by numerous factors connected with parameters of the material and conditions under which deformation takes place. One of such factors is the deformation rate. Therefore, additional examinations of polypropylene were conducted before and after purification for lower deformation rates ($6.7\times10^{-4}s^{-1}$). Decreasing the deformation rate should decrease the intensity of cavitation in both materials and at the same time intensify the difference between them.

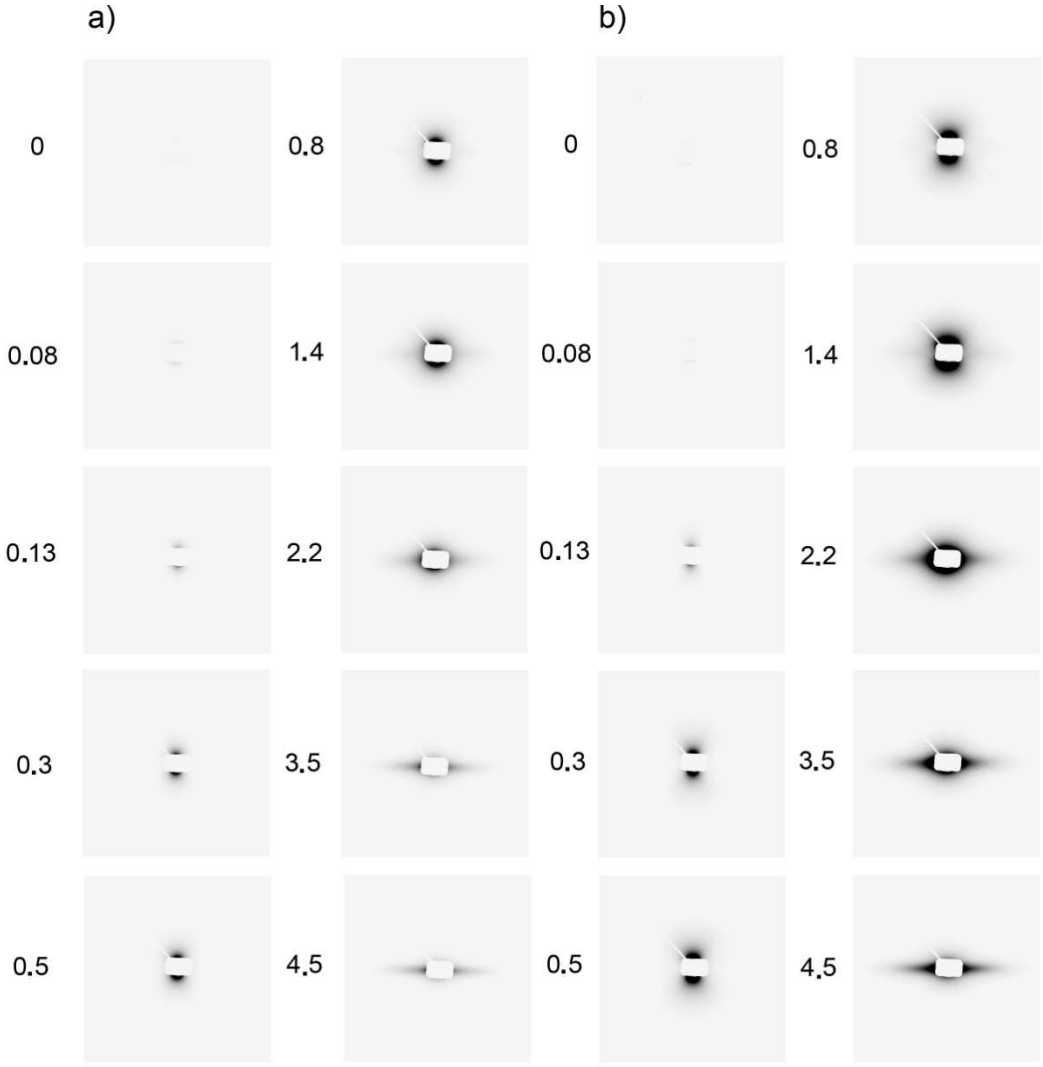

Fig. 26. Small-angle X-ray scattering patterns of a series of polypropylene samples: a) RS; b) PS. Numbers correspond to local strain of samples. Deformation rate $-6.7\times10^{-4}s^{-1}$. Direction of deformation – vertical.

Fig. 26 presents SAXS scattering patterns registered during *in situ* studies using synchrotron radiation for reference and purified polypropylene deformed at a rate of $6.7\times10^{-4}s^{-1}$ up to local strain of 4.5. Deformation of polypropylene samples prior to and after the purification process is accompanied by cavitation, however, the intensity of the phenomenon is significantly higher for materials after extraction of stabilizers and low molecular weight substances. At each stage of deformation of the examined materials one observes a substantial difference in the intensity of the scattering signal between the reference and the purified sample.

Fig. 27 presents volume strain measurements for samples prior to and after the purification process, deformed at a rate of $6.7\times10^{-4}s^{-1}$.

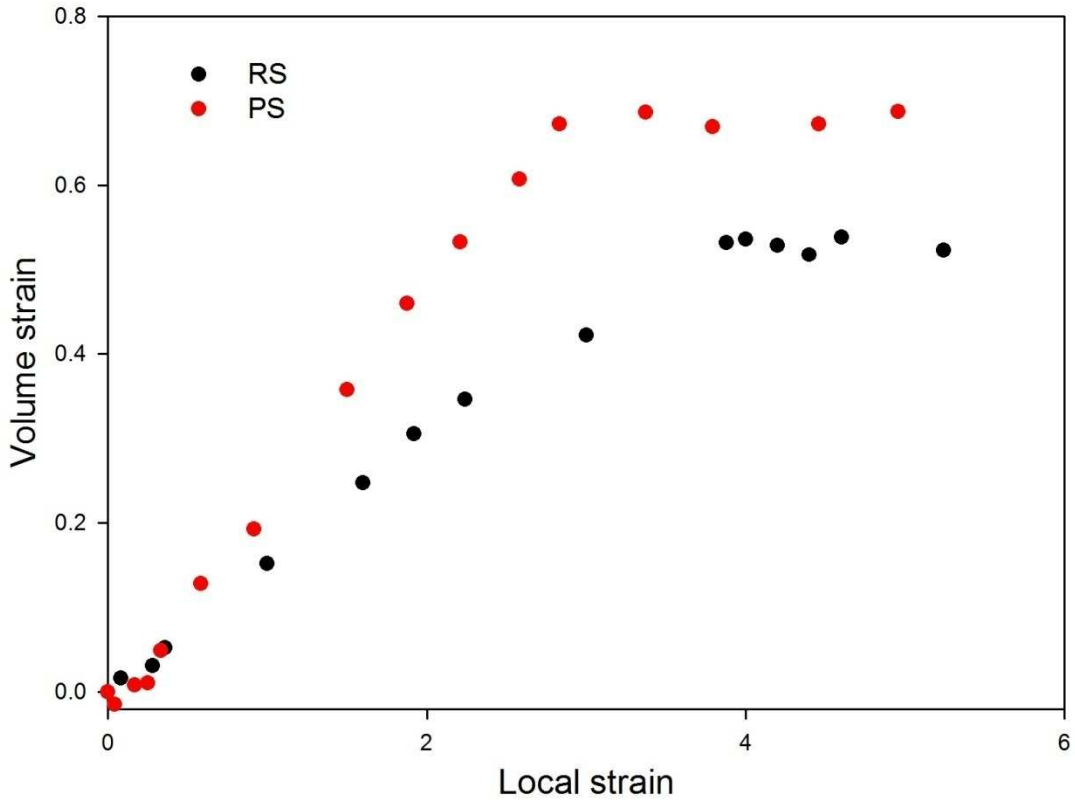

Fig. 27. Volume strain as a function of local strain for reference polypropylene (RS) and purified polypropylene (PS). Deformation rate $6.7\times10^{-4}s^{-1}$.

Tensile drawing of the unmodified polypropylene sample (RS) is accompanied by a substantial volume increase (up to 50%), resulting from cavities generated in the material. Purification of the material increases the intensity of cavitation, whose effect is an increase in volume strain by approx. 70%, presented in the Fig. 27. Extraction leading to removal of impurities from the amorphous phase of the material, i.e. stabilizers and low molecular weight fractions, results in an increase in cavity formation in the material by around 40%. The above presented data indicates that the amorphous

phase of crystalline polymers at temperature above its glass transition temperature differs markedly from low molecular weight analogous liquids. Polymers are not specially purified, opposite they contain various additives such as stabilizers, antioxidants, residue of catalysts, low molecular weight fractions, lubricants, light stabilizers etc. Despite of impurities and additives amorphous phase of crystalline polymers exhibit amazingly high strength in terms of cavitation stress, at the level of 10-20 MPa. It is even more astonishing when considering that all those substances and additives are rejected into amorphous layers during polymer crystallization. Cavitation in polymers seemingly is not of a heterogeneous character, unlike in unpurified low molecular weight liquids. The most probable reasons are: confinements of amorphous layers between crystalline lamellae and macromolecular chain entanglements, the factors that are absent in low molecular weight liquids.

5.2. Modification of the amorphous phase of polypropylene.

The results of the previous chapter unambiguously indicate that nucleation of cavitation is not of heterogeneous character. The other possibility is homogeneous nucleation of cavitation. This likelihood is supported also by unusually high negative pressure necessary for cavitation for several crystalline polymers: polypropylene (-13.7 MPa), poly(methylene oxide) (-35.8 MPa) and polyethylene (-15.1 MPa).

The amorphous phase of polymers is characterized by a more unordered structure than amorphous low molecular weight materials due to steric hindrances introduced by chemical bonds of long chains. Hence, an intrinsic element of polymers' amorphous phase is a fraction of so called "free volume" resulting from its incomplete packing. This results in difference in density between well-packed polymer crystals and amorphous phase. At the temperatures above glass transition amorphous phase exhibits certain dynamics of free volume - "empty" spaces change in time as a result of thermal movements of polymer chains. The presence of "empty" spaces (vapour or gas bubbles) in low molecular weight liquids is conducive to formation of cavities. I suggest that in polymers dynamic "empty" spaces may also initiate nucleation of cavitation. Size of these empty spaces is considerably smaller than the thickness of amorphous layers, though it can increase under the influence of mechanical stress during tensile drawing of a polymer, which is when they may become cavitation nuclei. Therefore, it seems that introducing molecules of a low molecular weight liquid penetrant into interlamellar regions, i.e. amorphous phase, should lead to at least partial filling of

the free volume of amorphous phase and thus decrease in size or significant elimination of the “empty” spaces, which constitute an integral part of the unordered regions. Introducing a low molecular weight liquid into amorphous phase, that is to a region where cavitation is initiated, should result in change in the intensity of the phenomenon.

5.2.1. Modification of the amorphous phase of polypropylene with chloroform.

From 1 mm thick film (PP2), obtained by compression moulding at the temperature of 230^{o}C and cooled between metal plates, samples were cut out for mechanical and X-ray studies. The first batch of samples (soaked sample – SS) has been placed in a vessel containing a penetrant (chloroform) for the period of at least 72 hours in order to obtain full saturation of the amorphous phase of the material with a low molecular weight liquid. The second batch of samples (reference sample - RS) provided reference material.

In order to estimate the amount of chloroform present in the examined material on completion of the conditioning process TGA examination has been conducted in air. Fig. 28 presents the relevant thermogram of weight loss.

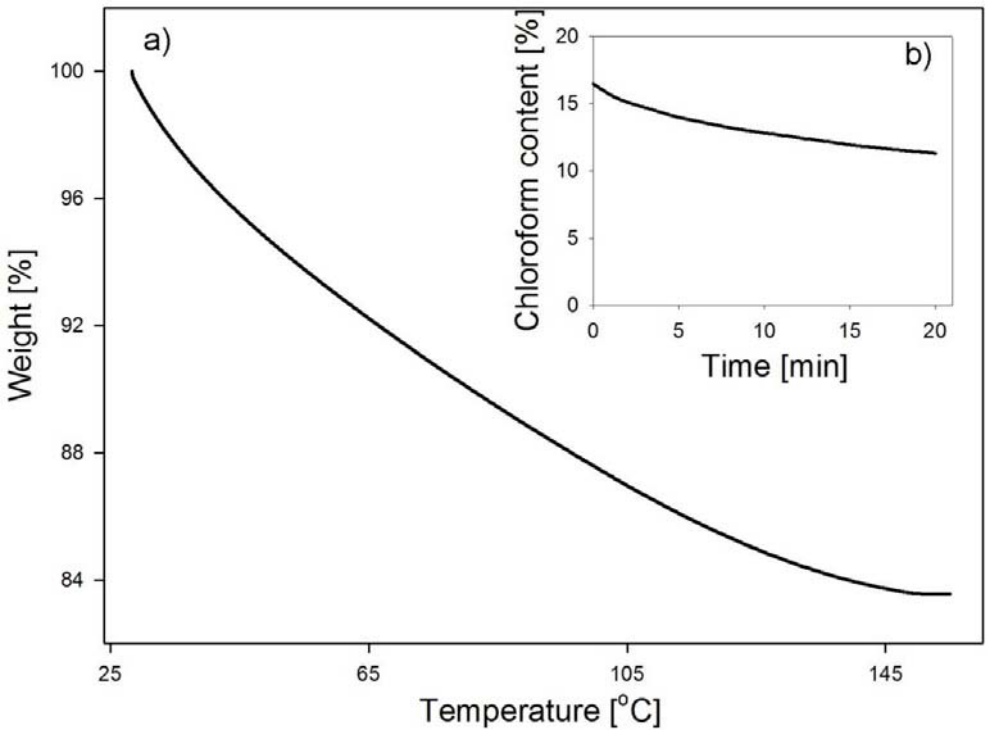

Fig. 28. Chloroform-soaked polypropylene: a) TGA thermogram of weight loss in air; b) kinetics of chloroform desorption for SS sample, after removal from a liquid, under laboratory conditions.

On the basis of the presented thermogram the amount of chloroform has been estimated at 16.5% (wt.) (11.3% vol.) in the analyzed material on completion of the conditioning process. Additionally the above figure (Fig. 28b) presents the kinetics of penetrant desorption at room temperature on extraction of the material from the conditioning vessel. Desorption of penetrant under laboratory conditions was found to be a relatively quick process, therefore all measurements were performed within a minute after removal of the sample from the conditioning vessel.

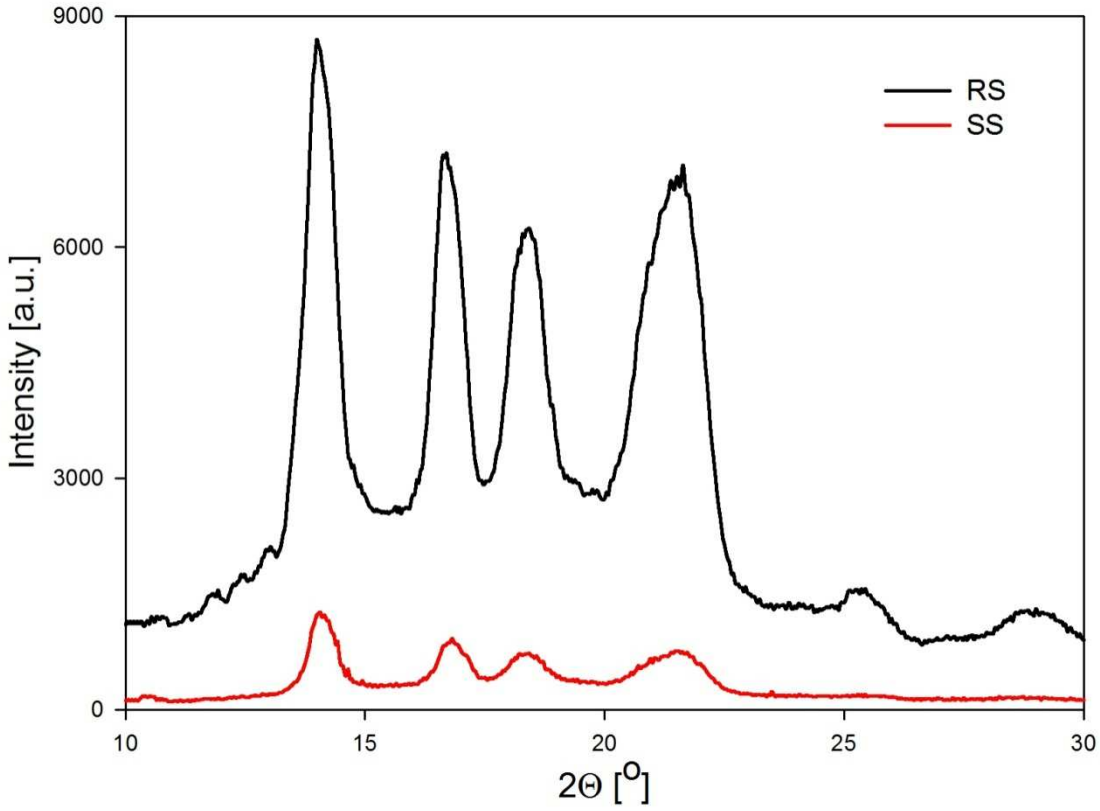

Fig. 29. Diffractograms of polypropylene samples: saturated with chloroform, SS, and reference, RS.

Fig. 29 presents WAXS diffractograms for reference and modified polypropylene. In the case of the SS sample significant reduction in the intensity of peaks is observed, which is the result of the introduction of chlorine atoms strongly absorbing X-ray radiation. It is hard to evidence the change that occurred in the structure of the analyzed material as a result of the introduction of low molecular weight penetrant on the basis of the presented diffractograms. Hence, a WAXS diffractogram was recorded for polypropylene sample prior to the conditioning process (RS) and for the material which was initially saturated with chloroform and next deprived of penetrant as a result of the drying process (RS-SS-RS).

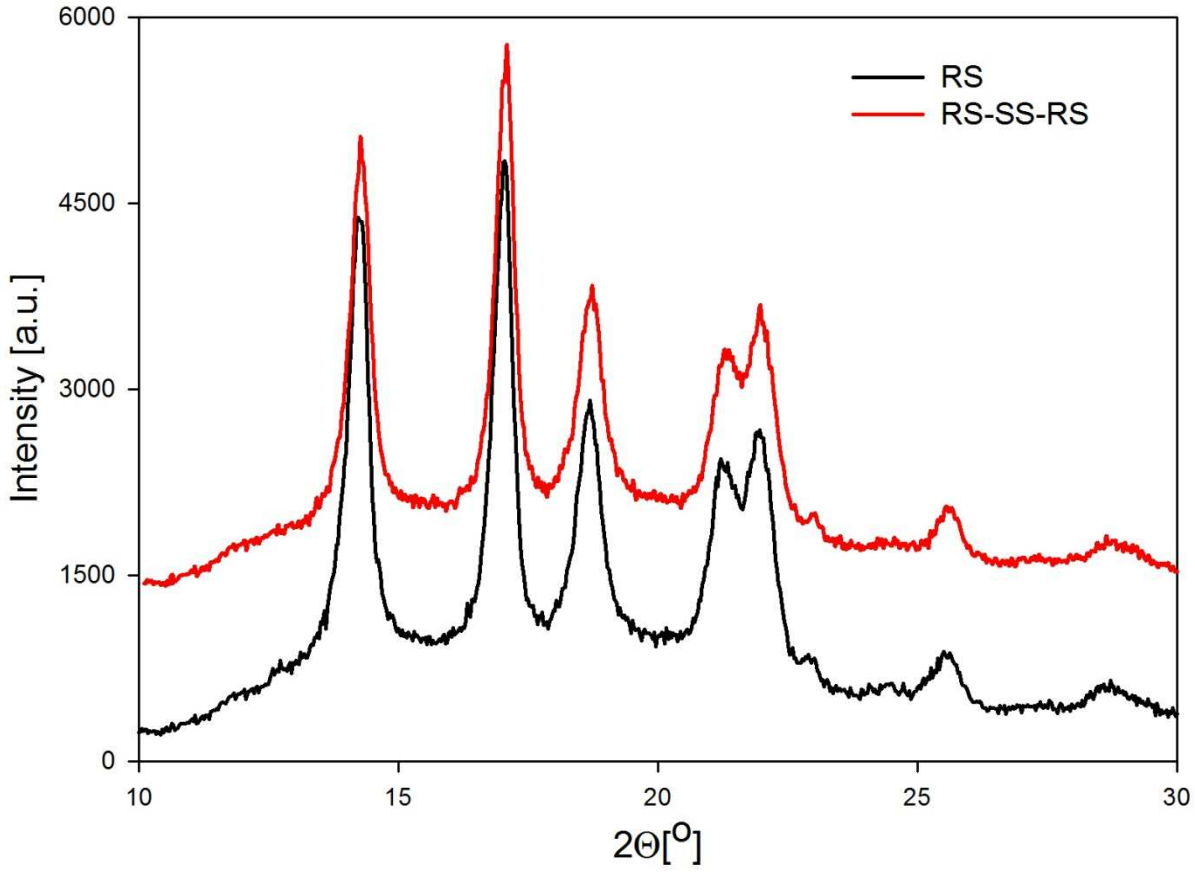

Fig. 30. Diffractograms of RS and RS-SS-RS polypropylene samples. Curves have been shifted along the vertical axis for better visualization.

Wide-angle X-ray scattering measurements presented in Fig. 30 indicate not only complete reversibility of the process of chloroform sorption, but also the lack of significant changes in the crystalline structure of polypropylene as a result of introduction and desorption of the penetrant. The presented results indicate that chloroform sorption occurs mainly in the area of amorphous phase of material and it is mainly there that the molecules of low molecular weight penetrant accumulate.

Fig. 31 presents results of a measurement of a long period as a function of time of sorption of a low molecular weight penetrant (chloroform). Clear changes in the values of a long period in the samples saturated with a low molecular weight penetrant (135.1 Å for reference sample, 163.9 Å for soaked sample), with minor changes in the crystalline regions, indicate an increase in the interlamellar distances as a result of strong swelling (deformation) of unordered regions with molecules of chloroform.

Using dynamic mechanical analysis (DMTA) viscoelastic properties of polypropylene were determined and the influence of the presence of penetrant on such material parameters as storage modulus (E'), loss modulus (E") and loss tangent (tg α) was described. Fig. 32 presents relations between the said parameters and temperature.

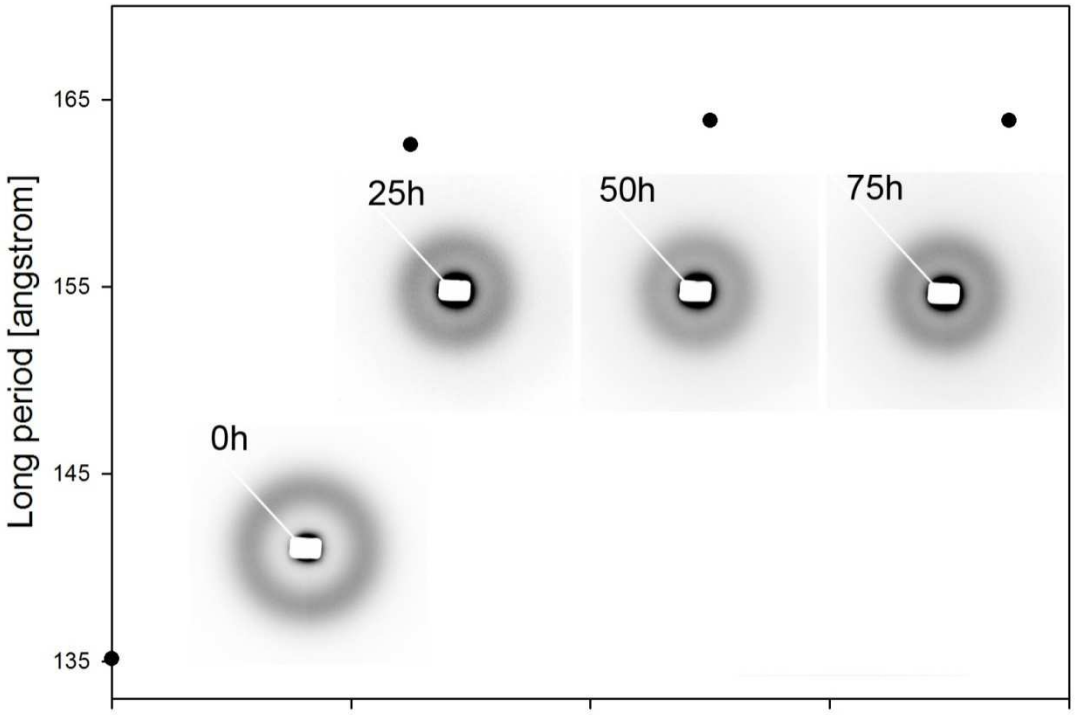

Fig. 31. Change in a long period of polypropylene as a function of time of sorption of chloroform.

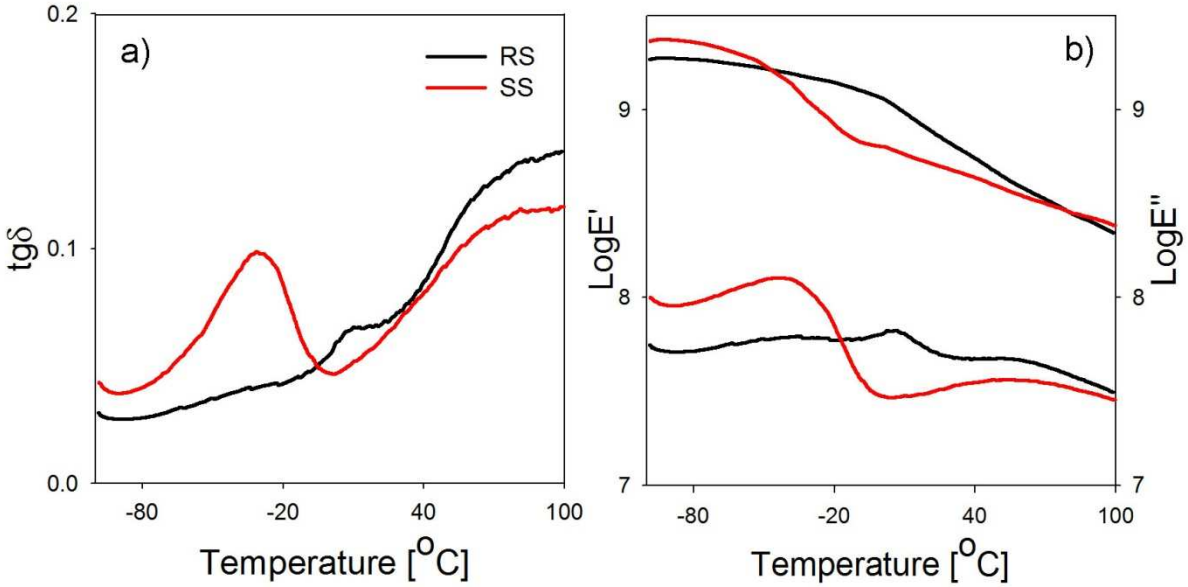

Fig. 32. Relations between loss tangent (a), storage modulus and loss modulus (b) and temperature of polypropylene samples determined by means of dynamic mechanical analysis (DMTA).

While analyzing the curves (presented in Fig. 32) of dependence of the said parameters on temperature, one can distinguish three relaxation transitions typical of unmodified polypropylene (RS sample): γ (approx. –40^{o}C), β (7^{o}C) (corresponding to processes taking place within the amorphous phase of material) and α (approx. 50^{o}C) (effect of complex changes occurring both in crystals and unordered regions). The introduction of chloroform molecules (SS sample) leads to significant decrease in glass transition temperature, which results in the shift of the maximum of relaxation process β towards lower temperatures, by 49^{o}C (to -42^{o}C). The presence of penetrant molecules in the low temperature range, below glass transition temperature, leads to the "stiffening" of material, which is manifested by a higher modulus of the soaked material recorded in this region (Fig. 32b). In the temperature range from -46^{o}C to 80^{o}C the modified material is characterized by a much lower modulus than the reference material. It is the result of strong plasticization of the amorphous material, below its glass transition temperature, due to the introduction of a low molecular weight penetrant. At the temperature of 80^{o}C the values of moduli of both materials become equal, which is the result of desorption of the modifier.

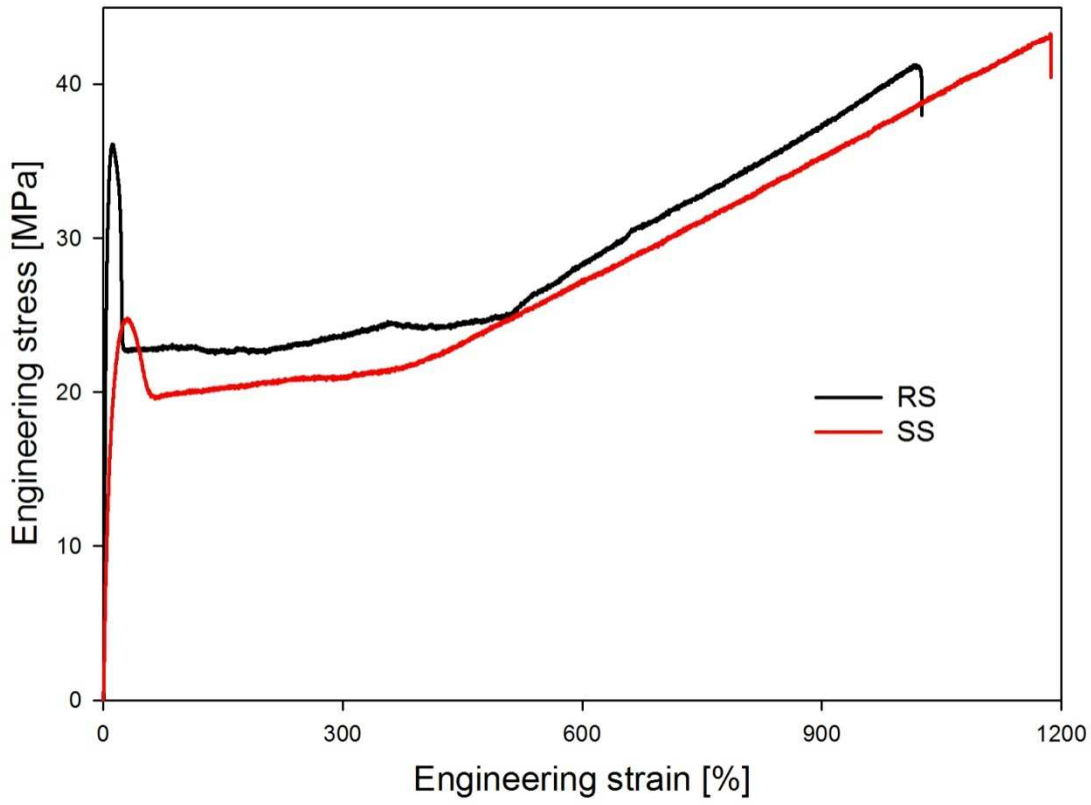

Fig. 33. Engineering strain - engineering stress curves for samples of unmodified polypropylene and saturated with chloroform. Deformation rate – $3.3\times10^{-3}s^{-1}$.

Fig. 33 presents engineering strain – engineering stress curves for polypropylene samples subjected to tensile drawing up to fracture. Deformation of both unmodified and chloroform-soaked polypropylene was accompanied by the necking process. Deformation of unmodified polypropylene within the region of macroscopic yield point was accompanied by intense whitening of the material, which is the evidence of intense cavitation. At the same time the sample, whose amorphous phase had been filled with chloroform molecules remained transparent up to rupture without evidencing cavitation. The analysis of curves presented in Fig. 33 indicates, moreover, strong dependence of stress at yield point on the presence of a penetrant filling the amorphous phase of material. The determined values are, respectively: 36.1 MPa for RS sample and 24.1 MPa for SS sample. The introduction of penetrant molecules therefore leads to decrease in stress at yield point of the material by 12 MPa. The parameters of the crystalline phase of soaked sample, as proved by X-ray examinations, remain unchanged as a result of chloroform sorption. The observed difference in stress at yield point between the reference and modified sample must be therefore the result of changes taking place in the unordered regions of the material. Therefore, I planned and carried out the following experiment: a sample saturated with chloroform, immediately after removal from a conditioning vessel, has been clamped in the apparatus for measuring mechanical properties and stress buildup in the sample as a function of time of desorption of the penetrant has been measured. Figure 34 presents the results of the experiment.

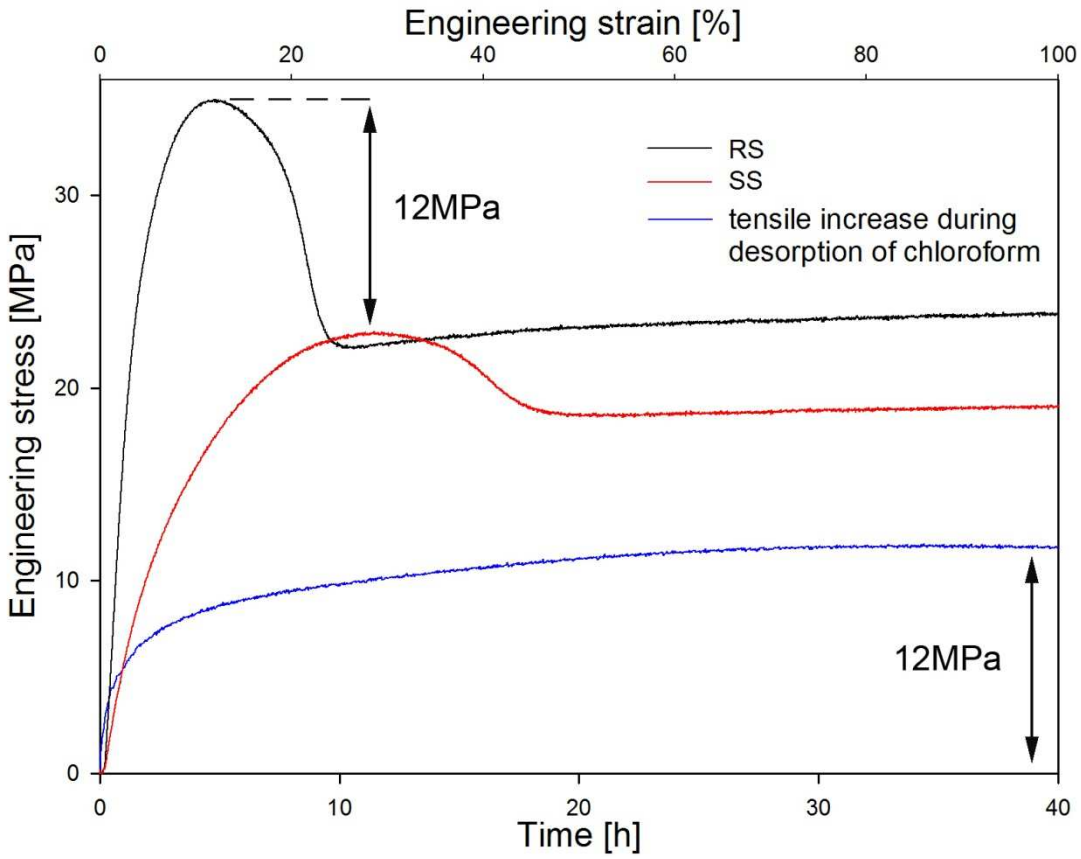

Fig. 34. Engineering strain – engineering stress for reference and chloroform-soaked polypropylene samples. Deformation rate – $3.3\times10^{-3}s^{-1}$. The blue curve shows the stress buildup on clamped swollen PP sample during evaporation of chloroform.

After approximately 40 hours since removal of the sample from the conditioning vessel stress buildup in the sample equal to 12 MPa was noted, which corresponds to the observed difference in stress at yield point between the dry and soaked sample. The introduction of the chloroform molecules leads to strong swelling of the amorphous phase, which results in its significant deformation (no changes in the crystalline structure of the material, change in the values of a long period). Highly swollen, hence deformed amorphous phase impresses the adjacent crystals with the force equal to the value of the observed difference in stress at yield point.

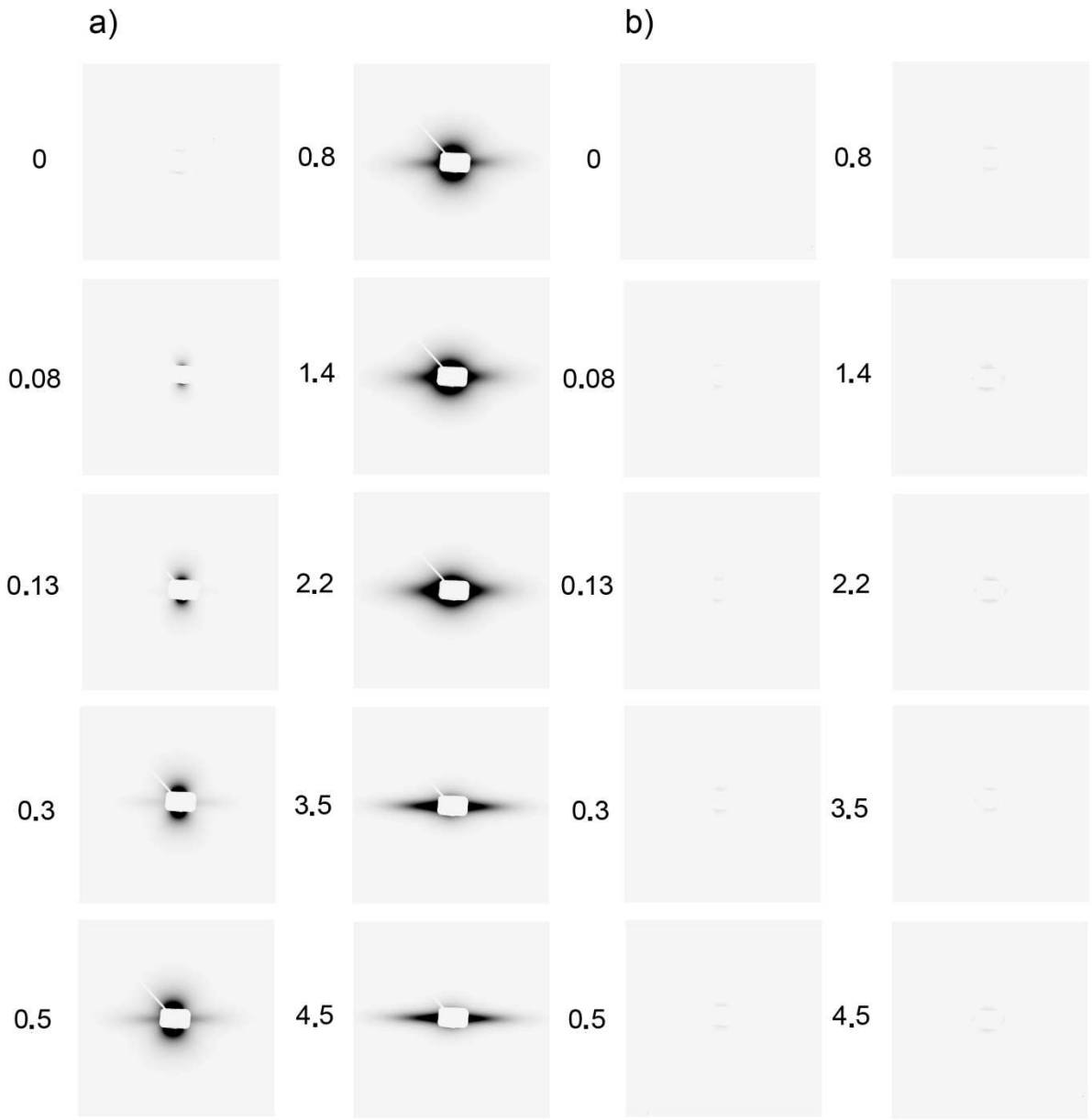

Fig. 35. Small-angle X-ray scattering patterns of a series of polypropylene samples: a) RS; b) SS. Numbers correspond to local strain of samples. Direction of deformation – vertical.

In order to establish the influence of the presence of molecules of a low molecular weight penetrant, within the amorphous phase of the material, on the phenomenon of cavitation accompanying deformation of unmodified material, small-angle X-ray scattering (SAXS) measurements were performed. Scattering patterns presented in Fig. 35 were performed during *in-situ* studies using synchrotron radiation.

In the case of unmodified polypropylene the first signals on SAXS scattering patterns evidencing the presence of cavitation in the material were already observed at the local strain equal to

0.08. The registered signal indicates that cavities at this deformation stage are of ellipsoidal shape, forced by the lamellar structure of the material, and are oriented by their long axis perpendicularly to the direction of deformation (signal in the meridional region on a scattering pattern). At further deformation stages an increase in the intensity of the registered signal is observed in the mentioned scattering pattern up to the local strain of 0.8. Meanwhile, a less intense, markedly thin signal is noted in the equatorial region on a scattering pattern for the deformed sample up to the local strain of 0.3. Such shape of scattering pattern obtained for the deformed material evidences the presence of dilatation gaps occurring during deformation of material. The characteristic feature of such discontinuities is the presence of highly deformed parts of material in the form of fibrils which create a peculiar kind of structure of the dilatation gaps. Openings occurring between the neighbouring fibrils, which are elongated parallel to the direction of deformation, contribute to X-ray scattering in the way presented in

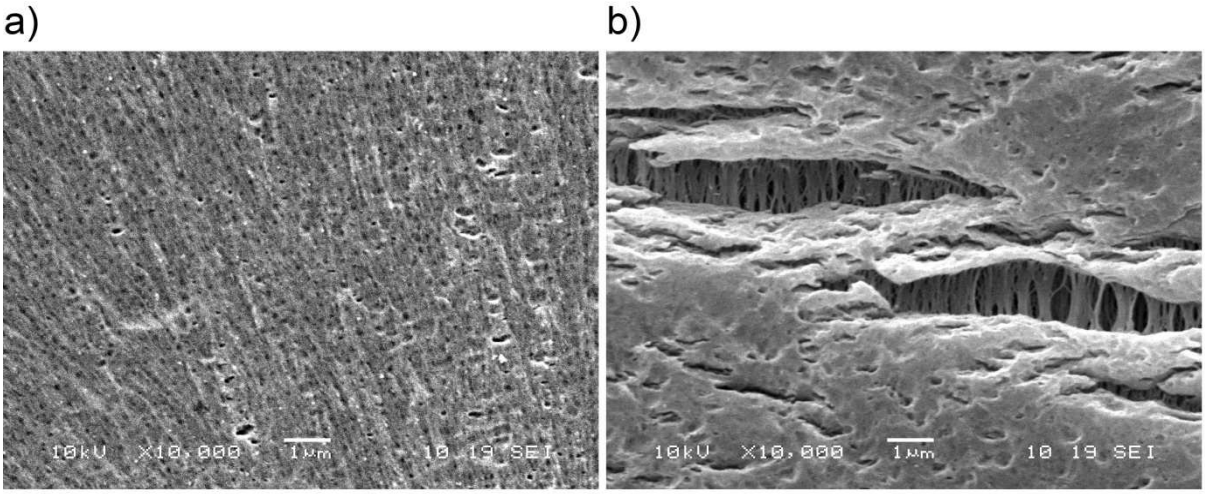

Fig. 36. Microphotographs of unmodified polypropylene sample deformed to the local strain of 0.5. Direction of deformation – vertical. a) polar region of spherulite; b) equatorial region of spherulite.

the mentioned scattering pattern. Deformation of unmodified polypropylene is therefore accompanied by formation of numerous cavities (Fig. 36a) as well as individual dilatation gaps occurring mainly in the equatorial region of spherulites (Fig. 36b).

In the case of unmodified samples with a higher degree of deformation (> 0.8) an increase in the intensity of the scattering signal is observed in the equatorial region at the expense of the signal in the meridional region. The observed change is an effect of the reorganization of the shape of cavities,

which orient themselves in the direction of the applied stress as a result of activation of subsequent plastic deformation mechanisms. Finally, for the samples with a degree of deformation of 3.5 or more, there occurs signal narrowing in the equatorial region of a scattering pattern, which evidences the high degree of orientation of markedly thin cavities. It is difficult, based on small-angle X-ray scattering measurements, to assess changes that occur in the dilatational gaps on further (> 0.8) stages of deformation, however, microphotographs presented later in this chapter indicate a rapid increase in their size combined with the reorganization of shape and destruction of fibrillar structure. Such changes in the morphology of the material are outside detection of SAXS method.

Scattering patterns presented in Fig. 35b performed for chloroform-soaked polypropylene, for local strains analogous to RS sample, indicate complete elimination of the phenomenon of cavitation. No signals indicating formation of discontinuities in the material, both cavities and dilatation gaps, are noted up to the local strain of 4.5. Filling the free volume of the amorphous phase of material successfully eliminates this kind of material response.

The presented WAXS measurements (Figure 29) indicate a very low intensity of scattering signals recorded for the samples saturated with chloroform. To confirm that the lack of signals on SAXS scattering patterns (Figure 35) for modified samples is an effect of elimination of cavitation and not the presence of chlorine atoms (which significantly stronger absorb X-rays than carbon atoms) filling the amorphous phase of material, small-angle X-ray scattering studies were performed for samples, from which a low molecular weight penetrant was removed after the deformation process. SS samples deformed to selected strains were fixed in a special frame, which enabled removal of the sample from a testing machine while retaining the strain state in the material. Next, the penetrant was removed from samples by drying at the temperature of 40^{o}C to constant weight. Analogous procedure was applied for unmodified material in order to obtain the reference data. For such prepared samples small-angle X-ray scattering (SAXS) measurements were conducted as presented in Fig. 37.

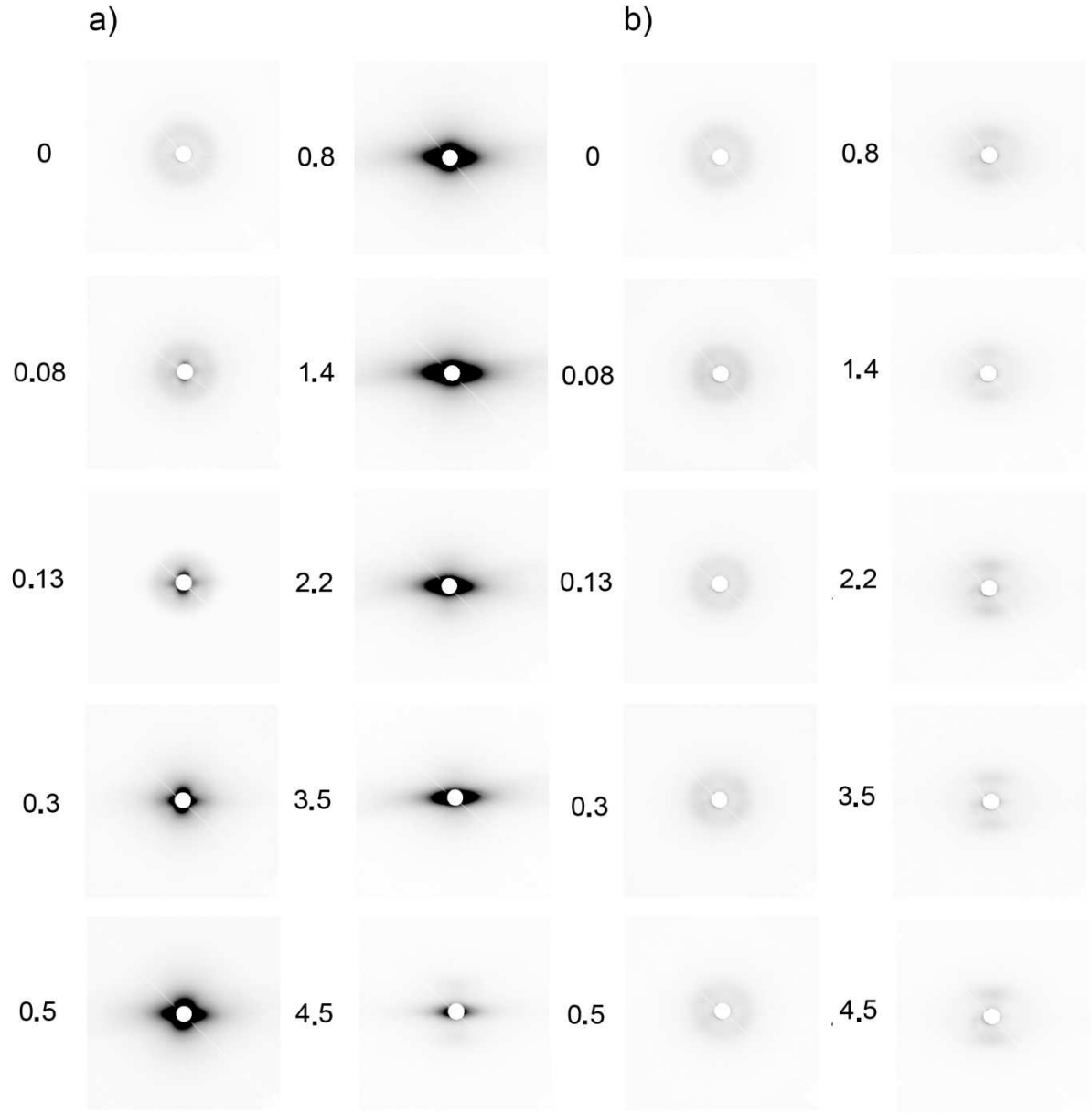

Fig. 37. Small-angle X-ray scattering patterns of a series of polypropylene samples: a) RS; b) SS. Numbers correspond to local strain of samples. Direction of deformation – vertical. SS samples, in the strained state, were being dried at the temperature of 40^{o}C in order to remove a low molecular weight penetrant. RS samples were subjected to analogous procedure.

The presented scattering patterns confirmed the results of *in-situ* small-angle X-ray scattering (SAXS) studies using synchrotron radiation. Deformation of unmodified polypropylene (Fig. 37a) is accompanied by an intensive cavitation process. The first cavities begin to appear at the local deformation equal to 0.08. At further stage of deformation one also observes appearance of dilatation gaps. The presence of this type of discontinuities is manifested by an additional signal in the equatorial region of scattering pattern. For RS polypropylene samples of a higher degree of

deformation**,** an increase in the intensity of the signal is registered in the equatorial region of scattering pattern at the expense of signal in the meridional zone. The observed changes are the result of the reorganization of the shape of cavities, at this stage of deformation of the material. Continuing deformation (> 1.4) make the cavities become thinner and elongated parallel to the direction of deformation.

Scattering patterns recorded for SS samples after removal of low molecular weight penetrant confirm earlier conclusions that filling the amorphous phase of material leads to elimination of cavitation during deformation of the material (Fig. 37b). Examinations performed after chloroform desorption not only indicate that the process of formation of discontinuities (cavities, dilatation gaps) could be entirely eliminated in SS samples, but also enable to trace the changes occurring in the lamellar structure on subsequent stages of deformation. Isotropic signal, typical of non-oriented material, transforms into a four-point pattern with the strain increase (0.3). Such image is an evidence of the formation of two populations of lamellae oriented at an acute angle to the direction of deformation. With the strain increase, the angle between the normals of lamellae and the direction of the applied force decreases. This evidences a systematic change in the direction of lamellar arrangement in the material. Finally, for the local strain of 0.8 or more, a two-point signal is observed in the polar region, which indicates lamellar arrangement (fragments of lamellae) perpendicularly to the direction of deformation. Such analysis was not possible for cavitating samples because of strong signal from cavities. Only for samples with high strain (4.5), the signal from lamellae can be observed, as in the case of a sample SS, in the meridional region of diffractogram, which testifies to the similar arrangement of lamellae in the material.

Appearance of cavitation, and change in the shape of cavities in particular, must be accompanied by change in the arrangement of crystals in the material. Specific organization of crystallites at various stages of deformation can be controlled using wide-angle X-ray diffraction (2D WAXS). Scattering patterns recorded for subsequent deformation stages of samples of unmodified polypropylene and saturated with a low molecular weight penetrant (after removal of penetrant) are presented in Fig. 38.

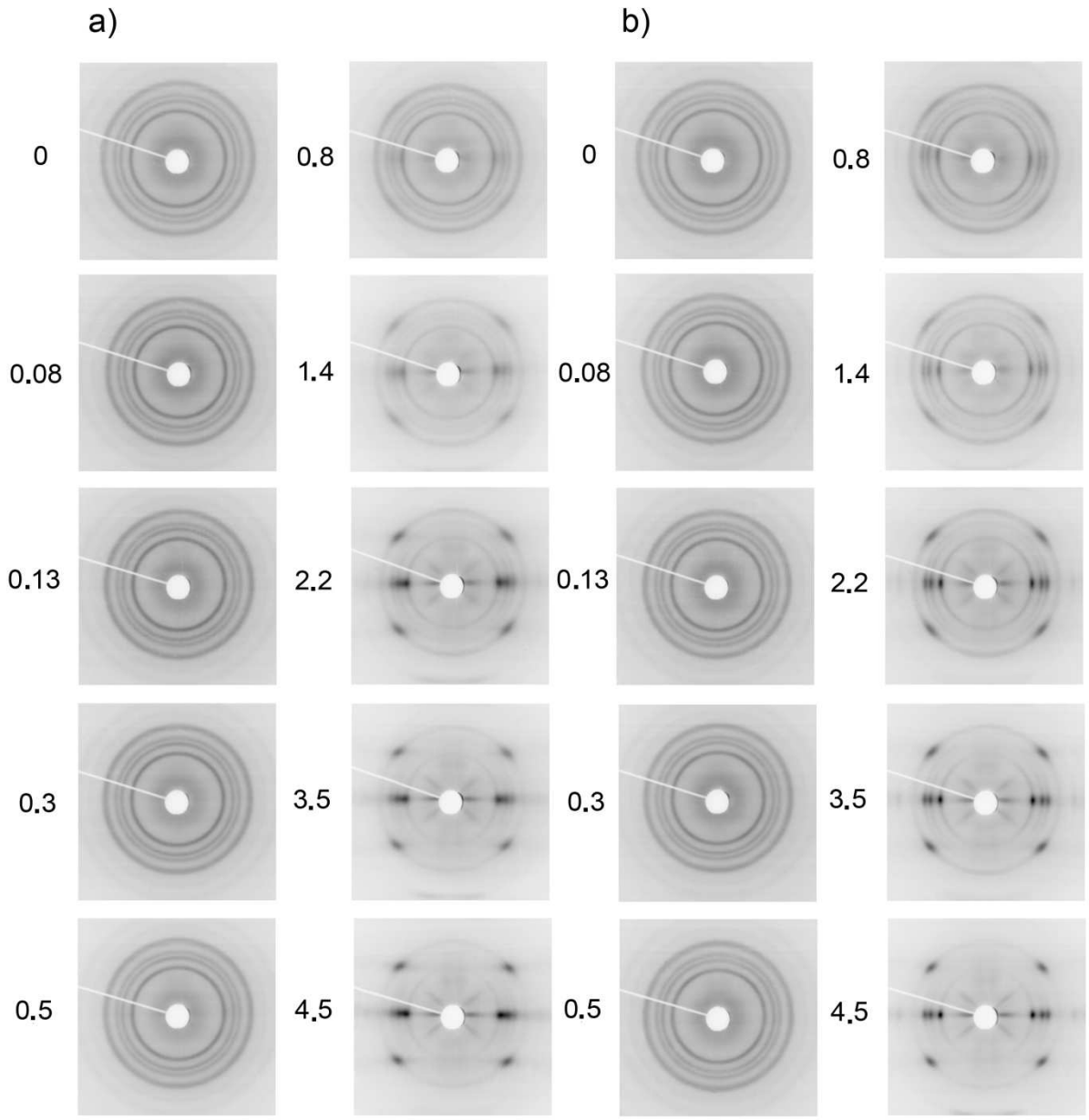

Fig. 38. WAXS scattering patterns for samples: a) RS, b) SS. Numbers correspond to local strain of samples. Direction of deformation - vertical.

The concentric rings represents diffraction from the following crystallographic planes: (110), (040), (130) and (111) together with (-131) and (041). With the deformed samples, diffraction patterns up to the local strain of 0.5 do not exhibit significant degree of orientation of crystallites in the examined materials. For the higher deformed samples (> 0.5), of both unmodified and modified polypropylene, one observes concentration of signals in the selected regions of diffraction circles.

Planes containing the axis of macromolecular chain [(110) (040) (130)] tend to orient themselves parallel to the direction of the applied stress (diffraction signal in the equatorial area). Meanwhile, the external circle, appearing as a result of overlapping of signals from three different crystallographic planes, all with the index l=1, not containing axes of macromolecular chains, transforms into a four-point pattern. This indicates the presence of two populations of lamellae in the material.

As the strain increases reflections from (110), (040) and (130) planes concentrate in equatorial zone of diffraction pattern forming so-called “zero layer” of x-ray fiber diffraction pattern. For pure uniaxial straining the intensities of reflections from all crystallographic planes containing macromolecular chains should increase in a similar way. Reflections from other planes (overlapping reflections from (111), (-131) and (041) at around $2\Theta=22^{o}$) will form first order layer of x-ray fiber diffraction pattern because the last number in crystallographic planes indices is 1. Changes in the arrangement of crystallites during deformation, both for RS samples (with cavitation) and SS (without cavitation), run similarly: the zero and first order layers are formed in patterns for both samples. The essential difference is the degree of concentration of individual signals. In the case of RS samples, concentration of signals in the equatorial region of a diffraction pattern is accompanied by their significant diffusing. Diffraction patterns recorded for SS samples remain sharp up to the local strain of 4.5.

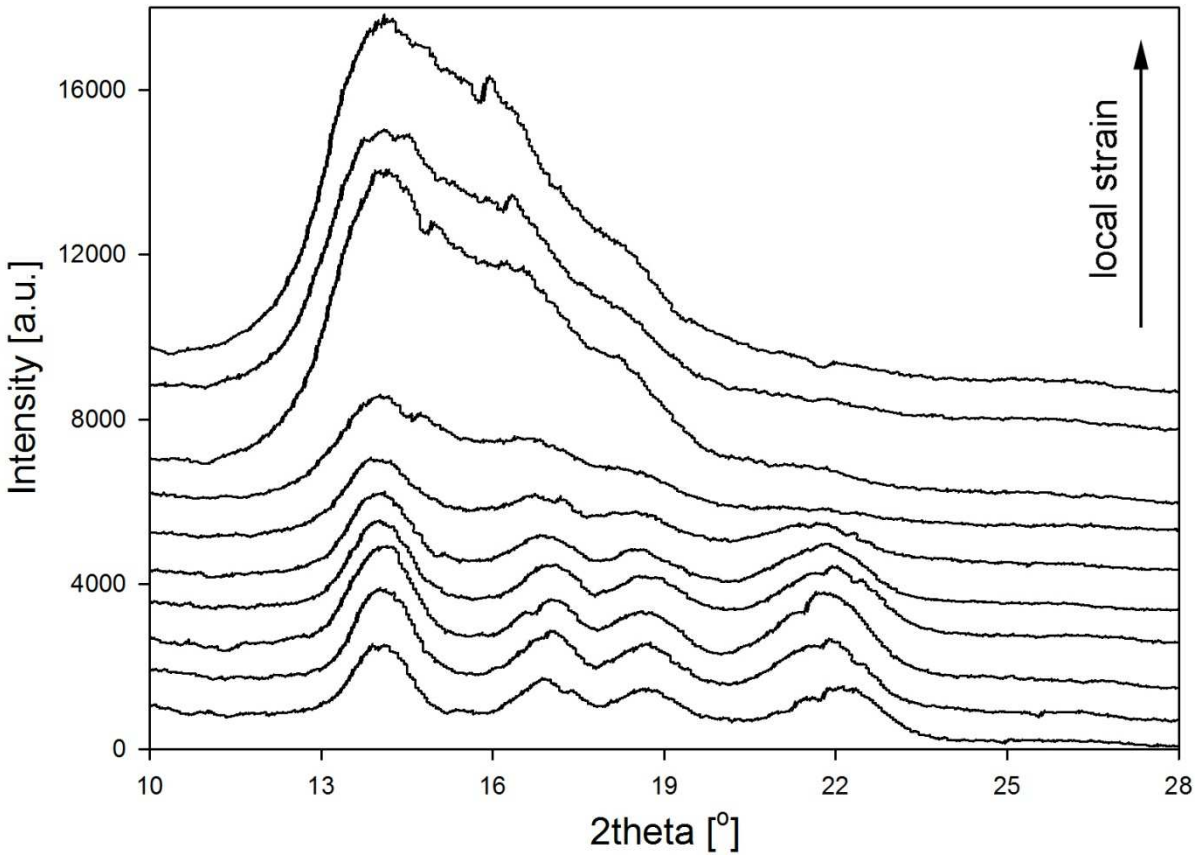

Fig. 39. Horizontally scanned diffraction profiles of WAXS scattering patterns for reference samples.

Fig. 39 presents diffraction profiles of the presented scattering images (Fig. 38) for reference material, horizontally scanned for individual local strains. In the case of cavitating samples an increase in the intensity of the obtained diffraction profile is observed on subsequent stages of deformation accompanied by a gradual decrease of the resolution of signals from individual crystallographic planes. The intensity ratio of signals from the crystalline component to the intensity of amorphous background for subsequent stages of deformation gradually decreases. For RS sample of local strain of 4.5 one observes only a broadened signal as a result of overlapping of a peak of the amorphous background with strongly reduced and diffused signals from the crystallographic planes.

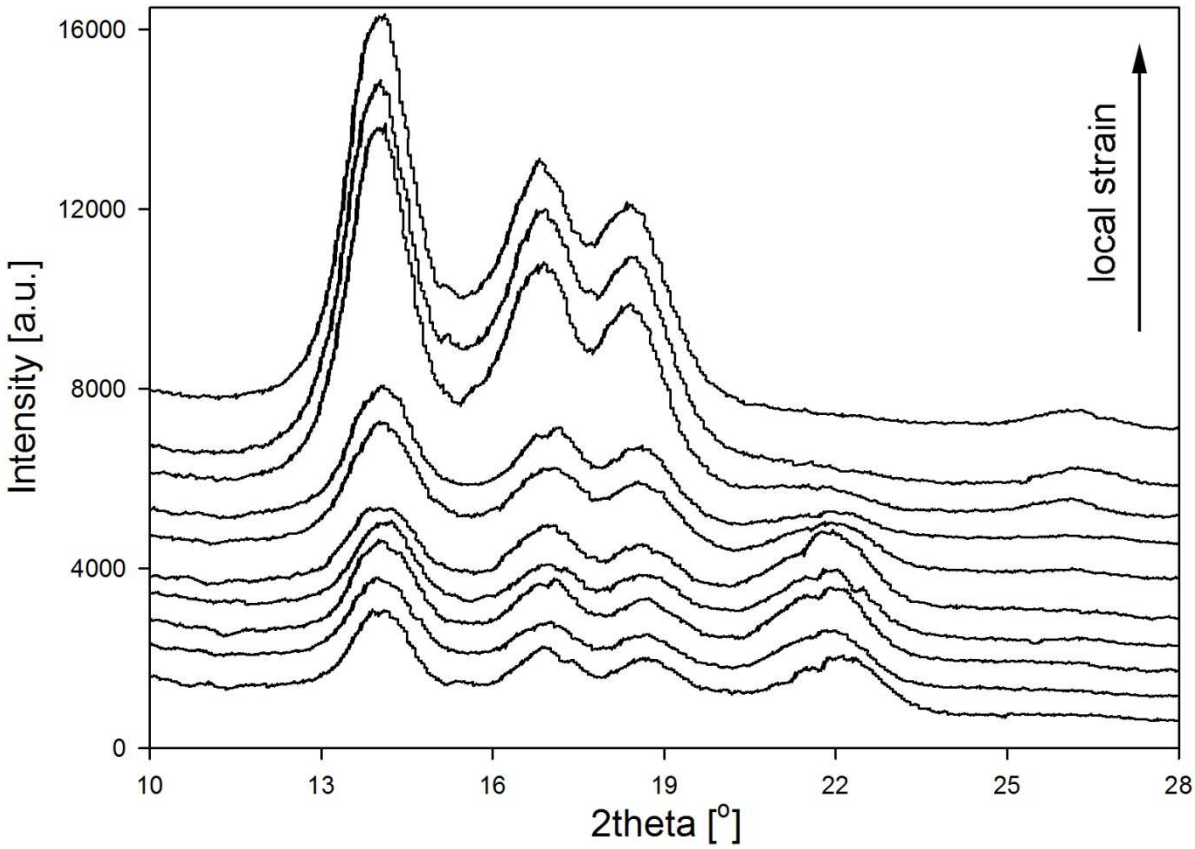

Fig. 40. Horizontally scanned diffraction profiles of WAXS scattering patterns for chloroform-soaked polypropylene samples.

Diffraction profiles obtained for samples saturated with a low molecular weight penetrant for subsequent deformation stages are presented in Figure 40. As in the case of cavitating material, a clear increase in the intensity of diffraction profile is observed in the samples with higher local strain, an effect of the concentration of signals from crystallographic planes of indices (hk0) or (0k0) in the horizontal region of scattering images. However, one does not observe a relative reduction in the intensity of peaks from the crystalline component in relation to the amorphous background. Signals from these planes remain sharp up to the local strain of 4.5.

Such strong change in the diffraction profile of cavitating samples (relative reduction in the intensity of peaks from the crystalline component) with no significant change in the degree of crystallinity (DSC thermograms discussed further in the chapter) proves strong changes in perfection of crystalline of lamellae. Lamellar distortion during deformation of non-cavitating samples is significantly weaker as evidenced by the shape of the diffraction profiles at different stages of deformation. Signals from the crystalline component remain sharp with regard to the signal originating

from the amorphous phase, up to local strain of 4.5. The presence of cavitation, therefore, induces lamellar imperfection by facilitating initiation of this type of material response.

Figures 41 and 42 present DSC thermograms recorded for the reference material and saturated with chloroform deformed to selected strains. Due to numerous phenomena and mechanisms activated during deformation of both the reference and the saturated with chloroform material (lamellar distortion, orientation of crystallites, defects in crystals caused by the presence of dislocations, reorganization of the crystalline structure induced by deformation of the material: monoclinic form – mezo phase), and relaxation of orientation during heating, interpretation of changes in shape and location of the melting peak is very difficult. Analysis of thermograms in a low temperature region (<100^{o}C) indicates the presence of mezo phase, whose formation in the deformed samples has been confirmed by the authors of the papers [13-15], both in cavitating samples and in the material soaked with a low molecular weight penetrant deformed to the local strain of 1.4 or more. The effect of cavitation on the presence of mezophase in the deformed material is relatively small. Therefore, diffusing of the diffraction signals observed on scattering patterns for RS sample (Fig. 38) may be additionally intensified by the presence of broad reflection from the mezophase plane (100), highly concentrated in the equatorial region of scattering images of the deformed samples, however it is strong lamellar distortion induced by cavitation and by a change in the direction of orientation of voids and dilatation gaps which influences the observed diffusing of diffraction signals on scattering patterns performed for cavitating samples. Diffraction signals in non-cavitating samples, due to relatively small degree of lamellar distortion, remain sharp within the entire analyzed deformation range. The presence of signal from mezophase only slightly influences the resolution of the peaks from different crystallographic planes – scattering signals for individual planes remain sharp up to the local strain of 4.5.

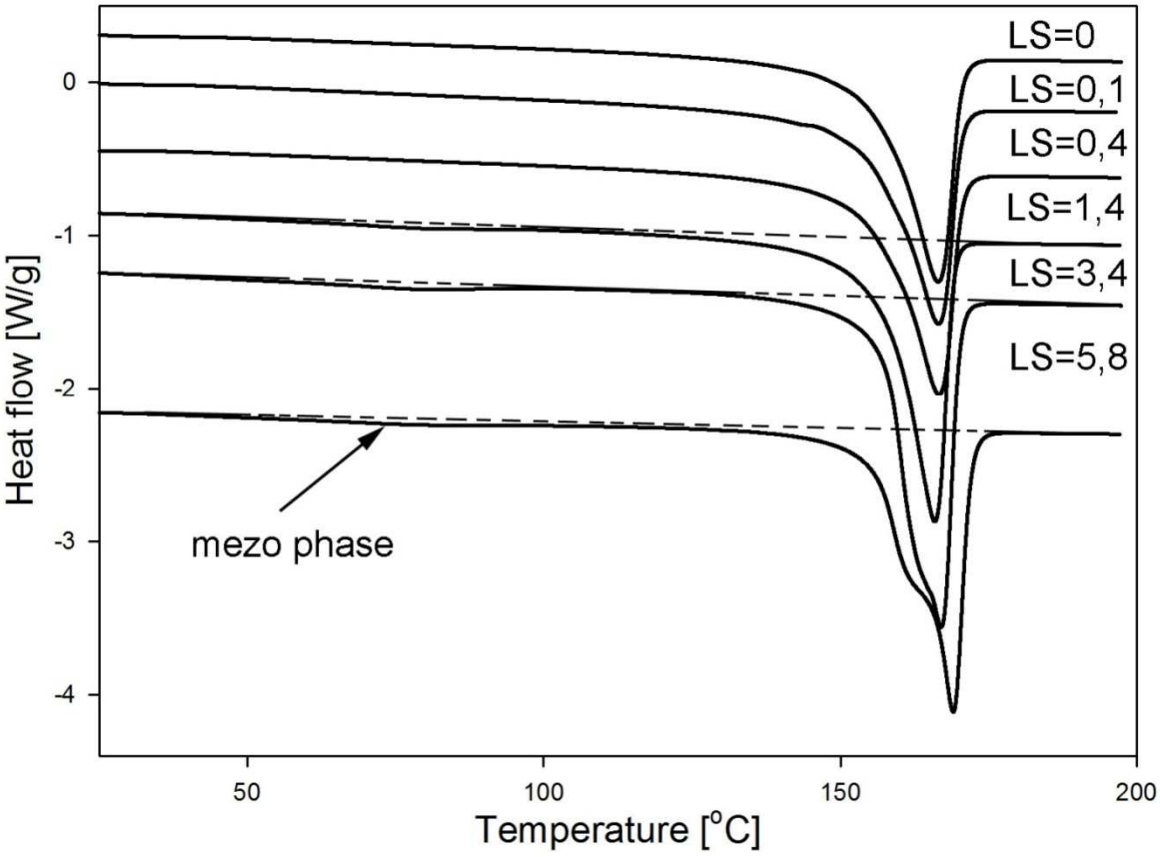

Fig. 41. DSC thermograms of a series of polypropylene samples (reference material). Numbers correspond to local strain of samples.

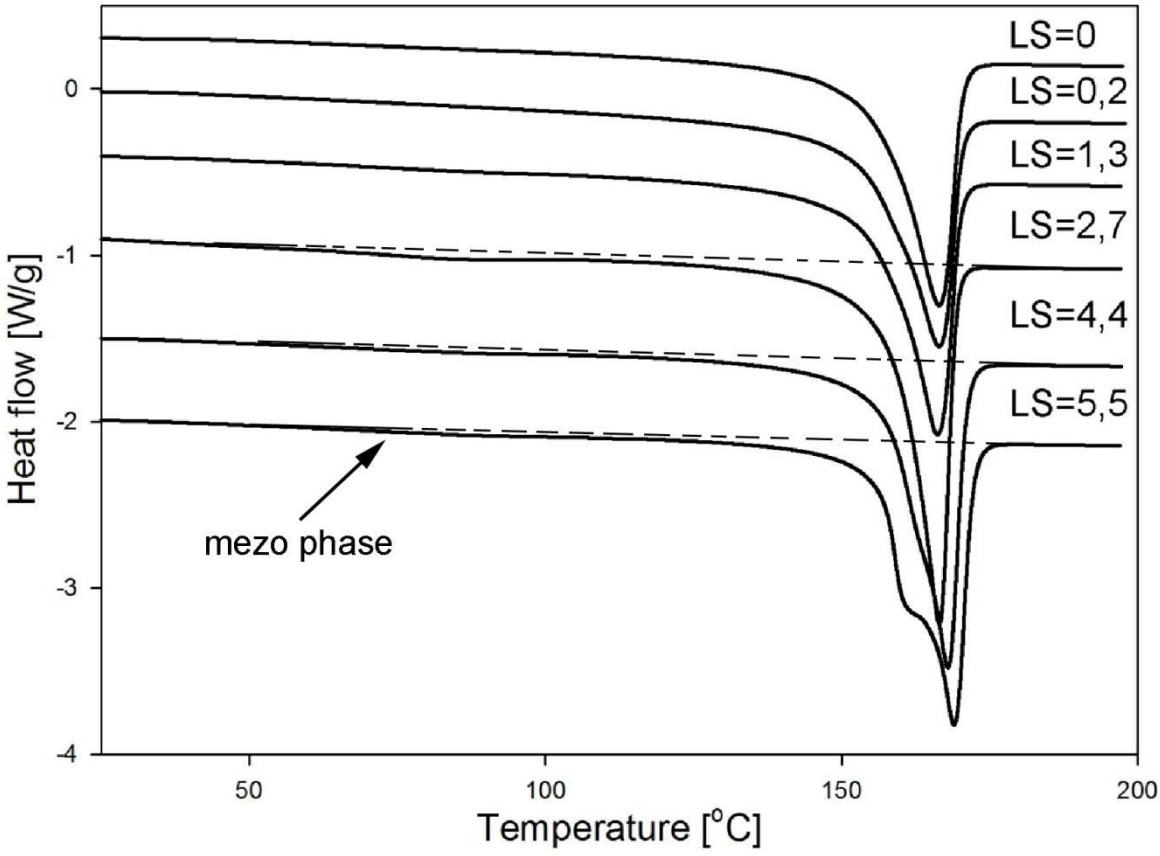

Fig. 42. DSC thermograms of a series of polypropylene samples (chloroform-soaked material). Numbers correspond to local strain of samples.

Change in the morphology of the samples accompanying deformation of the material can be traced using scanning electron microscopy. Figs. 43 presents exemplary microphotographs of the deformed samples of unmodified polypropylene and saturated with chloroform. Internal structure of the samples was exposed with the use of an ultramicrotome equipped with a diamond knife. The exposed surfaces were etched for 2 hours in etching mixture consisting of potassium permanganate dissolved in a mixture of concentrated sulphuric acid, orthophosphoric acid and distilled water.

Microphotographs of undeformed samples exhibit the typical spherulitic structure of polypropylene (Figs 43a and 43b). Deformation of unmodified material is accompanied by formation of discontinuities, first observed at the local strain equal to 0.3. Discontinuities, elongated perpendicularly to the direction of deformation, occur mainly in the equatorial regions of spherulites. However, it should be noted that the objects seen on SEM micrographs are outside of SAXS detection limit. Further deformation of the material is accompanied by increase in the number and size of discontinuities (cavities and dilatation microcracks). For the local strain of 0.8 and above, intense changes take place in the structure of the material, causing reorganization of the shape and size of cavities. For local strain 0.8 and above, discontinuities become elongated in the direction of the applied stress. SEM micrographs of RS sample (local strain of 2.2) present single large holes, which are remnants of dilatation microcracks and numerous cavities strongly elongated in the direction of deformation. Severe damage to crystalline lamellae occurred that is caused by cavitation and changes of cavities shape as the deformation increases: lamellae are no longer continuous, they are strongly fragmented and disrupted. The diffused x-ray reflections in the zero layer of x-ray fiber diffraction pattern in Fig.38 and analysed based on equatorial scans in Fig.39 is now quite obvious as they arise from highly fragmented crystalline lamellae.

Deformation of SS sample proceeds differently. Change in the shape of spherulites is observed, as in the case of RS sample, when the strain corresponding to macroscopic yield point is achieved, however at this stage and later, up to the strain equal to 2.2 formation of dilatational discontinuities is not observed in the material. Also at higher magnification cavities were not observed in the material. Lamellae in SS sample preserve their continuity up to high deformation ratio as it is clearly seen from SEM micrographs in Fig.43b. They evidently increase their length as seen on SEM images and decrease their thickness as can be deduced from respective long period determined from

SAXS patterns depicted in Fig. 37b. Significant thinning of lamellae begins with deformation of 0.3. The above presented facts, especially SEM images of deformed SS polypropylene sample in Fig.43b, constitute a strong evidence that deformation of lamellae can proceed without their severe fragmentation via crystallographic slips and most probably it is the cavitation, if activated, that triggers lamellae fragmentation.

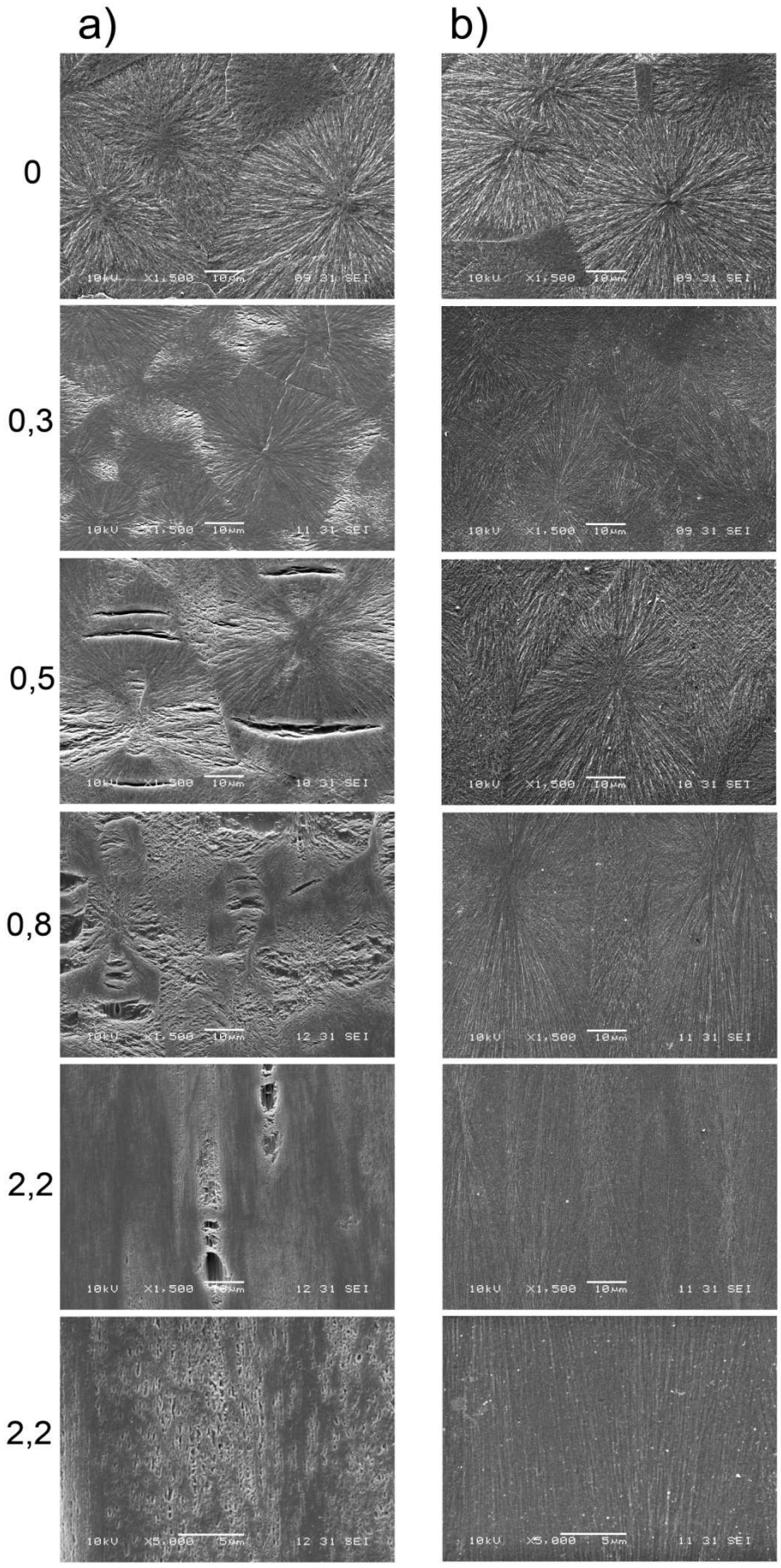
a)
b)
0
0,3
0,5
0,8
2,2
2,2
10kV X1,500 10µm 09 31 SEI
10kV X1,500 10µm 11 31 SEI
10kV X1,500 10µm 10 31 SEI
10kV X1,500 10µm 12 31 SEI
10kV X1,500 10µm 11 31 SEI
10kV X5,000 5µm 12 31 SEI
10kV X5,000 5µm 11 31 SEI

Fig. 43. SEM microphotographs of polypropylene samples: a) RS; b) SS. Microphotographs show etched longitudinal section of the sample. Number correspond to local strain of samples. Direction of deformation: vertical.

Conclusions presented in the previous chapters, supported by X-ray examinations, indicating appearance of cavitation in RS samples and excluding the phenomenon in the modified polypropylene samples are also confirmed by the results of volume strain measurements (Fig. 44). Deformation of samples of unmodified polypropylene is accompanied by a significant volume increase (by approx. 30%), an effect of formation of cavities and dilatation microcracks. Filling the free volume of the amorphous phase of a polymer with a low molecular weight penetrant eliminates the process of formation of discontinuities in the material, which is manifested by the lack of volume change of samples during their deformation.

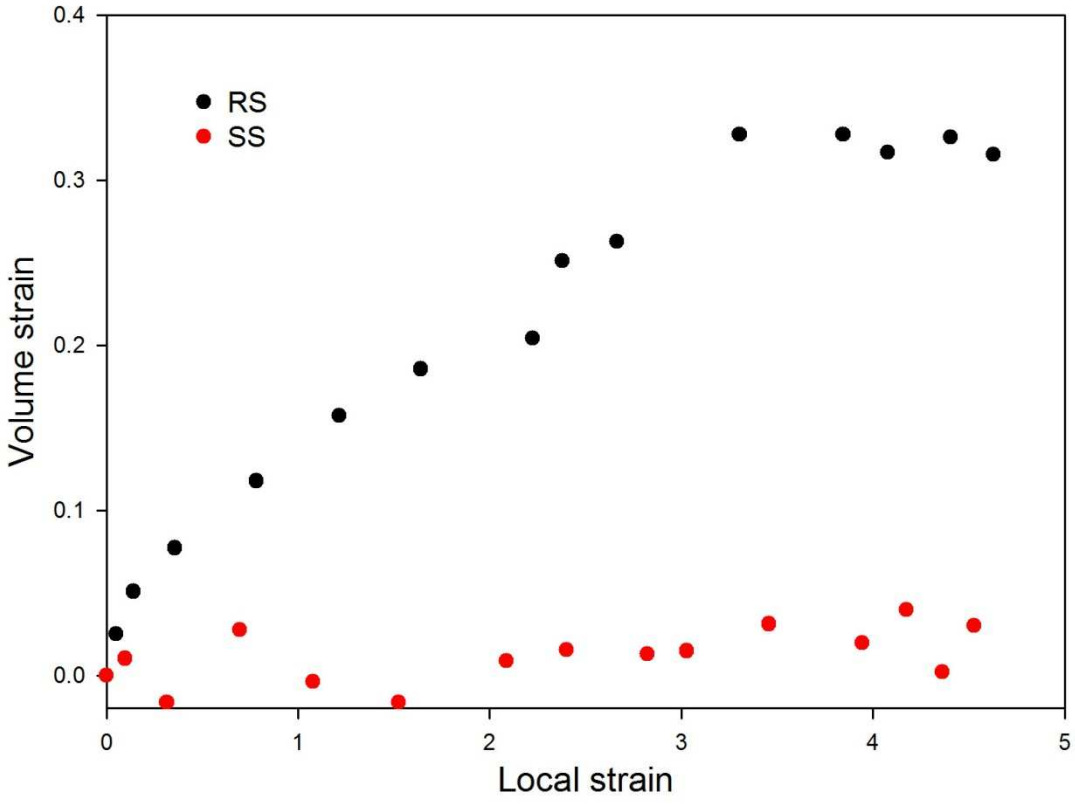

Fig. 44. Volume strain as a function of local strain for unmodified polypropylene (RS) and saturated with chloroform (SS).

In order to check whether the low molecular weight penetrant fills the free volume of the amorphous phase of the material, density measurements of reference and modified material were

performed. Macroscopic swelling of the sample should be in fact also related to the process of filling free spaces within the amorphous phase of a polymer. In such a case, the volume of the modifier introduced to the material should be higher than a change in volume of the sample as a result of saturation. Due to fast chloroform desorption, density measurements of fully saturated sample were not possible. The density measurement were performed approx. 16h after removal of the sample from the conditioning vessel. After 16h the sample has still a considerable content of the penetrant, however the rate of the desorption process is relatively slow. Relevant measurements and calculations are as follows:

-parameters of the sample before saturation:

m_0=0,03451g, d_0=0,09075g/cm^3 => $V_0=m_0/d_0$=0,03803cm^3

-parameters of the sample after saturation:

m_1=0,03653g, d_1=0,9300g/cm^3 => $V_1=m_1/d_1$=0,0393cm^3

-mass of chloroform in the saturated sample:

$m_m=m_1-m_0$=0,03653g-0,03451g=0,00202g

-chloroform volume in the saturated sample:

$V_m=m_m/d_m$=0,00202g/1,48g/cm^3=<u>0,00136cm^3</u>

-volume change of the sample as a result of introduction of the penetrant:

$V_s=V_1-V_0$=<u>0,00127cm^3</u>

The volume of a low molecular weight penetrant (V_m) introduced during modification of the material is higher than the change in the volume of the sample as a result of saturation (V_s). This indicates filling of pores of the free volume of amorphous phase of the material at the level of 0.24% of the volume of the sample before saturation**.** One may assume that in the sample fully saturated with low molecular weight molecules of a penetrant (immediately after removal of the sample from the conditioning vessel), the degree of saturation of the free volume of the amorphous phase is much higher.

5.2.2. Modification of the amorphous phase of polypropylene with hexane.

In order to determine the influence of the penetrant used to saturate the amorphous phase on the phenomenon of cavitation accompanying deformation of polypropylene, the modification process has been carried out using a liquid of a markedly different physicochemical properties, i.e. hexane.

Samples for mechanical and X-ray measurements had been cut out from 1mm thick film (PP2), prepared by compression molding. The first batch of samples (soaked sample – SS) was placed in a vessel containing a penetrant (hexane) for a period of at least 100 hours, so as to saturate the amorphous phase of the material with a low molecular weight liquid. The second batch of samples (reference sample – RS) served as a reference material.

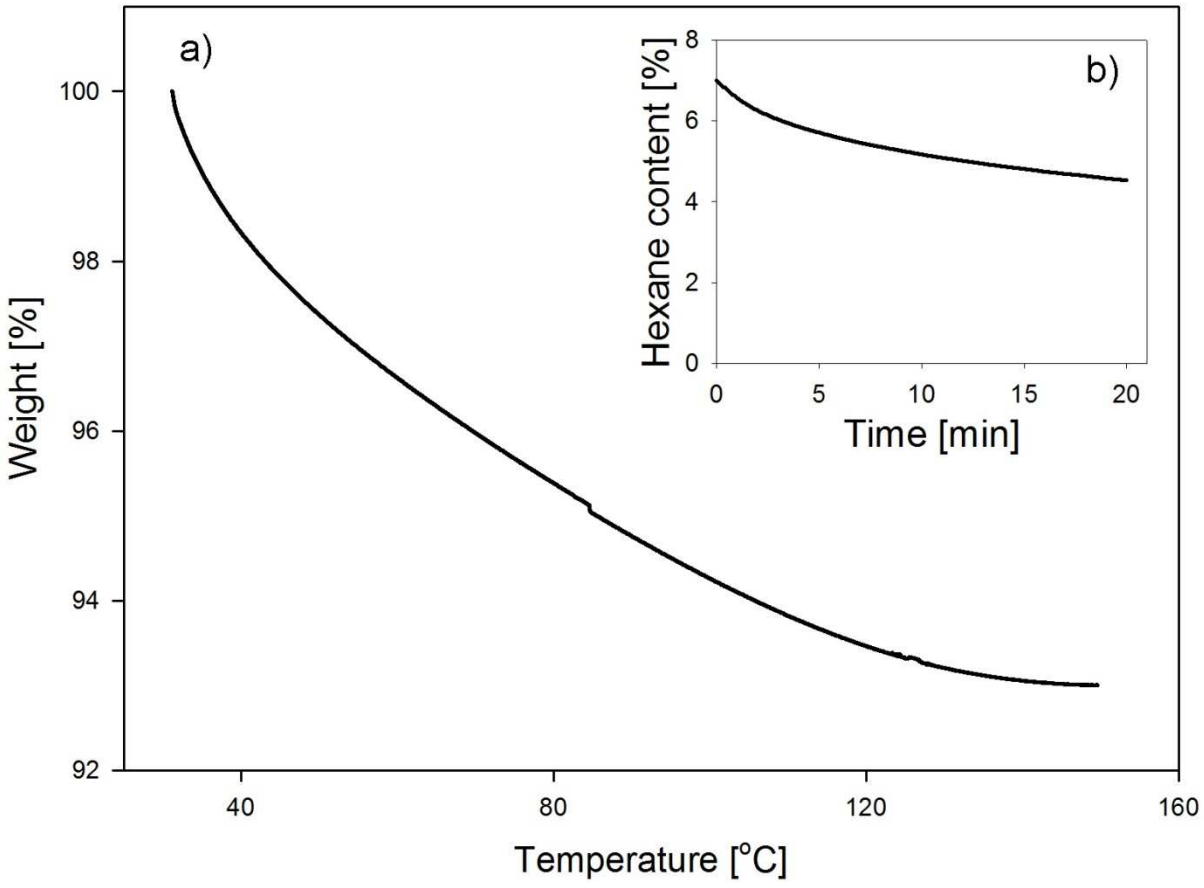

Fig. 45. Hexane-soaked polypropylene: a) TGA thermogram, b) desorption kinetics of hexane under laboratory conditions, after removal from a liquid.

In order to assess the amount of penetrant present in the examined material after completion of the conditioning process, TGA measurement has been taken. Figure 45a presents the relevant thermogram. On the basis of the above thermogram the amount of hexane in the material after completion of saturation has been determined as 7% (weight) (10.7% volume). Fig. 45b presents the desorption kinetics of penetrant under laboratory conditions after removal of the material form a

conditioning vessel. Desorption of penetrant under laboratory conditions is a relatively quick process, therefore all measurements were taken within a minute after removal of the sample from a conditioning vessel.

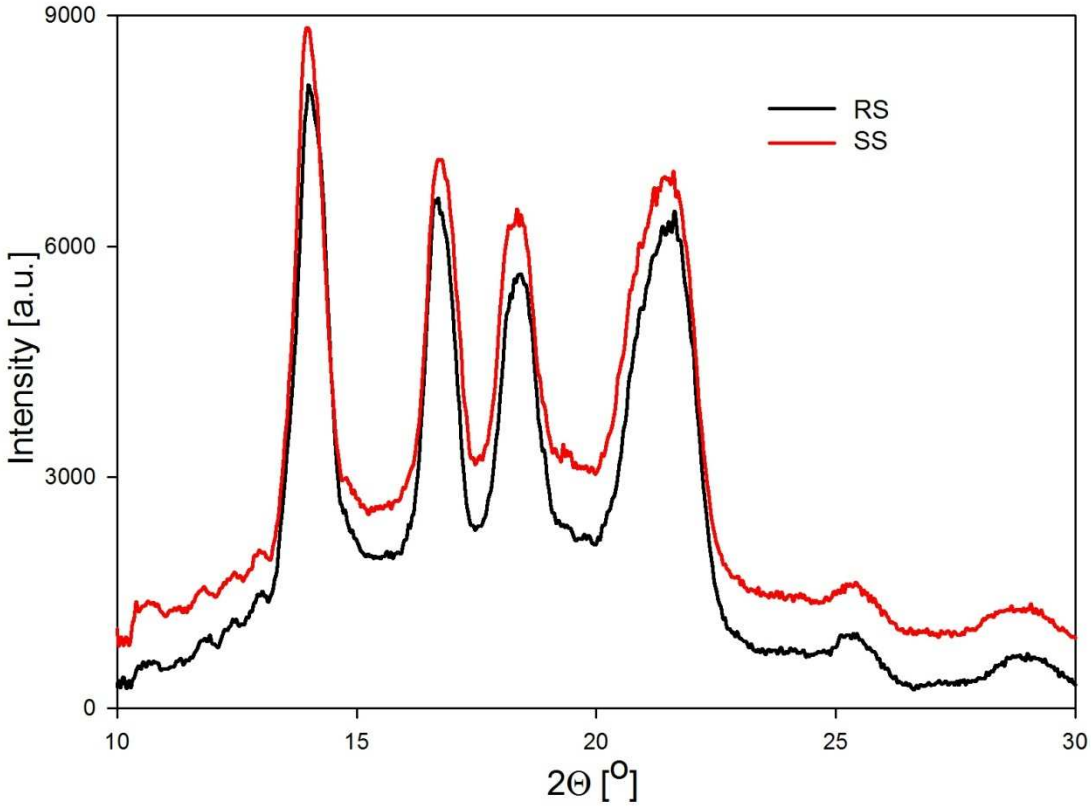

Fig. 46. Diffractograms of polypropylene samples: saturated with hexane, SS, and reference, RS. The curve for SS sample shifted upward for better visualization.

Figure 46 presents WAXS diffractograms for the modified polypropylene, SS, and the unmodified, RS. The presented diffraction profiles indicate no significant differences of diffraction reflections in height and width, which indicates no changes in the crystalline structure of the material caused by the penetrant.

Wide-angle X-ray diffraction measurements using a special system of diaphragms increasing angular resolution and considerably eliminating instrument broadening of reflections have also been performed. Figure 47 presents relevant diffraction profiles for the peaks corresponding to subsequent crystallographic planes.

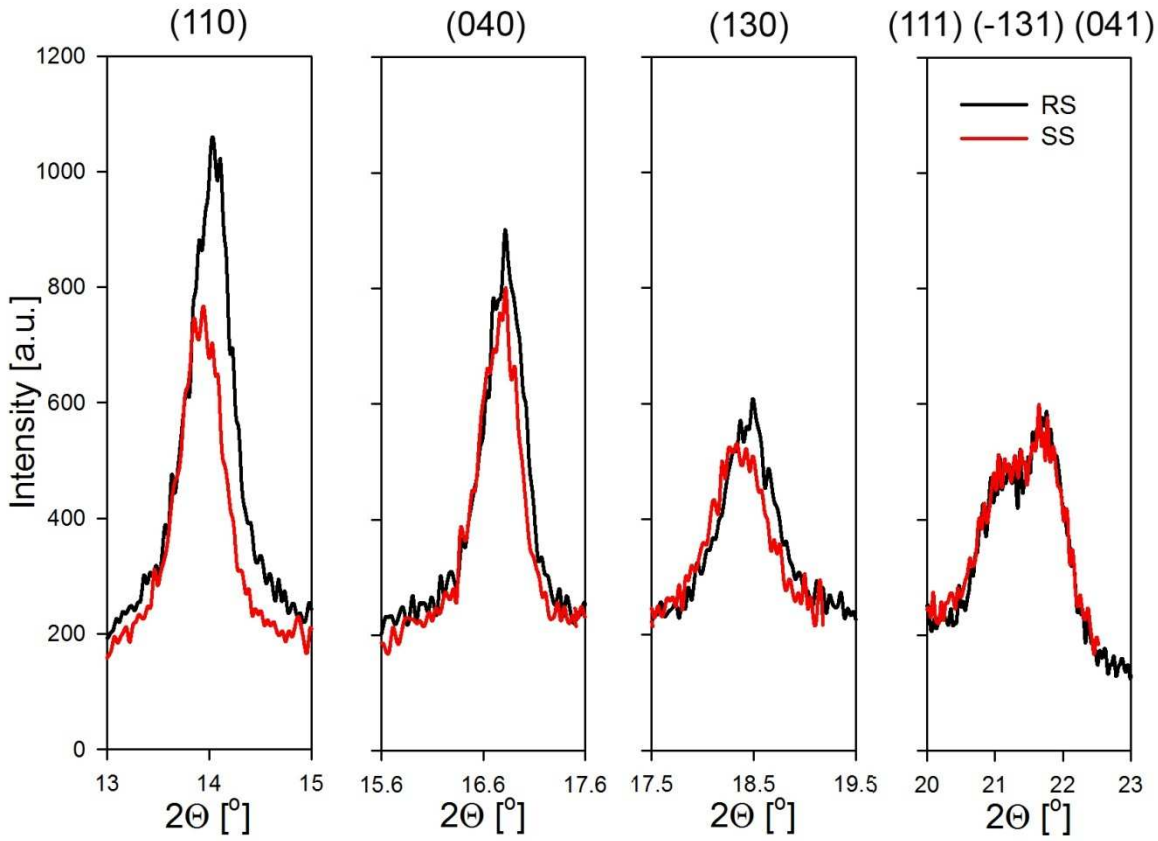

Fig. 47. X-ray diffractograms of polypropylene samples.

Increased resolution of the registered data allowed to observe minor changes in the positions of peaks corresponding to crystallographic planes of (hk0) index. Changes in the position of these peaks occurred towards lower values of 2θ angle, which indicates an increase in interplanar distances in selected directions.

The presented measurements of wide-angle X-ray scattering point to relatively small changes taking place in the crystalline phase of the material as a result of introduction of a low molecular weight penetrant. No significant changes within crystals proves that hexane is mainly localized in the amorphous phase of the material. However, the swollen amorphous phase exerts a significant stress onto lamellae that causes their crystallographic cells to deform along certain crystallographic planes.

In the case of polypropylene saturated with chloroform it was impossible to perform a similar analysis due to strong absorption of X-rays by atoms of chlorine. One can only assume that the presence of chloroform in the material leads to very similar changes in the material structure at the unit cell level.

Basing on small-angle X-ray scattering measurements, changes in the values of a long period as a function of sorption time of hexane have been determined. The results are presented in Figure 48.

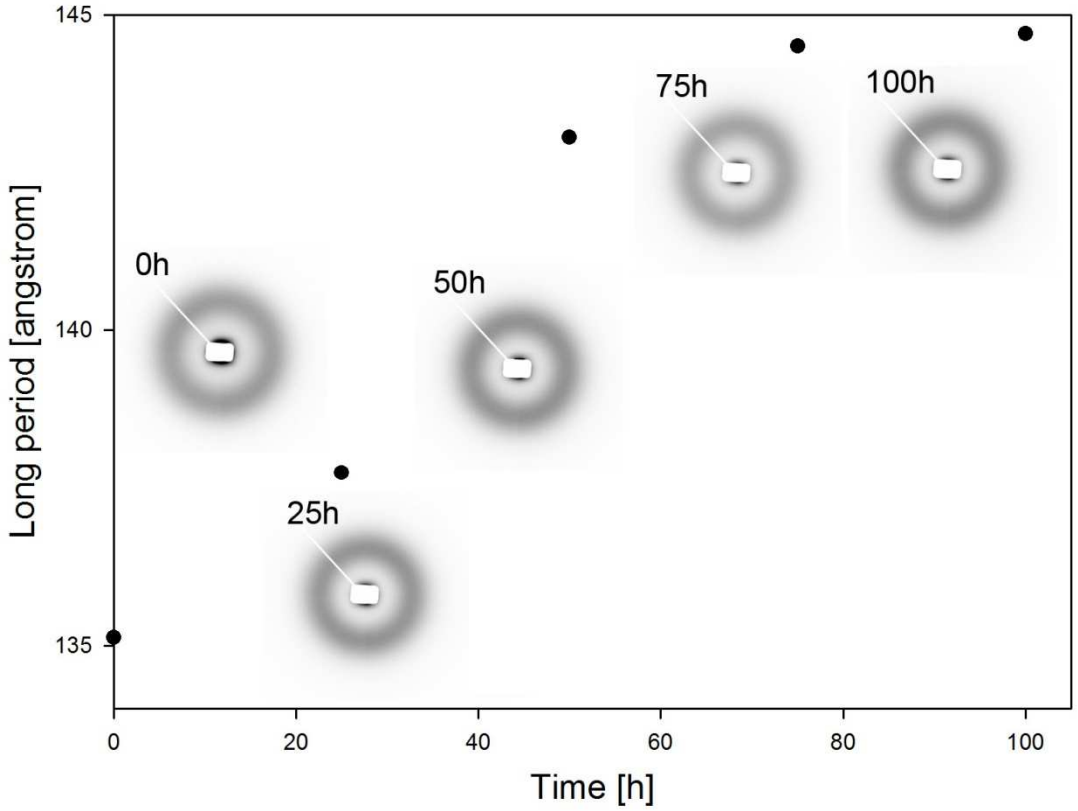

Fig 48. Change in a long period of polypropylene as a function of time of sorption of hexane.

The presented data suggest that as a result of sorption of a low molecular weight penetrant a significant change in the value of a long period has occurred. For reference sample the value of this parameter was 135.1 Å and after full saturation of the material with the penetrant it increased to 144.7 Å. Minor changes in the crystalline regions combined with an increase in the values of a long period indicate strong swelling of the amorphous phase resulting in deformation of the unordered amorphous regions. A direct result of the observed changes is increase in interlamellar distances as a result of introduction of hexane molecules.

Viscoelastic properties of polypropylene have been determined using dynamic mechanical analysis and the influence of the presence of hexane on the material parameters such as storage modulus (E '), loss modulus (E") and loss tangent (tg α) as a function of temperature has been discussed. Figure 49 presents relations between the said parameters and temperature.

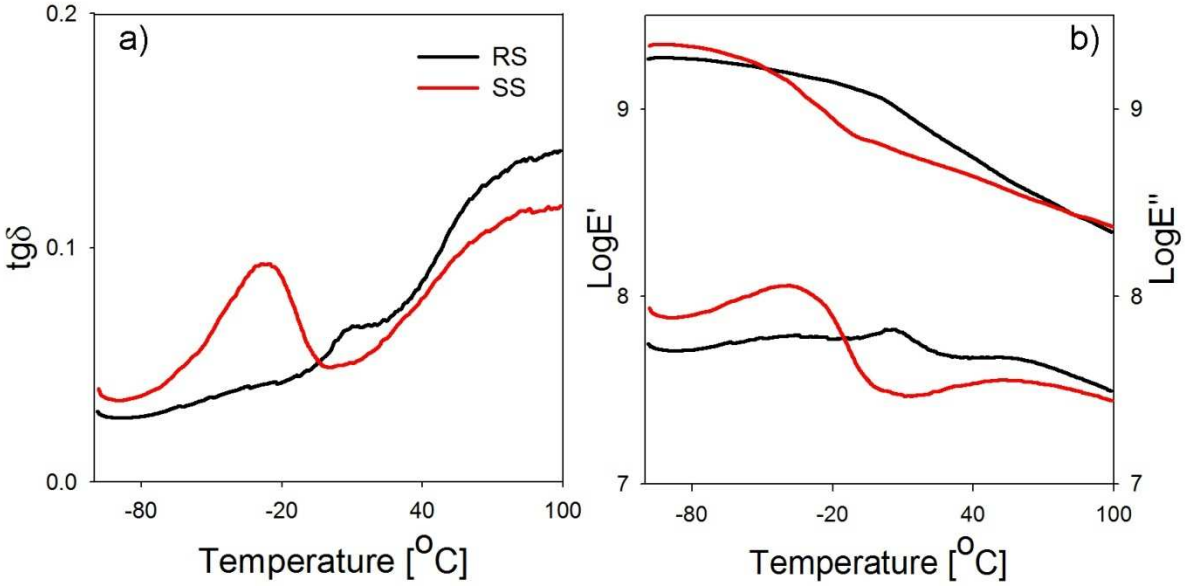

Fig. 49. Relations between loss tangent (a), storage modulus and loss modulus (b) and temperature of reference and soaked polypropylene sample determined by means of dynamic mechanical analysis (DMTA).

For reference material (RS, unmodified polypropylene), one can distinguish the following relaxation transitions: γ (around –40°C), β ((7°C) (corresponding to processes taking place within the amorphous phase of the material); β relaxation transition corresponding to material's transition from a state of high elasticity to a glassy state) and α (around 50° C) (an effect of complex changes occur ring both in crystals and in the unordered regions). Introduction of penetrant's molecules (SS sample) leads to a clear shift of glass transition temperature towards lower values by as much as 46°C, up to -39°C. The presence of penetrant's molecules, in a low temperature range, below glass transition temperature of the material, leads to "stiffening" of the material, which manifests itself in a higher modulus of the saturated material recorded in this area (Figure 49b). In a temperature range from -48°C to 78°C, above glass transition temperature, the modified material is characterized by a significantly lower modulus than the reference material. This is the result of strong plasticization of the material, below its glass transition temperature, as a result of introduction of a low molecular weight penetrant. At the temperature of 80°C values of moduli of both materials become equal, an effect of desorption of the modifier as a result of heating of the sample during DMTA experiment.

Figure 50 presents engineering strain - engineering stress curves for polypropylene samples subjected to tensile drawing up to rupture. Deformation of the unmodified polypropylene and saturated with hexane did not proceed in the same manner although both materials were accompanied by the micronecking process. During deformation of the unmodified material strong whitening occurred in the macroscopic yield point region, whereas the sample whose amorphous phase had been filled with molecules of penetrant remained transparent up to rupture. Analysis of curves presented in Figure 50 also points to strong dependence of stress at yield point on the presence of hexane filling amorphous phase of the material. The determined values of yield stress are 35 MPa for RS sample and 24.5 MPa for SS sample, respectively. Thus, the stress difference at yield point between the reference and the saturated sample is 10.5 MPa. If the crystalline phase of the saturated sample is not penetrated by a low molecular weight penetrant, we should expect that the critical shear stress of the active crystal slip planes will not be significantly different in the dried and modified samples. The observed stress difference at yield point between the reference and the modified sample has to result from changes in the amorphous phase of the material. To verify this assumption I performed the following experiment: a sample saturated with hexane, immediately after removal from a conditioning vessel, has been clamped in the apparatus for measuring mechanical properties and stress buildup in the sample as a function of desorption time of the modifier has been measured. Figure 51 presents results of the experiment.

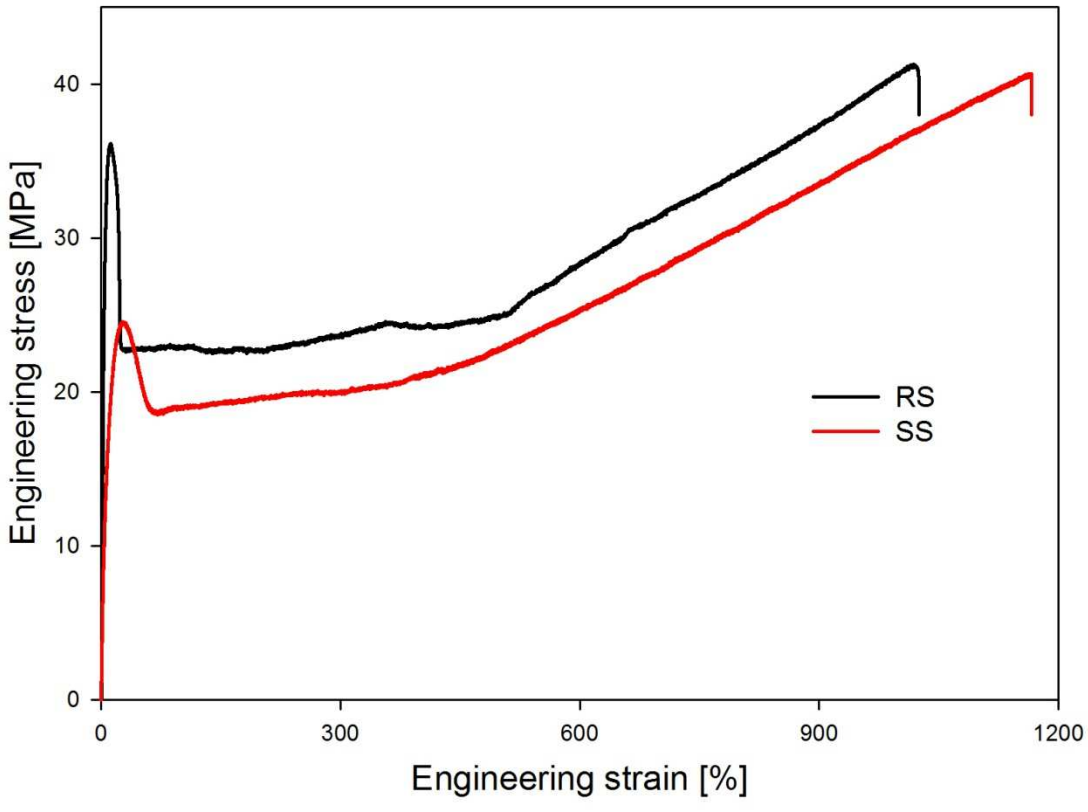

Fig. 50. Engineering strain - engineering stress curves for samples of reference polypropylene and saturated with hexane. Deformation rate – $3.3\times10^{-3}s^{-1}$.

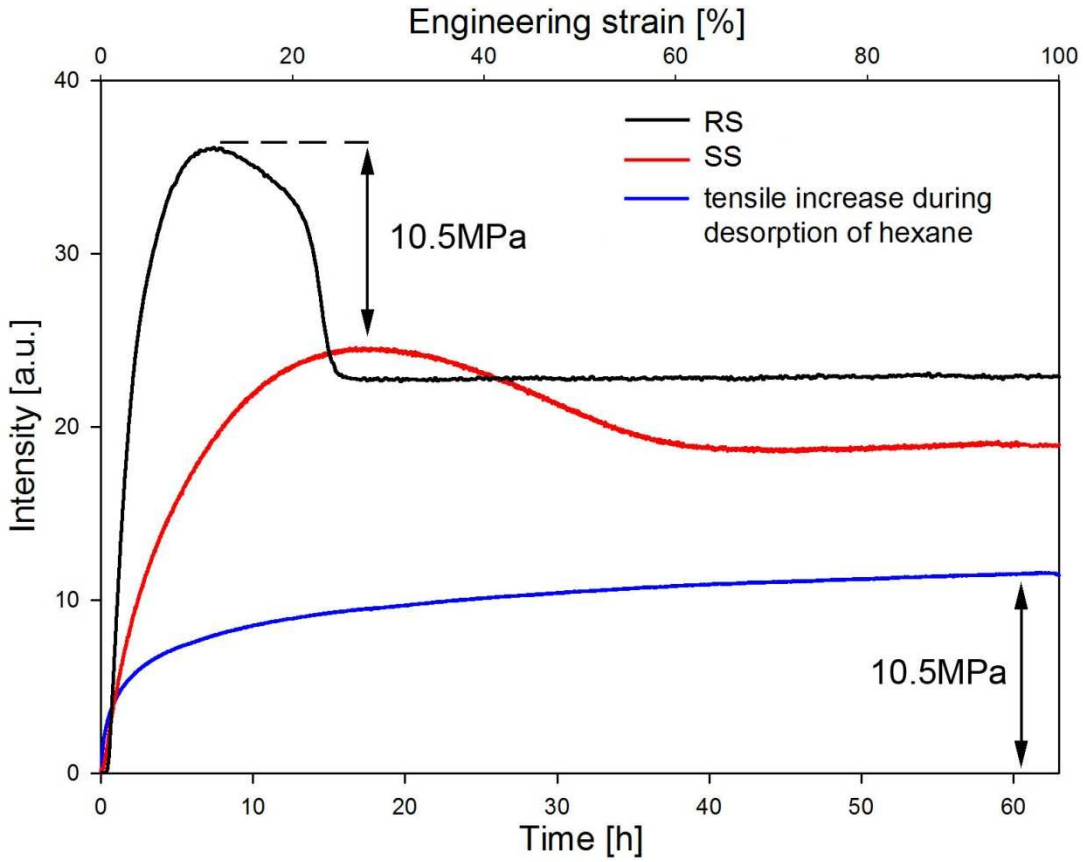

Fig. 51. Engineering strain - engineering stress curves for samples of reference polypropylene and saturated with hexane. Deformation rate – $3.3\times10^{-3}s^{-1}$. The blue curve shows the stress buildup on clamped swollen PP sample during evaporation of hexane.

After approximately 60 hours after removal of the sample from the conditioning vessel tensile increase in the sample equal to 10.5 MPa occurred, which corresponds to the observed stress difference at yield point between the dry and the soaked sample. Introduction of hexane molecules leads to strong swelling of the amorphous phase, resulting in its considerable deformation (no change in the structure of the crystalline phase of the material, change in the value of a long period). Distinctly swollen and stretch amorphous phase acts on the adjacent crystals with a stress equal to the value of the observed stress difference at yield point.

In order to assess the impact of the modifier filling the amorphous phase of the material on the phenomenon of cavitation during tensile drawing, *in-situ* small-angle X-ray scattering (SAXS) studies using synchrotron radiation have been conducted. Figure 52 presents SAXS scattering patterns

recorded for samples of reference polypropylene and saturated with hexane deformed to local strain up to 4.5.

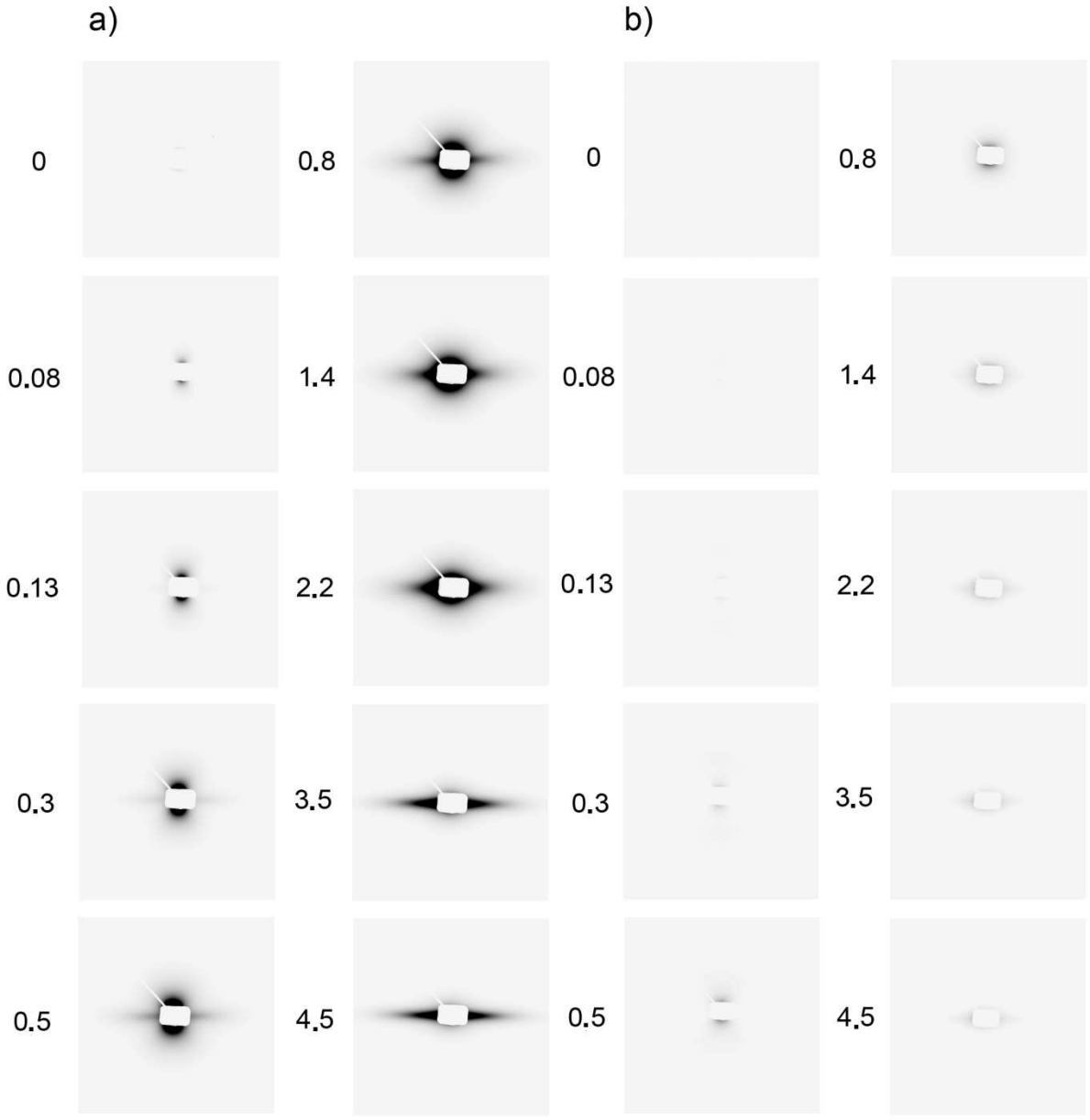

Fig. 52. Small-angle X-ray scattering patterns of a series of polypropylene samples a) RS; b) SS. Numbers correspond to local strain of samples. Direction of deformation – vertical.

Deformation of the reference sample proceeds as presented (Fig. 35) in the previous chapter. Deformation of the unmodified material is accompanied by an intensive process of formation of discontinuities in the material (cavities and dilatation microcracks)

SAXS scattering patterns recorded for polypropylene saturated with hexane presented in Figure 50b, for local strains analogous to RS sample, indicate complete elimination of the

phenomenon of cavitation. Up to the strain of 4.5 one does not observe any signals indicating formation of discontinuities in the material, such as cavities or dilatation microcracks. Filling the free volume of the amorphous phase effectively eliminates this response mechanism of the material. Only relatively weak signals from the crystalline-lamellar structure of the material can be observed.

Figure 53 presents volume strain measurements performed for samples of reference and hexane-soaked polypropylene. Deformation of unmodified polypropylene samples is accompanied by a strong volume increase (up to around 30%), a result of formation of cavities and dilatation microcracks. Filling the free volume of amorphous phase of a polymer with a low molecular weight penetrant eliminates formation of discontinuities in the material, which manifests itself in a lack of volume changes of samples during their deformation.

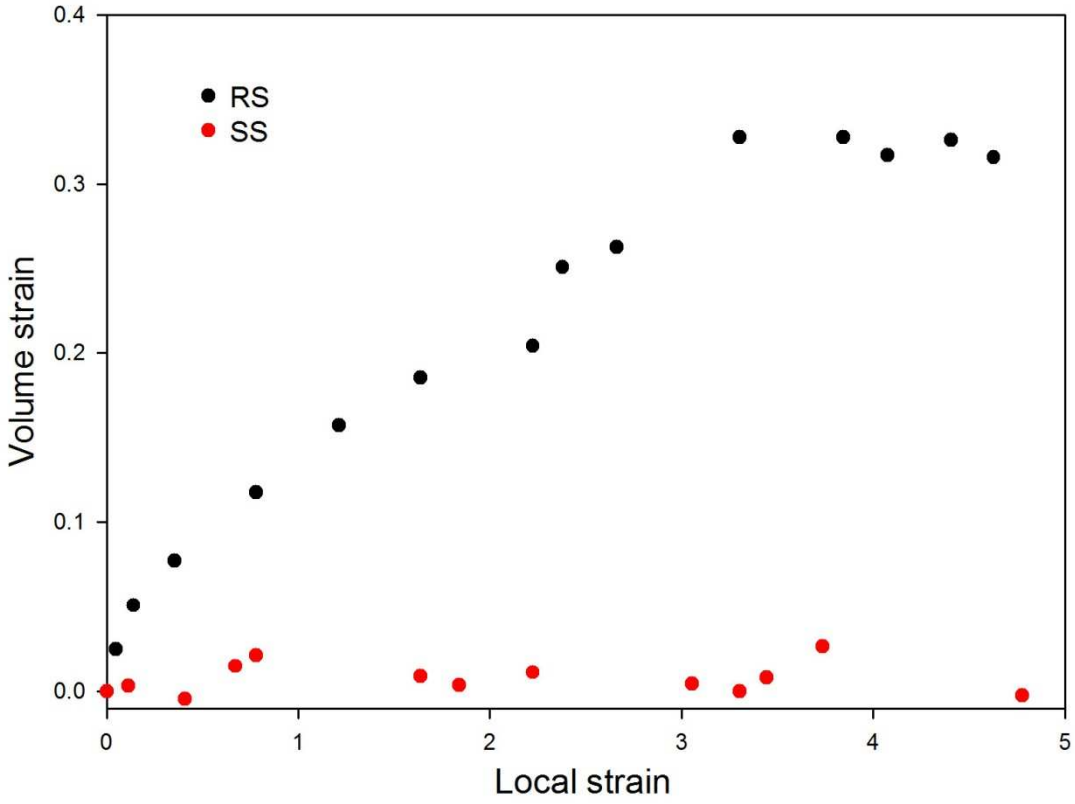

Fig. 53. Volume strain as a function of local strain for unmodified polypropylene (RS) and hexane-soaked (SS).

Density measurements were performed for the material modified with hexane, as in the case of polypropylene saturated with chloroform. Due to fast desorption of penetrant density measurements of the soaked sample were conducted approx. 16h after removal of the sample from a conditioning vessel (still significant content of the modifier, but relatively slow process of desorption of hexane). Relevant measurements and calculations are as follows:

-parameters of the sample before saturation:

m_0=0,05158g, d_0=0,09075g/cm^3 => $V_0=m_0/d_0$=0,0568cm^3

-parameters of the sample after saturation:

m_1=0,05286g, d_1=0,8998g/cm^3 => $V_1=m_1/d_1$=0,0587cm^3

-mass of hexane in the soaked sample:

$m_m=m_1-m_0$=0,05286g-0,05158g=0,00128g

-hexane volume in the soaked sample:

$V_m=m_m/d_m$=0,00128g/0,66g/cm^3=<u>0,00194c</u>m^3

-volume change of the sample as a result of introduction of the modifier:

$V_s=V_1-V_0$=<u>0,00186cm^3</u>

Similarly to the sample saturated with chloroform, the volume of hexane (V_m) introduced during modification of the material is higher than the change in the volume of the sample as a result of saturation (V_s). This indicates partial filling of pores of the free volume of amorphous phase of the material. In the given experiment conditions an excess of hexane in relation to the degree of swelling of the sample is 0.14% of the volume of the sample before saturation. Therefore, one can conclude that also in this case there is a relatively high degree of filling of the free volume of amorphous phase of the material, especially for the samples with a maximum degree of saturation (immediately after removal from the conditioning vessel) with a low molecular weight penetrant.

5.3. Modification of the amorphous phase of polyethylene.

Samples for tests were cut out from film, 1mm thick, prepared by compression moulding. The first batch of samples (soaked sample - SS) was placed in a vessel containing a penetrant (chloroform) in order to obtain full saturation of the amorphous phase with a low molecular weight liquid, whereas the second batch of samples (reference sample - RS) was not subjected to conditioning and provided reference material. The process of saturation of material with chloroform was run for at least 72 hours (up to full saturation of the amorphous phase).

In order to determine the quantity of chloroform present in the examined material on completion of the conditioning process, the TGA thermogram presented in Figure 54a has been recorded.

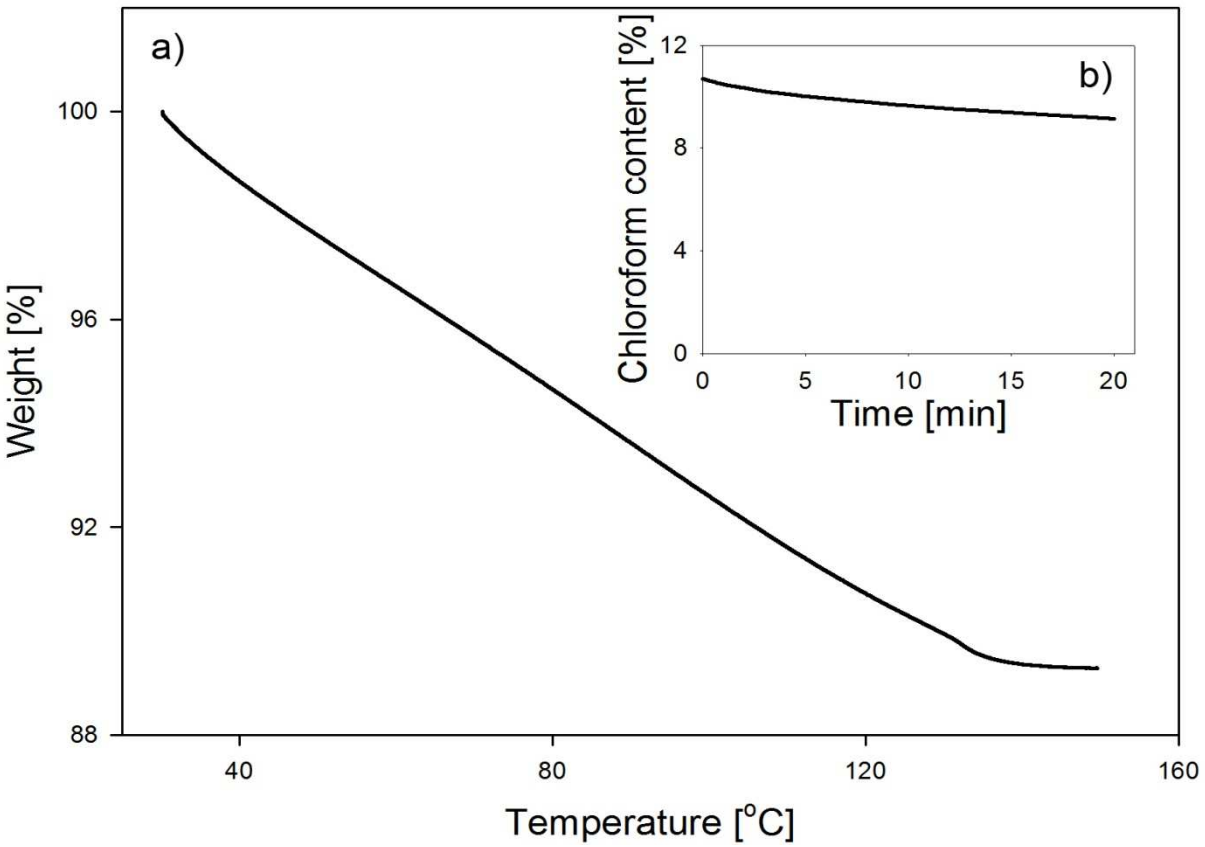

Fig. 54. Chloroform-soaked polyethylene: a) TGA thermogram; b) desorption kinetics of chloroform for SS sample under laboratory conditions, after removal from a liquid.

On the basis of the above thermogram the amount of chloroform in the examined material on completion of saturation has been determined as 10.7% (wt.) (7.2%vol.). Figure 54b also presents desorption kinetics of a modifier at room temperature after removal of the material from the conditioning vessel. The desorption of penetrant under laboratory conditions was found to be a relatively slow process, however some changes in the chloroform content after removal of the sample

from a liquid made it necessary to perform all measurements within max. 2 minutes after removal of the samples from the conditioning vessel.

Figure 55 presents WAXS diffractograms of RS and SS samples. The nature of the presented curves demonstrates no significant changes in the crystalline structure of the material as a result of chloroform sorption. Only decrease in the intensity of individual peaks is observed with the saturated sample, an effect of the introduction of chlorine atoms strongly absorbing X-ray radiation.

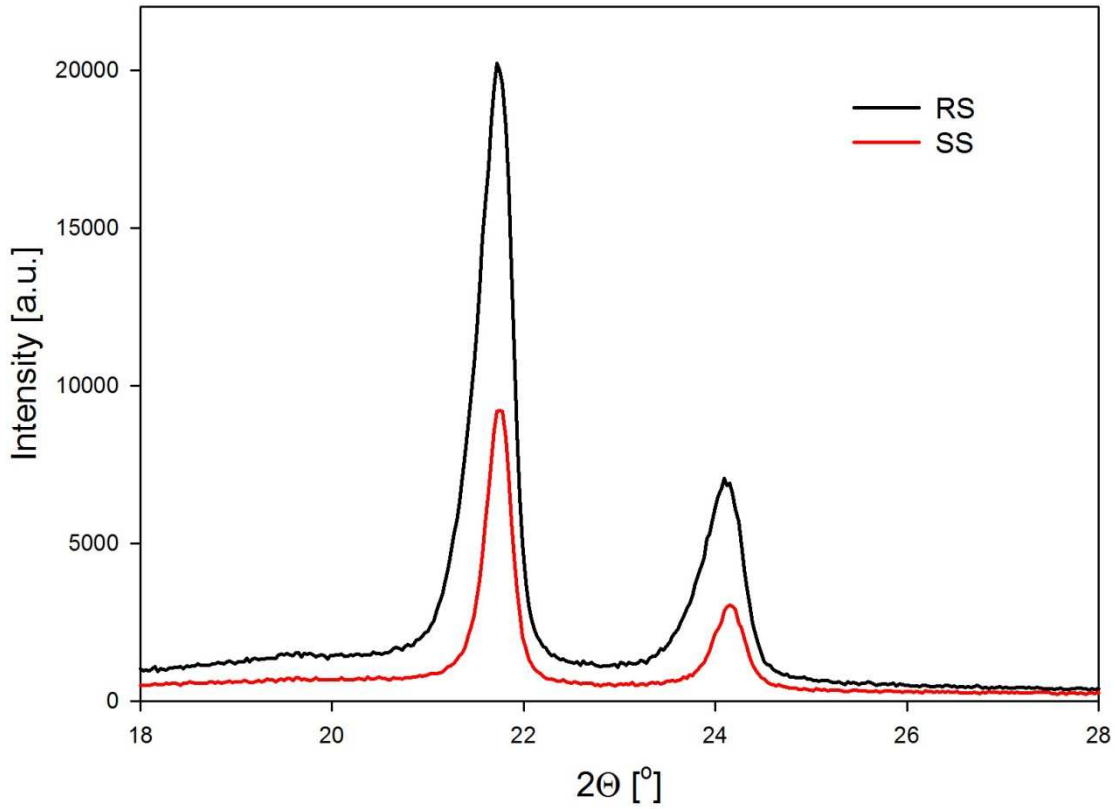

Fig. 55. Diffractograms of polyethylene samples.

Figure 56 also presents diffractograms of a polyethylene sample prior to the conditioning process (RS) and of the material saturated with chloroform and then deprived of the penetrant as a result of the drying process (RS-SS-RS). Presented wide-angle X-ray scattering measurements demonstrate not only complete reversibility of the sorption process of chloroform, but also the absence of any changes in polyethylene crystals as a result of the introduction and desorption of a penetrant. No changes in the parameters of polyethylene crystals prove a low molecular weight penetrant to be localized in the amorphous phase of the material.

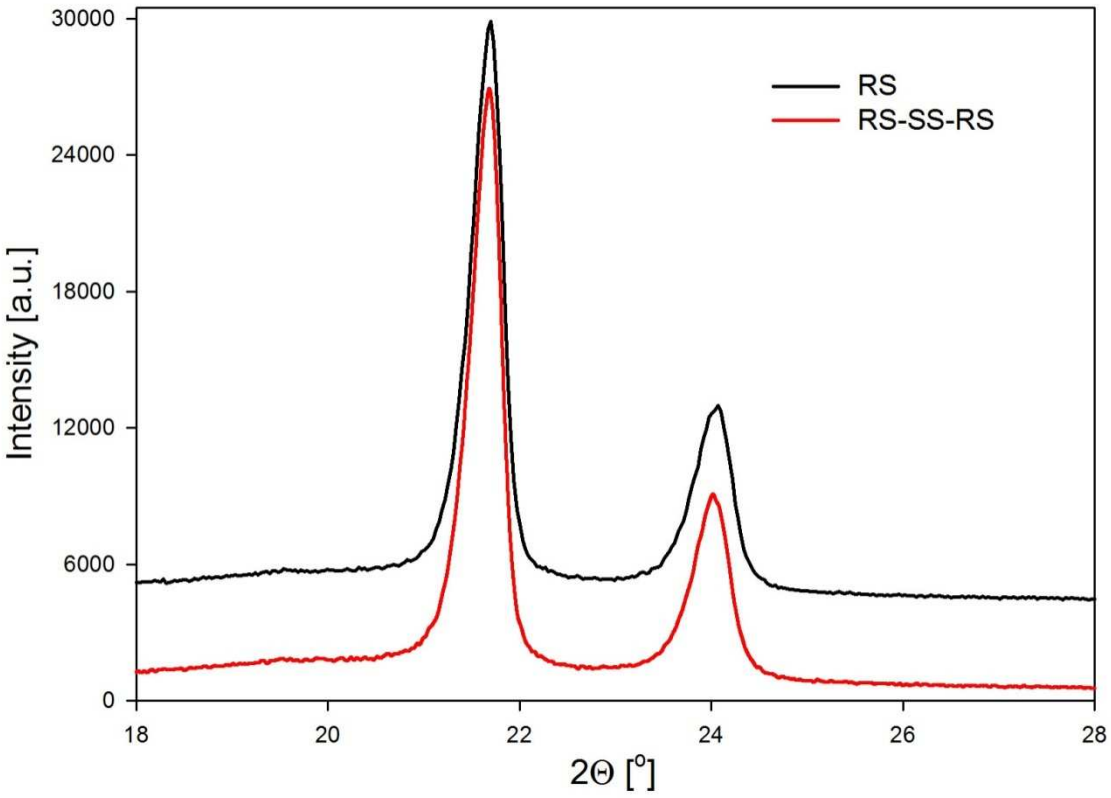

Fig. 56. Diffractograms of polyethylene samples. Curves have been shifted along the vertical axis for better visualization.

Fig. 57 presents results of measurements of a long period of polyethylene samples as a function of sorption time of a low molecular weight penetrant (chloroform).

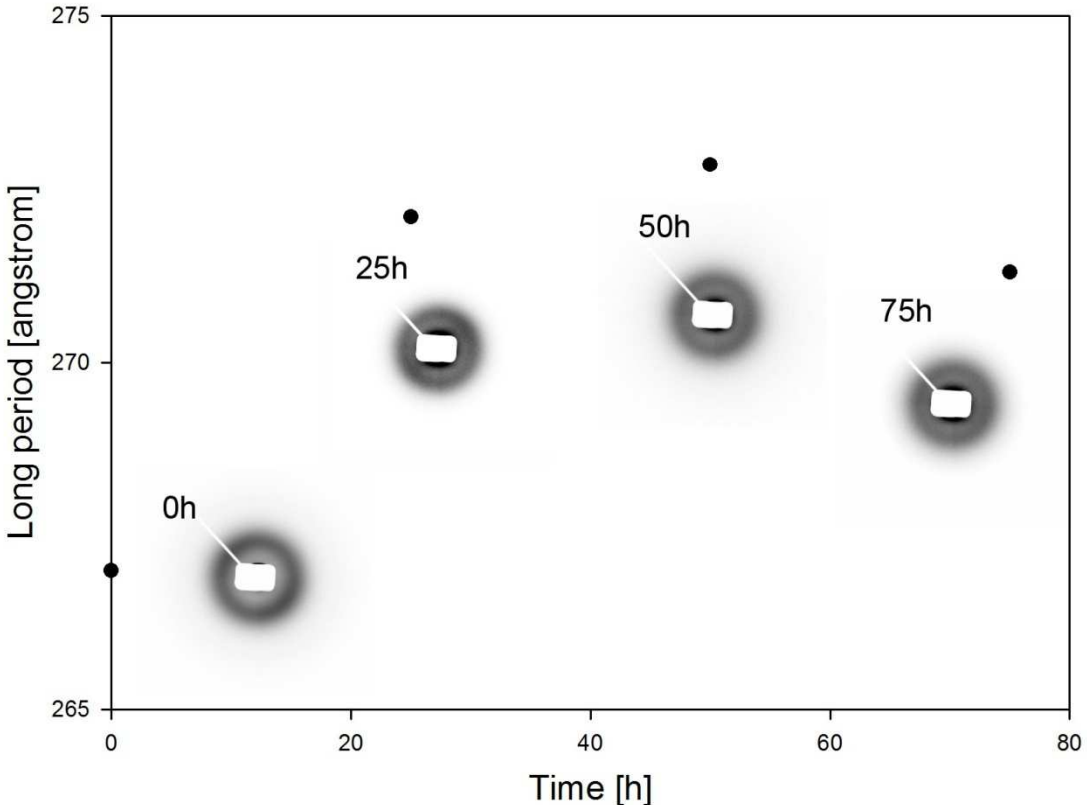

Fig. 57. Change in a long period of polyethylene as a function of time of sorption of chloroform.

Changes in the values of a long period in the samples saturated with a low molecular weight penetrant (266.8 Á for reference sample, around 272 Á for soaked sample), with minor changes in the crystalline regions, indicate an increase in the interlamellar distances as a result of strong swelling (deformation) of unordered regions with molecules of chloroform.

Using dynamic mechanical analysis (DMTA) viscoelastic properties of the analysed materials such as storage modulus (E '), loss modulus (E) and loss tangent (tg α) have been determined. Figure 56 presents relations between the said parameters and temperature.

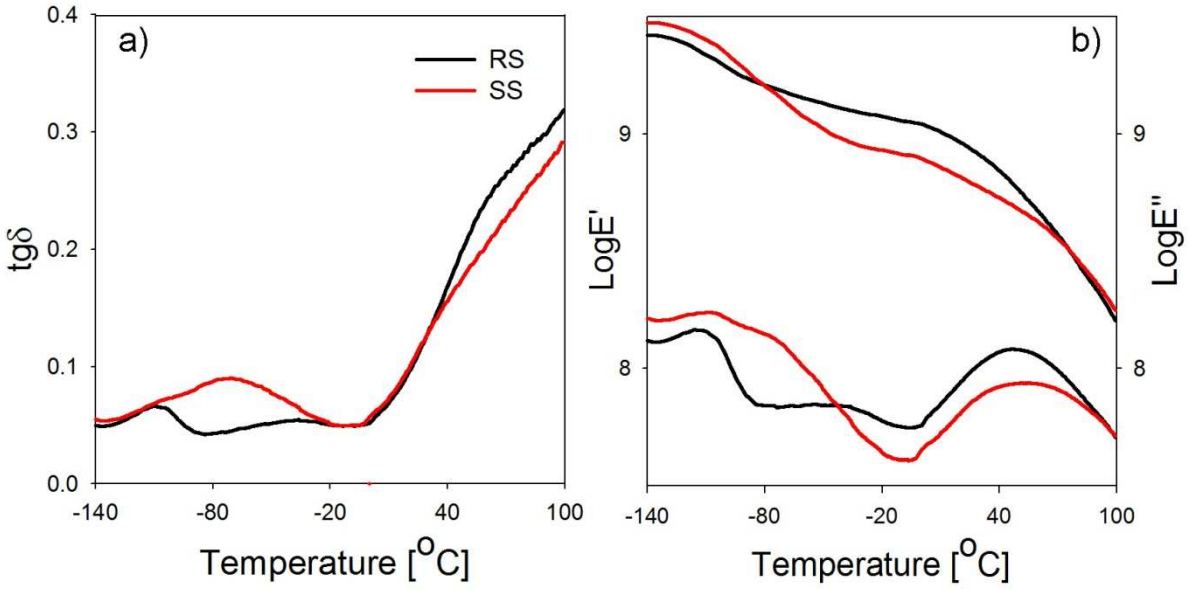

Fig. 58. Relations between loss tangent (a), storage modulus and loss modulus (b) and temperature of polyethylene samples determined by means of dynamic mechanical analysis (DMTA).

On the thermogram of unmodified polyethylene one can distinguish two relaxation processes: low temperature (γ) (-115^{o}C) corresponding to material's transition from the state of high elasticity to glassy state (glass transition temperature) and high temperature (α) (47^{o}C) associated with complex relaxation processes taking place in crystals. The introduction of penetrant molecules leads to significant changes in viscoelastic properties of the material. The visible effect is a shift of glass transition temperature of polyethylene towards higher values (-79^{o}C) that is probably caused by freezing of penetrated chloroform. In addition, one observes a small peak with a maximum at the temperature of -109^{o}C, in the region of glass transition temperature of unmodified polyethylene, which may indicate that part of the amorphous phase of material is free of penetrant molecules when chloroform is mostly frozen. The presence of molecules of chloroform, whose melting temperature is -63^{o}C, in a low temperature range leads to the "stiffening" of material, which manifests itself in a higher modulus of the soaked material recorded in this region of temperature (Figure 58b). For higher

temperatures, ranging from -80^{o}C up to a high temperature region, in which the stiffening of material occurs as a result of chloroform desorption, the modified polyethylene is characterized by a lower modulus in relation to the reference material as a result of an increased mobility of macromolecules and penetrant molecules.

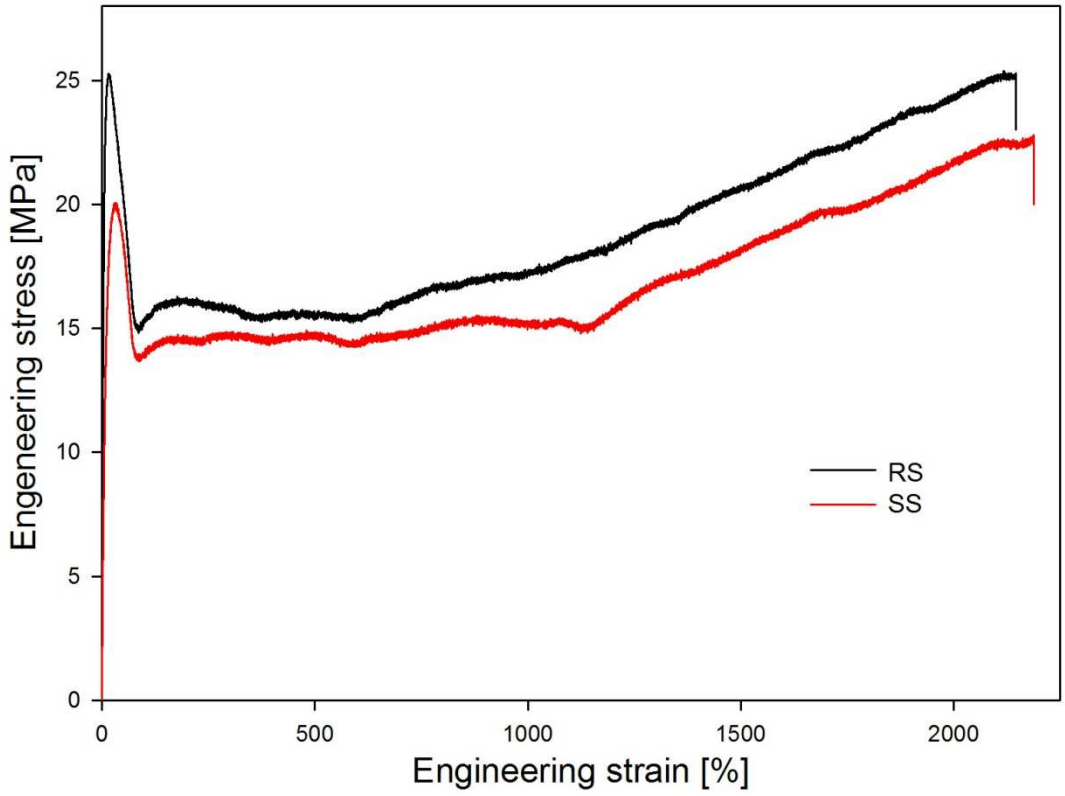

Fig. 59. Engineering strain - engineering stress curves for samples of unmodified polyethylene and saturated with chloroform. Deformation rate – $3.3\times10^{-3}s^{-1}$.

Figure 59 presents engineering stress - engineering strain curves for polyethylene samples subjected to tensile drawing. Deformation of unmodified polyethylene and saturated with chloroform was accompanied by the necking process. During deformation of the unmodified polyethylene strong whitening of the material occurred in the macroscopic yield point region, whereas the sample saturated with chloroform remained transparent up to rupture. Analysis of curves presented in figure 57 also points to strong dependence of stress at yield point on the presence of penetrantr filling the amorphous phase of material. The determined values are 25 MPa for RS sample and 20.1 MPa for SS sample, respectively. The introduction of penetrant molecules thus leads to decrease in stress at yield point by 4.9 MPa. The parameters of the crystalline phase of the soaked sample, as proved by X-ray examinations, remain unchanged as a result of sorption of chloroform. Thus, the observed difference in stress at yield point between the reference and the modified sample must be an effect of changes taking place in unordered regions of the material. Therefore, I performed the following experiment: a

sample saturated with chloroform, immediately after removal from a conditioning vessel, has been clamped in the apparatus for measuring mechanical properties and stress buildup in the sample as a function of time of desorption of the penetrant has been measured. Figure 60 presents the results of the experiment. After approximately 90 hours after removal of the sample from the conditioning vessel a stress buildup in the sample equal to 4.9 MPa was noted, which corresponds to the observed difference in the stress value at yield point between the dry and the soaked sample.

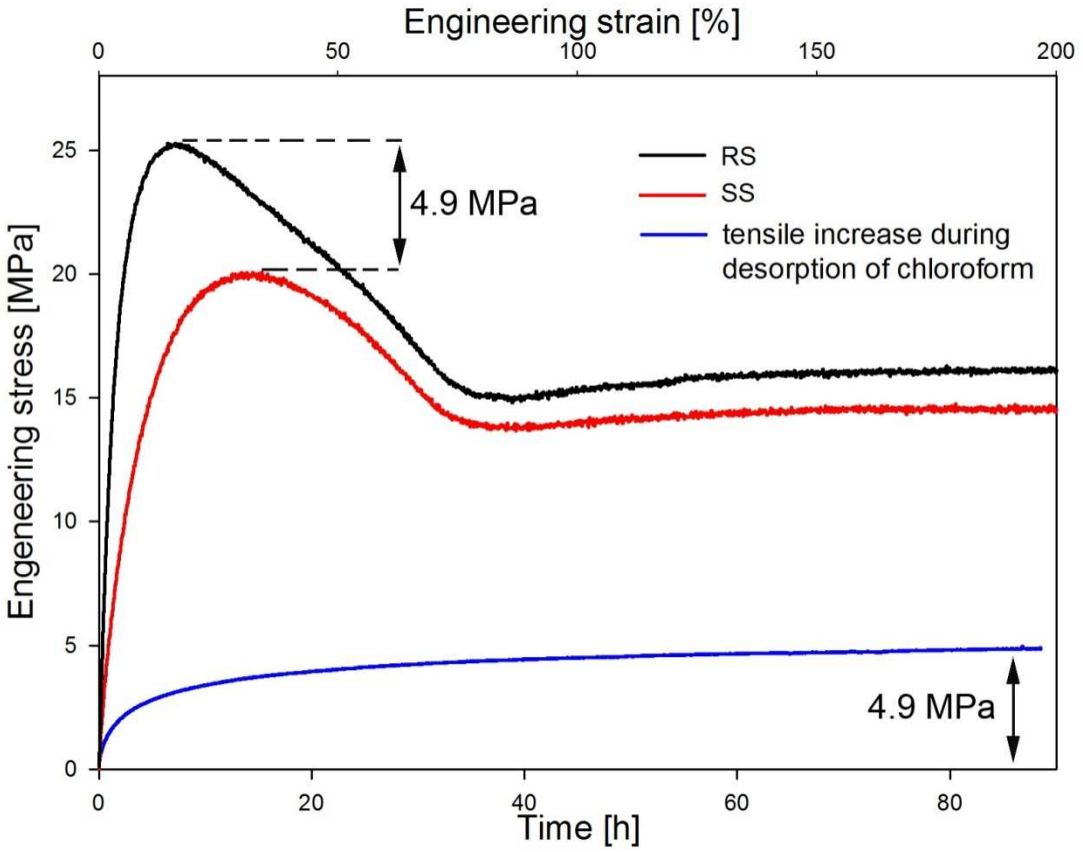

Fig. 60. Engineering stress - engineering strain curves for samples of reference and chloroform-soaked polyethylene. Deformation rate – $3.3\times10^{-3}s^{-1}$. The blue curve shows the stress buildup on clamped swollen PE sample during evaporation of chloroform.

The introduction of chloroform molecules leads to strong swelling of amorphous phase, which results in its considerable deformation (no changes in the structure of the crystalline phase of the material, change in the value of a long period). Distinctly swollen and stretched amorphous phase impresses the adjacent crystals with a force equal to the observed difference in the stress values at the yield point.

In order to assess the impact of the penetrant filling the amorphous phase of material on the phenomenon of cavitation during tensile drawing, *in-situ* small-angle X-ray scattering (SAXS) studies using synchrotron radiation have been conducted. Figure 61 presents SAXS scattering patterns

recorded for subsequent deformation stages of unmodified and chloroform-soaked polyethylene samples.

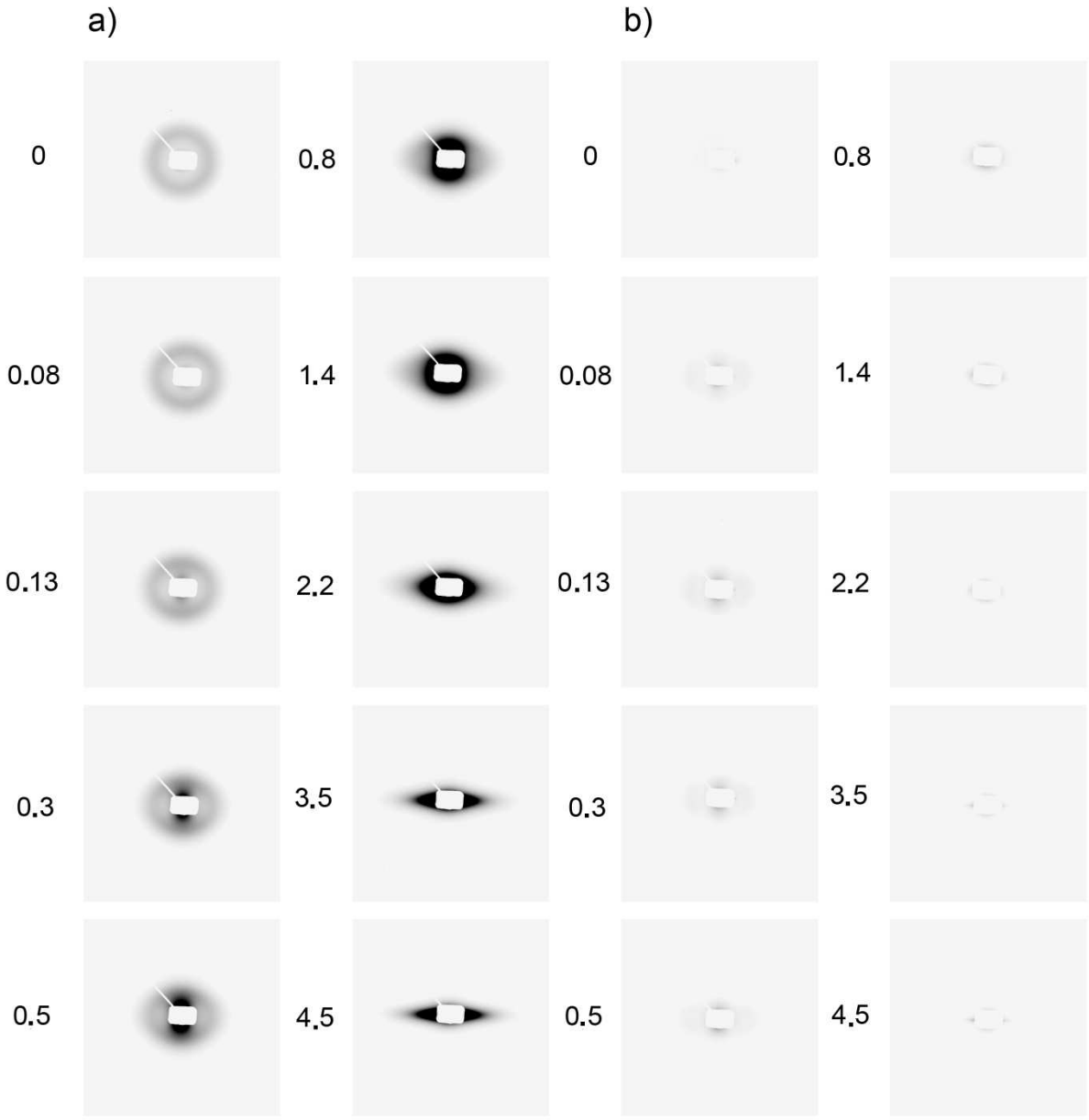

Fig. 61. Small-angle X-ray scattering patterns obtained *in situ* during deformation of a series of polyethylene samples a) RS; b) SS. Numbers correspond to local strain of samples. Direction of deformation – vertical.

Analysis of the presented scattering patterns proves a significant influence of the filling of the free volume of amorphous phase with a low molecular liquid on the phenomenon of cavity formation in polyethylene during its deformation. With unmodified polyethylene, the first signals on SAXS scattering patterns, indicating formation of discontinuities in the material, are observed at the local strain of 0.3. The recorded signal suggests that cavities at this stage of deformation, similarly as in the case of polypropylene, are of ellipsoidal shape and are oriented by their long axis perpendicularly to the

direction of deformation (signal in the meridional region on a scattering pattern). At further deformation stages an increase in the intensity of the registered signal occurs in the said region of scattering pattern, up to the local strain equal to 0.8. At this stage the maximum intensity of signal in the scattering pattern was reached and further deformation of the material is accompanied by strong scattering in the equatorial region at the cost of signal in the meridional region. This indicates change in the shape of cavities in relation to the direction of deformation. Cavities initially oriented perpendicularly to the direction of the applied stress, beyond the local strain of 0.8 are oriented parallel. Above the local strain of 2.2 one observes a strong, thin signal, mainly in the equatorial region, indicating strong orientation of cavities generated in the material parallel to the direction of the applied stress.

Deformation of polyethylene penetrated with a low molecular liquid is not accompanied by the process of formation of cavities. On the presented scattering patterns (Fig. 61) up to the local strain of 4.5 one does not observe signals indicating formation of discontinuities in the examined material. Filling the free volume of amorphous phase of the material effectively eliminates generation of cavities.

Conclusions drawn on the basis of small-angle X-ray scattering measurements are also confirmed by the volume strain measurements performed for the examined materials (Figure 62). Deformation of unmodified polyethylene is accompanied by a strong volume increase of the sample (up to approx. 25%), as a result of cavities generated in the material. X-ray examinations showed that the first cavities appear at the local strain equal to 0.3. Volume strain measurement, as a method less sensitive to subtle changes occurring in the material, demonstrates that only at a strain equal to 0.7 detectable discontinuities are generated in the material.

Volume strain measurements performed for polyethylene modified with chloroform prove the absence of changes in the morphology of the material (presence of cavitation) which would result in volume increase of the sample.

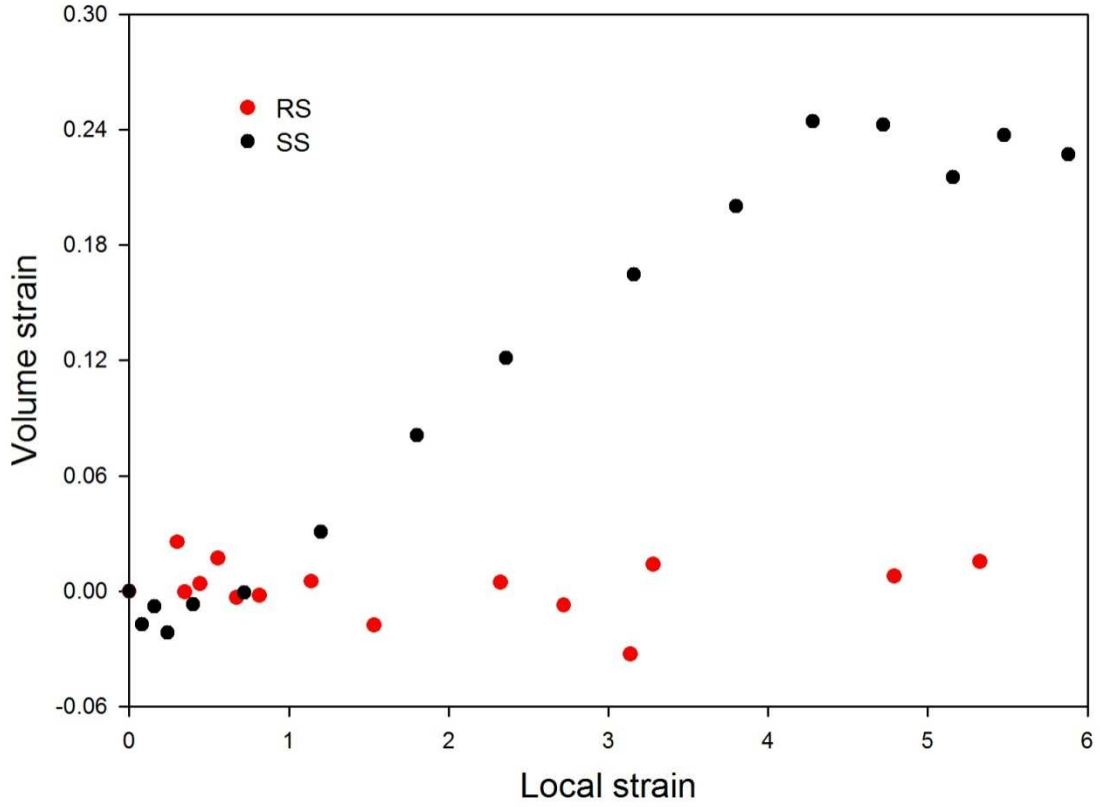

Fig. 62. Volume strain as a function of local strain for unmodified (RS) and chloroform-soaked (SS) polyethylene.

5.4. Modification of the amorphous phase of polyamide 6.

In the case of polyamide 6 I chose water as a low molecular weight penetrant of its amorphous phase. There are several reports indicating that water infused into amorphous phase of polyamide 6 while crystalline phase is unaltered (see for example Seguela et al. [23] and references cited there). Three types of samples of polyamide 6 of different water content have been prepared. Samples for studies were cut out from 1 mm thick film, prepared by compression moulding. In order to standardize the water content and the crystalline structure of the analyzed material, the prepared samples were annealed under vacuum at 105^{o}C to a constant weight. After drying, the first batch of samples (DS - dry sample) was immediately placed in a container with phosphorus (V) oxide. The applied procedure enabled to retain low water content in the samples. Another group of samples (MS – moist sample) was subjected to conditioning under laboratory-like conditions (temperature 23ºC, relative humidity around 50%). The last batch of samples (WS – wet sample) was immersed directly in distilled water to obtain a material with the maximum content of penetrant. For each group of samples conditioning in the given conditions ran for at least 72 hours.

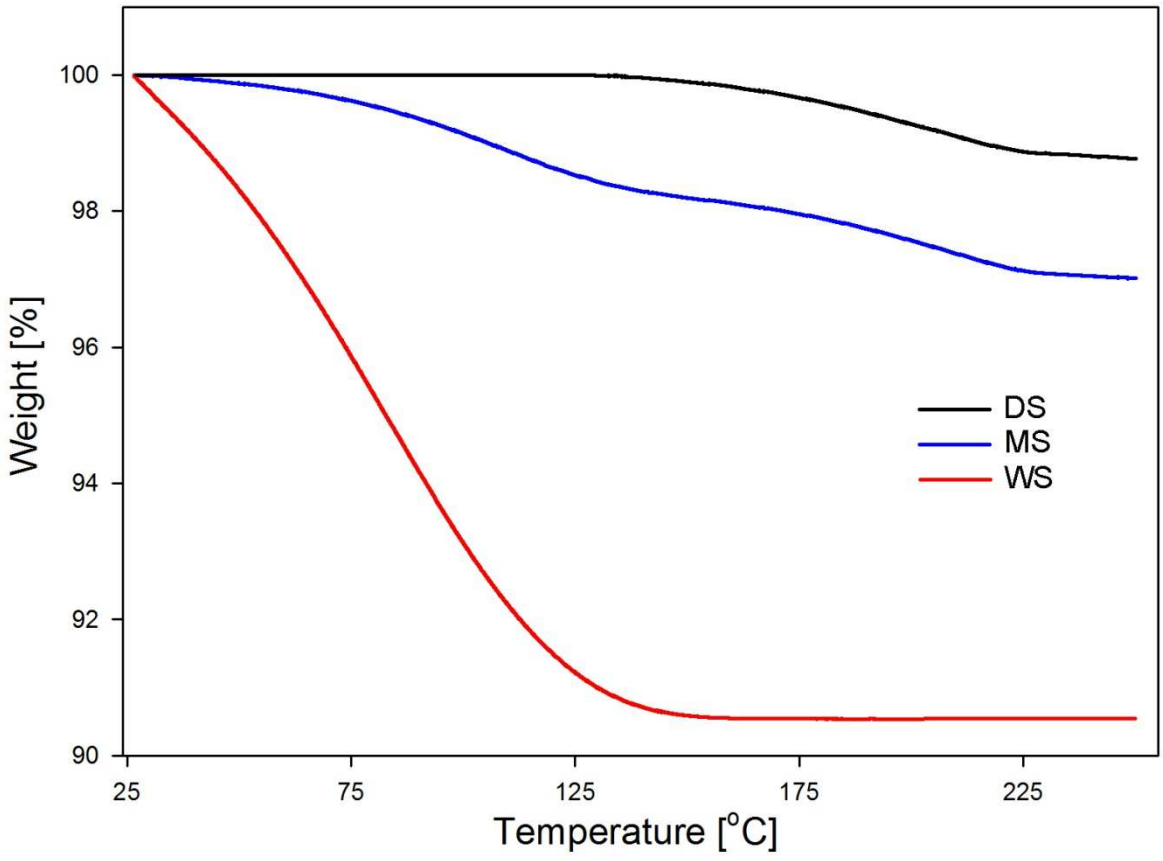

Fig. 63. TGA thermograms of polyamide 6 samples of different water content.

Figure 63 presents TGA thermograms recorded for samples of polyamide 6 of different water content. The conditioning procedure of the samples discussed in the previous paragraph, allowed to obtain the material of clearly different modifier content (water). As expected, samples placed in a container filled with a highly hygroscopic substance immediately after the annealing process, were characterized by the lowest humidity (1.1%). Samples conditioned at the humidity around 50%, due to a natural tendency of polyamide 6 to absorb water, contained nearly three times more water (2.95%). Samples immersed directly in water contained the highest amount of water. For such conditioned samples water content was estimated as 9.45%.

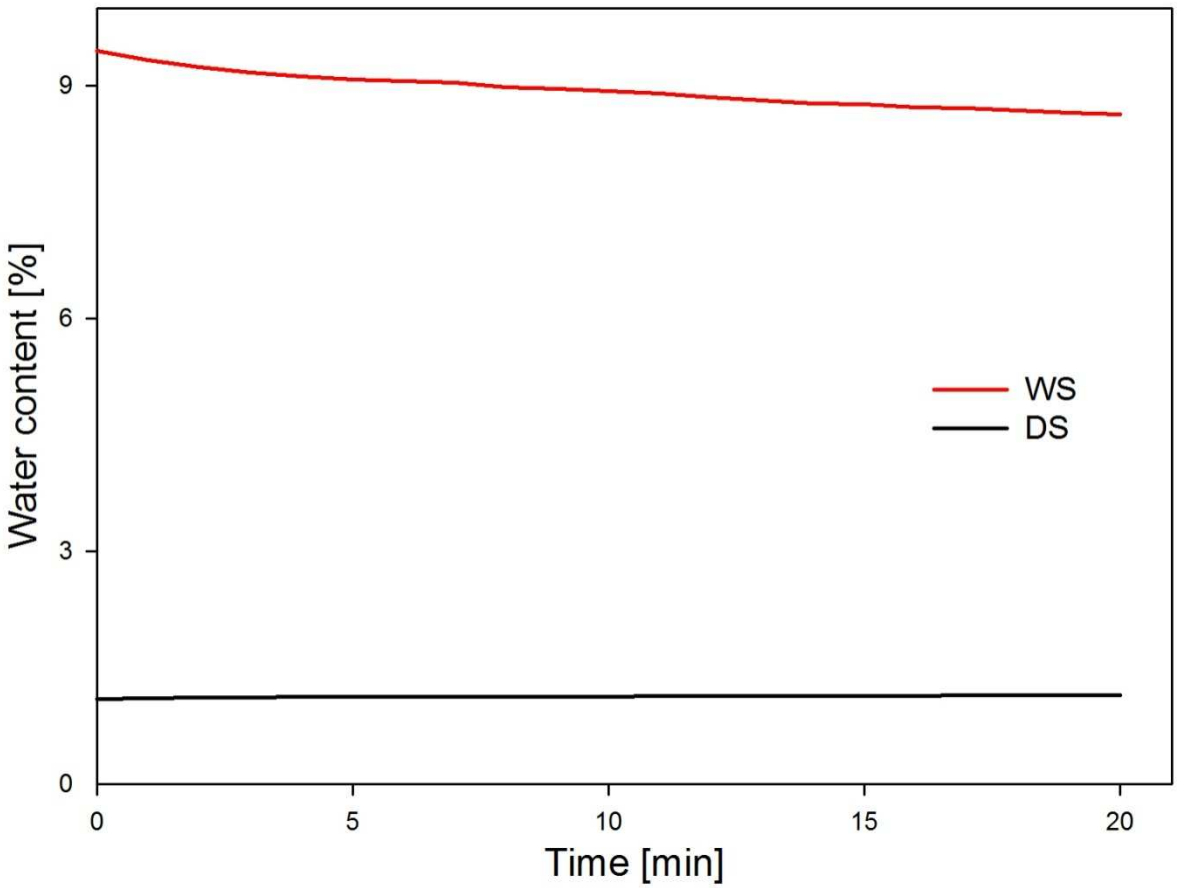

Fig. 64. Kinetics of sorption (for DS sample) and desorption of water (for WS sample) under laboratory conditions, relative humidity around 50%, temperature 23^{o}C.

Sorption of water by DS samples after removal from a conditioning vessel, as well as desorption of penetrant at room temperature for samples with the highest water content – WS (Fig. 64) removed from a liquid, are relatively slow processes. Hence, one could assume relative stability of the penetrant content in the examined material, especially during mechanical and X-ray studies.

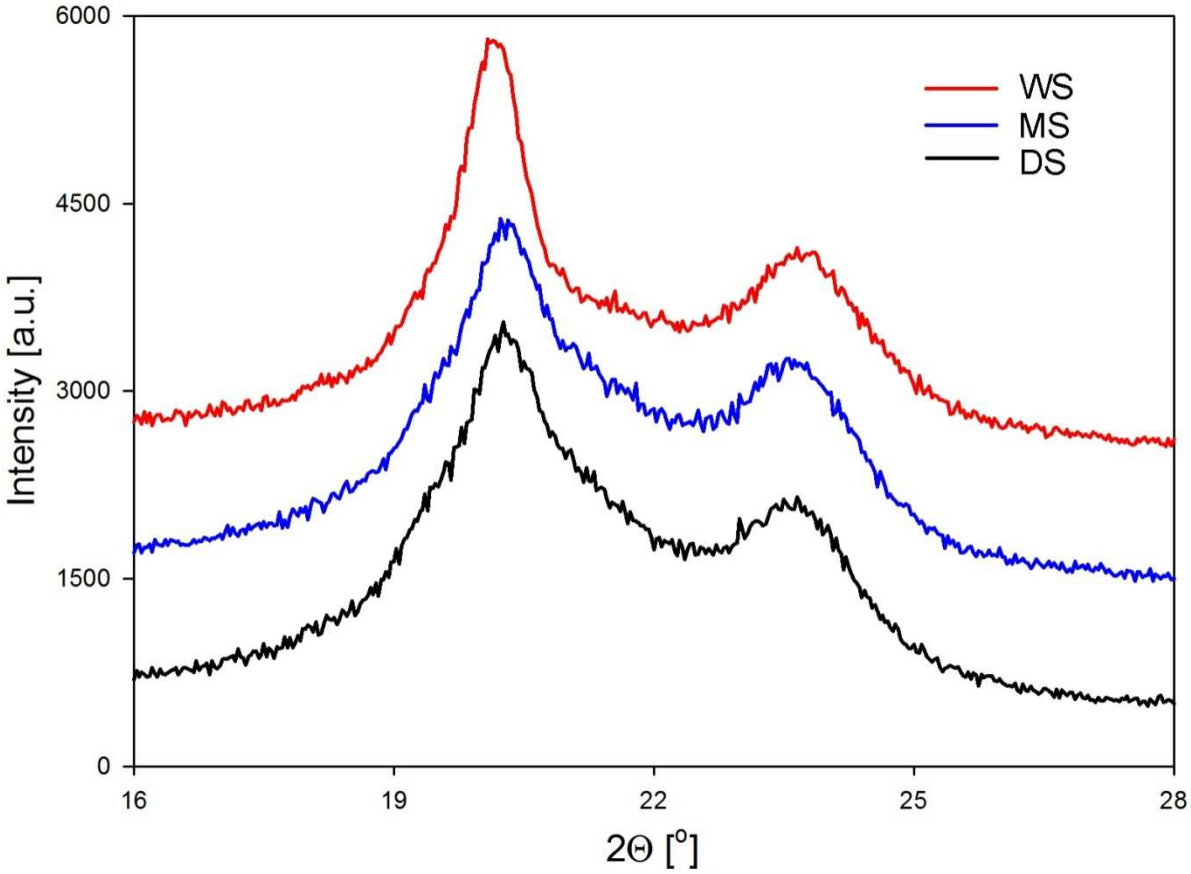

Fig. 65. Diffractograms of PA6 samples of different water content. Graphs have been shifted along the vertical axis for better visualization.

Fig. 65 presents WAXS diffractograms for polyamide 6 samples of different water content. The presented profiles indicate no significant changes in the crystallographic structure of the samples [α-phase – monoclinic with characteristic peaks located at 2θ=20.3^{o} and 23.3^{o}, corresponding to crystallographic planes (200) and (002) + (202)], as a result of introduction of a modifier, which is confirmed by the literature data [16] demonstrating that during sorption of water, modifier is preferentially accumulated in the amorphous phase of the material.

One can only observe a slight separation [shift of the maximum of the peak corresponding to crystallographic plane (200) towards lower values of 2theta angle and shift of the signal from **(**002) + (202) planes towards higher values of 2theta angle] of the registered peaks of the crystalline component. The phenomenon was registered during wetting and annealing of polyamide 6 [24-26]. Separation of peaks of the crystalline component initiated by wetting of the material is a reversible process. In both cases, the change in the position of the mentioned signals is interpreted as a change in the crystal perfection [24-26].

Fig. 66 presents measurement results of a long period as a function of time of sorption of a low molecular weight penetrant (water). Changes in the values of a long period in the samples saturated with a low molecular weight penetrant (84.4 Á for reference sample, 88.1 Á for water-

soaked sample), with insignificant (if any) changes in the crystalline regions, indicate an increase in the interlamellar distances as a result of strong swelling (deformation) of unordered regions with molecules of water.

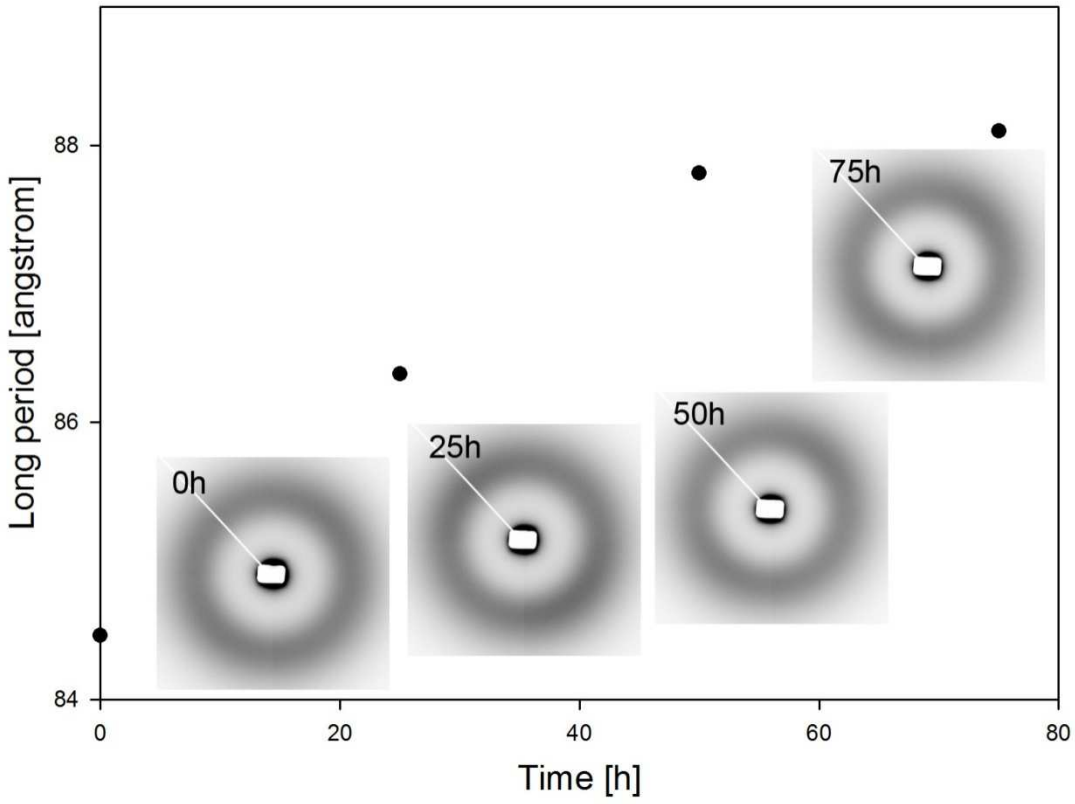

Fig. 66. Change in a long period of polyamide 6 as a function of time of sorption of water.

Viscoelastic properties such as storage modulus (E '), loss modulus (E") and loss tangent (tg α) have been determined for samples of different degree of water content using dynamic mechanical analysis (DMTA). Figure 67 presents relations between these parameters and temperature. The presented curves indicate the presence of relaxation processes α and β typical of polyamide 6. Relaxation transition α, corresponding to glass transition of material at the temperature of 58^{o}C for DS sample, is strongly related to the degree of saturation of the amorphous phase with water. Increasing the amount of water in the amorphous phase of the material leads to temperature decrease corresponding to α transition. For WS sample, a strong signal from the amorphous phase, strongly plasticized by the introduced water, is observed at the temperature of -25^{o}C and a signal at the temperature of 60^{o}C from relaxation processes of the same type, taking place in the part of the material resistant to sorption of the used penetrant.

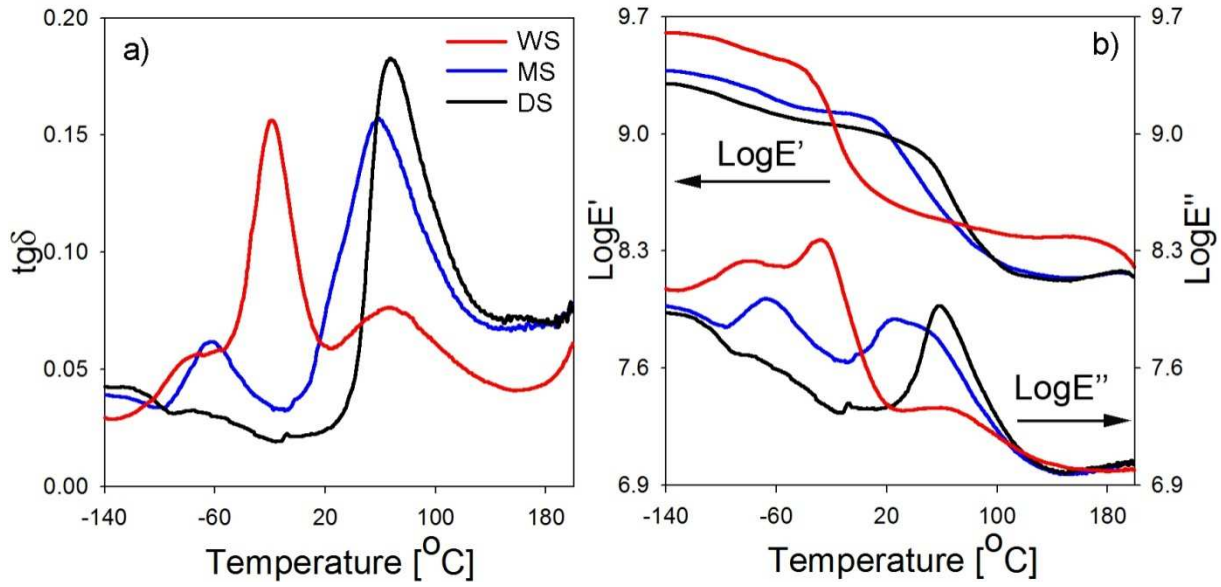

Fig. 67. Relations between loss tangent (a), storage modulus and loss modulus (b) and temperature for polyamide 6 samples of different water content determined by means of dynamic mechanical analysis (DMTA).

β relaxation processes, corresponding to relaxation of amide groups in the presence of hydrogen bonds, also strongly depend on the degree of water in the material. For the sample with the lowest water content, β relaxation transition takes place at the temperature of -46°C, whereas in the case of the HS samples the presence of additional molecules of water in the amorphous phase of the material leads to reduction of the maximum of the relaxation transition by 18°C, to -64°C. Due to apparatus limitations temperature of β relaxation peak could not be determined for WS sample.

Figure 68 presents engineering stress - engineering strain curves for samples of polyamide 6 of different water content, subjected to tensile drawing. The test was conducted up to rupture of the sample. Deformation of DS samples was accompanied by the necking process. For samples with the highest water content deformation proceeded in a homogenous manner, along the entire gauge length of the sample. In the case of MS samples deformation ran in an intermediate manner - a neck was formed, though the degree of its localization was relatively low. Analysis of curves presented in the Fig. 68 points to strong dependence of stress at yield point on the water content in the material. The values are 65 MPa for DS sample, 56 MPa for MS sample and 25 MPa for WS sample respectively. Therefore, introduction of penetrant's molecules leads to reduction of stress at yield point. The observed decrease is strongly related to the amount of water absorbed by the material. Parameters of the crystalline phase of the water-soaked sample, as proved by X-ray examinations, remain unchanged as a result of sorption of the modifier. Hence, the observed difference of stress at yield point between the reference and the modified sample has to result from changes taking place in the unordered regions of the material. Therefore, I planned and carried out the following experiment:

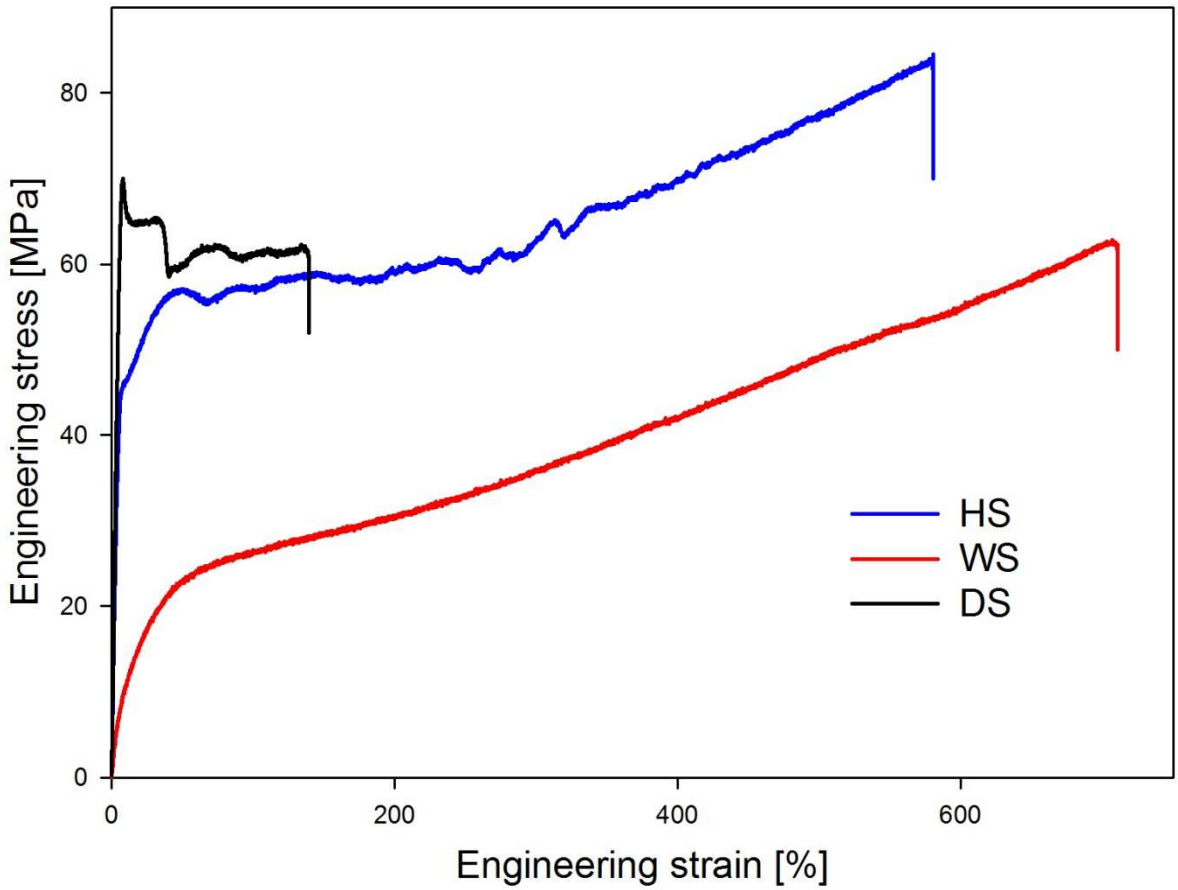

Fig. 68. Engineering stress - engineering strain curves for samples of polyamide 6 of different water content. Deformation rate – $3.3\times10^{-3}s^{-1}$.

a sample saturated with water (9.45%), immediately after removal from a conditioning vessel, has been clamped in the apparatus for measuring mechanical properties and stress buildup in the sample as a function of time of desorption of the penetrant has been measured. Figure 69 presents the results of the experiment. After over 65 hours since removal of the sample from the conditioning vessel stress buildup in the sample equal to 6.8 MPa was noted. The obtained value was significantly smaller than the observed difference in stress at yield point between MS and WS sample. Hence, an additional experiment (tensile drawing) was carried out for the sample saturated with water (WS) and next removed from the liquid and stored under laboratory conditions for 65 hours (Fig. 69). As a result of desorption of water (in laboratory conditions for 65 hours) tensile increase at yield point, of 6.8 MPa, was noted in relation to WS sample (Fig. 69, black curve), which corresponds to the measurement value of tensile increase in the sample as a result of desorption of modifier (Fig. 69, blue curve). Desorption of water from polyamide 6 under laboratory conditions is not efficient enough to reduce the amount of the modifier in the material up to the level corresponding to MS sample. One may only assume, as in the case of the aforementioned materials, that the reduction of stress at yield point depends only on the degree of saturation of the amorphous phase with a low molecular penetrant.

Also in the case of polyamide 6 distinctly swollen amorphous phase acts on the adjacent crystals with a force equal to the value of the observed difference in stress at yield point between materials of different water content, proportionally to the amount of water filling the unordered regions.

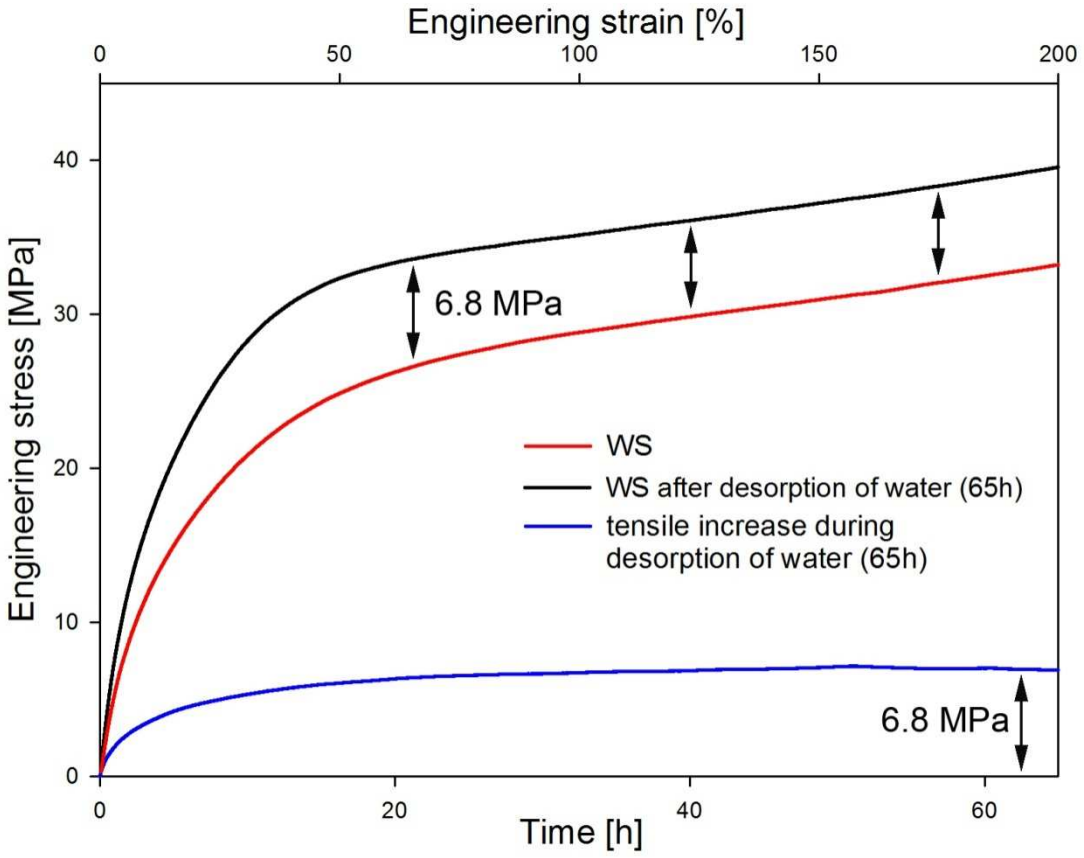

Fig. 69. Engineering strain - engineering stress curves for samples of polyamide 6 saturated with water and sample WS deformed 65hours after removal from a conditioning vessel. The blue curve shows the stress buildup on clamped swollen PA6 sample during evaporation of water.

In order to assess the influence of the water content in the amorphous phase of polyamide 6 on cavitation during tensile drawing, small-angle X-ray scattering studies (SAXS) have been conducted. As it was mentioned, SAXS method is a very useful tool for examination of cavities in materials. Figure 70 presents SAXS scattering patterns registered for subsequent deformation stages during *in-situ* studies using synchrotron radiation. Analysis of the presented scattering patterns proves how strongly the phenomenon of formation discontinuities in the material is influenced by the degree of saturation of the amorphous phase with water. Deformation of MS sample, that is material whose degree of saturation with water is close to the level corresponding to a typical water content in the material during its use in standard conditions, is accompanied by cavitation, however, the intensity of the process is relatively small. This is confirmed by the results presented in the paper [17], which suggested the possibility of formation of cavities in polyamide 6. However, according to the authors of

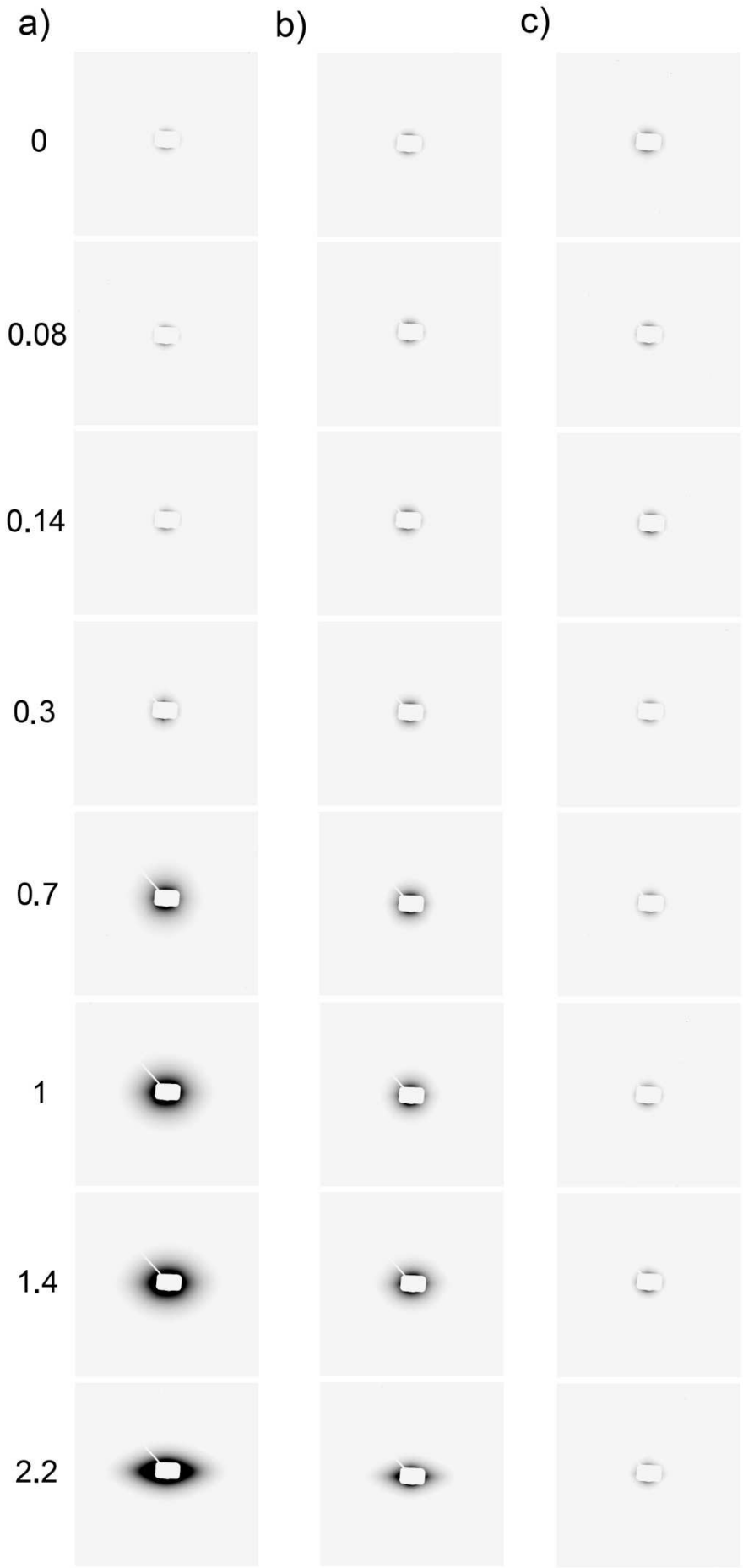

Fig. 70. Diffractograms of small-angle X-ray scattering of a series of samples of different water content: a) DS; b) MS; c) WS. Figures correspond to local strain of samples. Direction of deformation – vertical.

the mentioned paper, cavities formed during deformation, are instable due to small size and close during deformation or shortly after the release of stress. The first SAXS signals from cavities are observed at the local strain of 0.7 (Fig. 70b). At this deformation stage cavities of ellipsoidal shape, as in the case of polyolefins, are oriented by their long axis perpendicular to the direction of deformation.

The presence of objects with such parameters is confirmed by a signal in the meridional region on a SAXS scattering pattern. Such a shape of cavities is forced by the lamellar structure of the material. Studies on polyamide 6, based on microphotographs recorded using transmission electron microscopy and the process of contrasting samples with the use of osmium oxide, presented by Galeski et al. [17], indicated the possibility of formation of cavities, particularly intensively in the equatorial region of a spherulite, in which the specific arrangement of crystallites facilitates formation of ellipsoidal cavities in the interlamellar regions. At further deformation stages, at the local strain exceeding 1, one can also note on a scattering pattern a signal from cavities oriented parallel to the direction of deformation (signal in the equatorial region.) The observed effect is the result of changes in the interlamellar distances and lamellar fragmentation taking place at this stage of plastic deformation. At the local strain equal to 2,2 a thin, intensive signal is observed on a scattering pattern, mainly in the equatorial region, indicating strong orienation of the cavities generated in the material parallel to the direction of the applied stress.

Drying of polyamide 6 (DS sample), whose effect is reduction of the water content in the material up to 1.1%, considerably influences the process of cavity formation during deformation of the material (Fig. 70a). The first signals from cavities on SAXS patterns begin to appear at the local strain of 0.3. As in the case of MS samples, cavities are initially elongated perpendicular to the direction of the applied stress. At further stages of deformation, as a result from changes taking place in the lamellar structure of the material, one also observes changes in the shape of cavities (signal in the equatorial region on a diffractogram). Although the initial shape of cavities observed in DS samples and the process of their reorganization recorded as a result of activation of subsequent plastic deformation mechanisms is similar to the mechanism of cavitation in MS sample, the intensity of the the cavitation process is much stronger in the dried samples.

A reverse effect has been observed for WS samples (Figure 70c). Maximum saturation of the amorphous phase of the material with water led to the complete elimination of cavitation during tensile

drawing of such modified material. On presented scattering patterns, up to the local strain of 2.2, no signals indicating the presence of cavities generated during deformation of the material were recorded.

Fig. 71 presents measurements of volume strain as a function of the local strain for the given materials. Analysis of these results confirms results obtained from X-ray measurements. In the case of material with the lowest water content, strong increase in volume accompanying deformation was observed, up to 30%. Such a strong change in the parameters of a sample is the result of intensive cavitation during deformation of the material. Only initially tensile drawing of DS sample is accompanied by the negative volume change, which can be accounted for by better packing of the material as a result of the applied stress. At further stages of deformation of the material, when the first signals from cavities are recorded on SAXS scattering patterns, one observes a strong increase in volume as a result of cavitation.

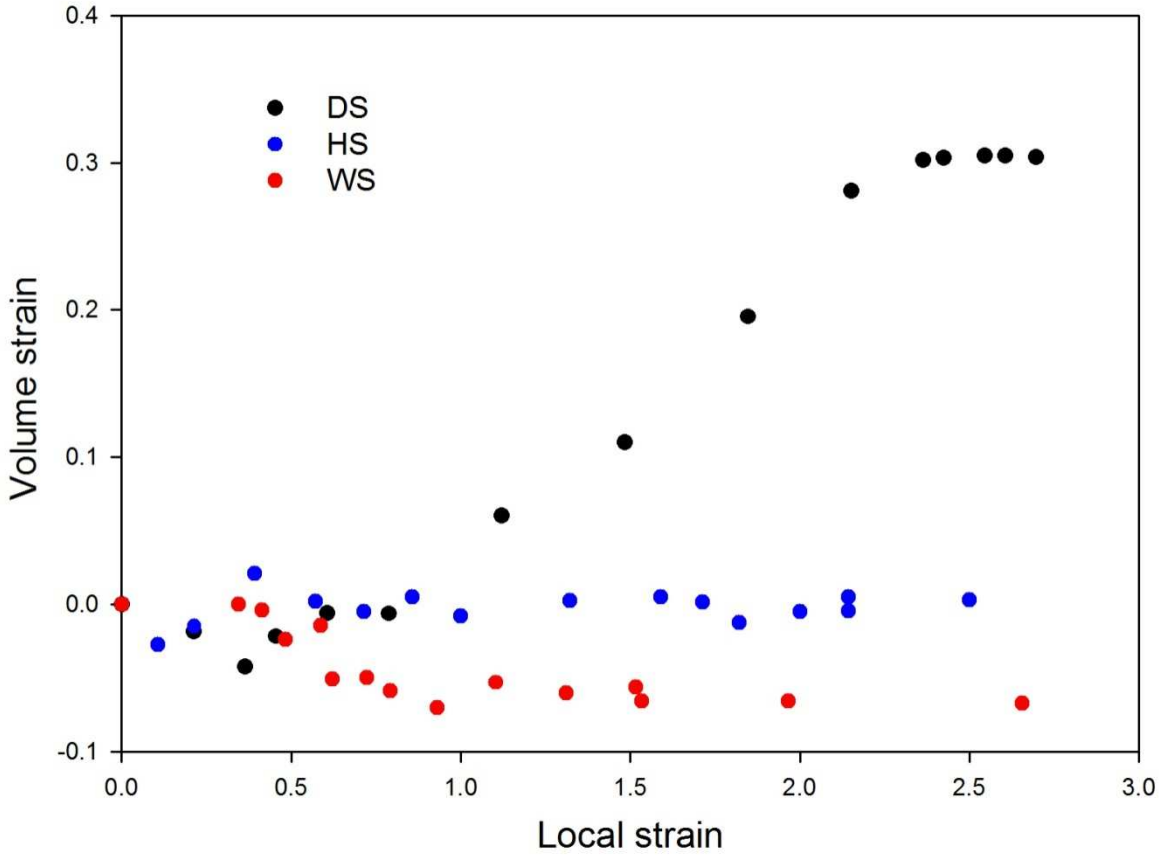

Fig. 71. Volume strain as a function of local strain for polyamide 6 of different degree of saturation with water.

Also volume strain measurements during deformation of the material with the maximum degree of water saturation demonstrate that cavitation in the material is completely eliminated as a result of filling the amorphous phase with the penetrant. Relation between the volume strain and the

degree of deformation of WS sample, presented in Figure 71, does not exhibit typical changes observed in the strongly cavitating materials. One observes a few per cent decrease in the volume of the sample as a result of tighter packing of the material, resulting from plasticization of the material with molecules of water, elimination of cavitation and orientation of the amorphous material as a result of tensile drawing.

In the case of polyamide 6 conditioned in laboratory conditions, no significant changes in the volume of the samples at subsequent stages of deformation are observed. Increase in volume, a result of relatively weak cavitation registered during X-ray examinations (Figure 71b), is compensated by changes in the structure of the material leading to closer packing of the material.

5.5. The influence of cavitation on the course of deformation of polypropylene.

Mechanical properties of polymers strongly depend on parameters such as temperature and deformation rate. By changing the value of the above parameters one can influence the macroscopic properties of polymer materials. There are reports [18-20], whose authors demonstrated the influence of these factors on the stress at yield point for a series of polymers of very different kinds. The following dependency has been observed: an increase in the stress value at the macroscopic yield point with an increase in deformation rate or a decrease in temperature at which the material deformation was conducted.

Figure 72 presents strain rate positive jump experiment for polypropylene sample**.** The strain rate jumps were made when the drawing reached the plastic flow region. During the experiment the temperature of the sample was monitored at different stages of deformation.

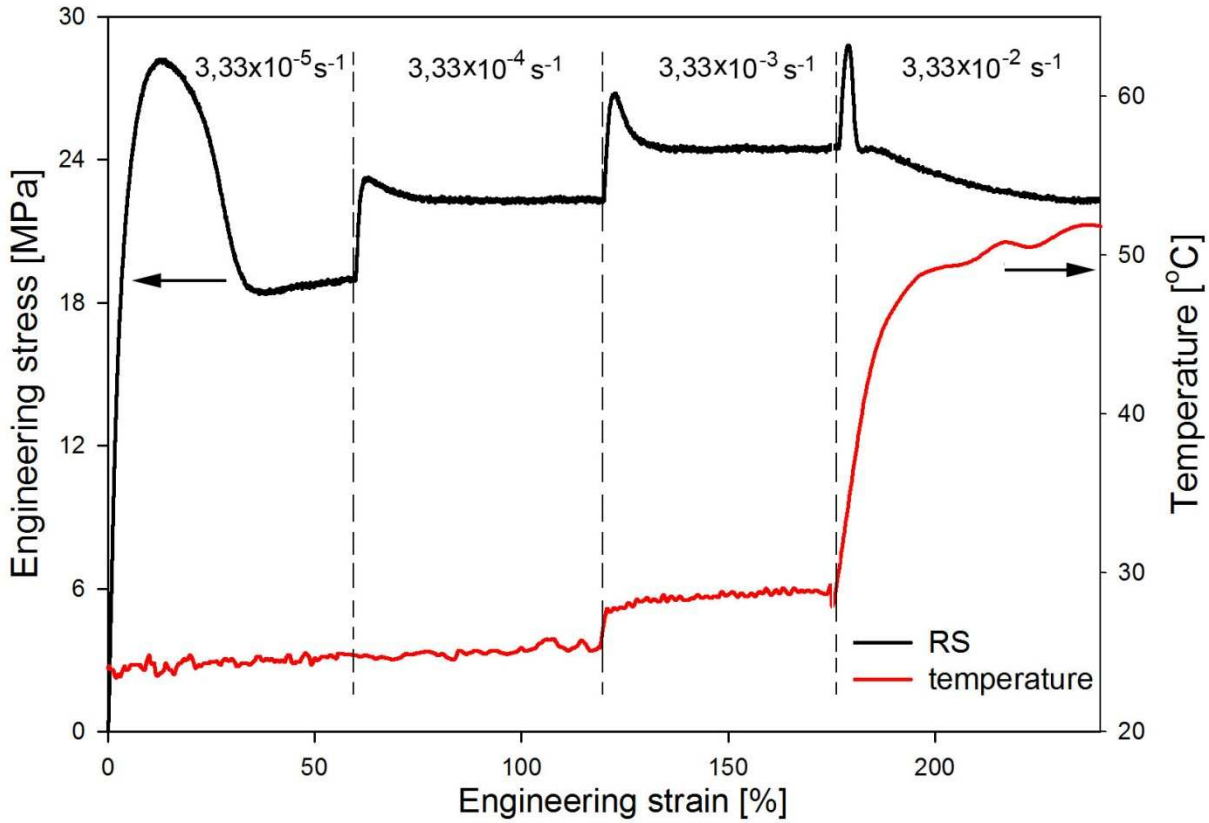

Fig. 72. Strain rate positive jump experiment for polypropylene. The base strain rate was $3.33\times10^{-5}s^{-1}$ and jumps were made by one decade increase of the strain rate. The red curve represents the maximum temperature of the sample (deformation zone) during deformation of the sample.

At low deformation rates ($3.33\times10^{-5}s^{-1}$, $3.33\times10^{-4}s^{-1}$), deformation of the sample is not accompanied by a significant thermal effect. Therefore, after increasing the deformation rate (from $3.33 \times 10^{-5}s^{-1}$ to $3.33 \times 10^{-4}s^{-1}$), deformation of the material takes place at a higher plastic flow stress

value**.** The next positive jump in a deformation rate of a sample (from $3.33\times10^{-4}s^{-1}$ to $3.33\times10^{-3}s^{-1}$) is accompanied by a temperature change within the deformation zone by around $3^{o}C$. However, a relatively small temperature increase results in a smaller increase in the value of plastic flow stress of the material deformed at a higher rate (by 2.11 MPa) as compared to the first change in the tensile rate of the sample (by 3.64 MPa). Very strong temperature increase, by $23^{o}C$, is observed within the deformation zone after the next change in the deformation rate of the sample (from $3.33\times10^{-4}s^{-1}$ to $3.33\times10^{-3}s^{-1}$). Such a strong thermal effect leads to reduction of the flow stress value by 2.21MPa of the material deformed at the rate of $3.33\times10^{-2}s^{-1}$, in spite of the expected increase of the plastic flow stress as the plastic flow is strain rate controlled. Strain rate jump experiment of crystalline polymers, in this case of polypropylene, is accompanied by two complementary effects: an increase in the plastic flow stress values, resulting from increase in the deformation rate of the sample, and a decrease in the plastic flow stress due to temperature increase within the deformation zone. The influence of temperature during a strain rate jump experiment of the sample deformed at low rates is negligible. Only an increase in the plastic flow stress value resulting from an increase in the deformation rate of the sample is observed. At higher deformation rates temperature increase generated as a result of changes in the structure of the material during plastic deformation of the material plays a dominant role. This accounts for the observed decrease in the plastic flow stress values after change in the deformation rate of the sample.

Figures 73 and 74 present SAXS scattering patterns and volume strain measurements recorded for samples subjected to tensile drawing to local strain of 4.5 drawn at different rates. Analysis of the presented results indicate a strong dependence of the intensity of cavitation accompanying deformation of polypropylene on the deformation rate. Increasing deformation rate leads to intensification of formation of discontinuities in the material. Such a dependence, already observed in papers [21, 22] results from an increase in the stress value during plastic flow of the material, as a result of increase in the deformation rate of the sample due to localization of deformation and formation of a neck. This is when cavitation occurs, prior to full activation of the deformation mechanisms of the crystalline phase.

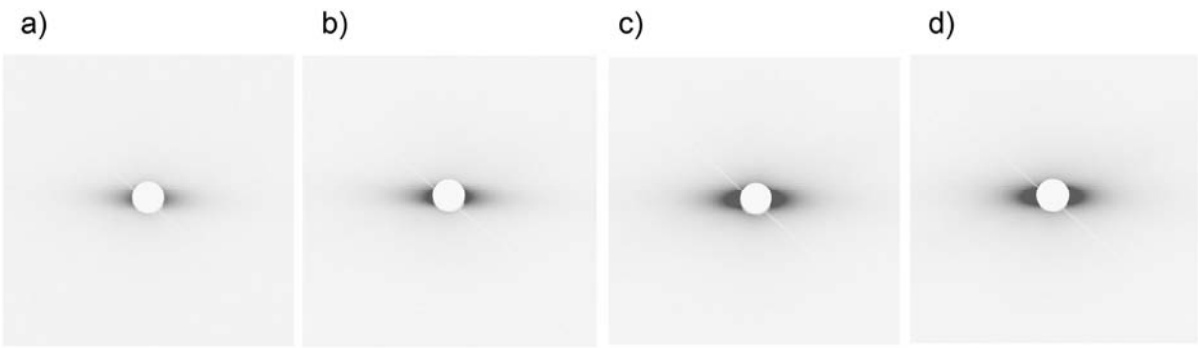

Fig. 73. Small-angle X-ray scattering patterns of polypropylene samples deformed at different rates: a) $3.33\times10^{-5}s^{-1}$, b) $3.33\times10^{-4}s^{-1}$, c) $3.33\times10^{-3}s^{-1}$, d) $3.33\times10^{-2}s^{-1}$. Local strain: 4.5. Direction of deformation – vertical.

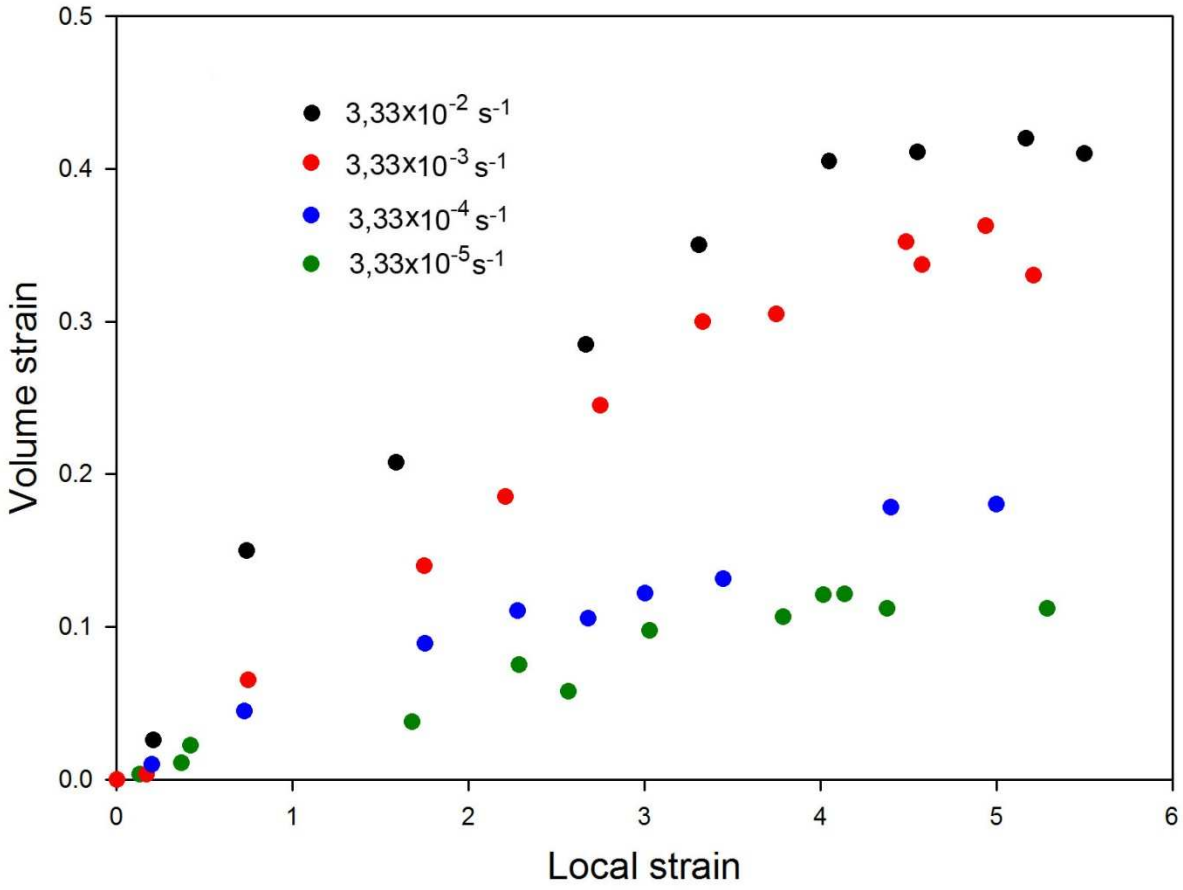

Fig. 74. Volume strain as a function of local strain for polypropylene deformed at different rates.

Changes of deformation rate in a strain rate jump experiment lead to a change in the stress of plastic flow of the deformed material. Depending on the temperature generated in the deformation zone, after changing the deformation rate, further deformation of the material takes place at higher or lower value of plastic flow stress. Increasing the deformation rate also leads to an increase in the intensity of cavity formation in the material (Fig. 73 and 74). In order to assess how the phenomenon of cavity formation affects a kind of “rivalry” between an increase or decrease in the deformation rate and an increase or decrease in the temperature generated in the deformation zone, i.e. two “factors that are neutralizing each other”, a strain rate jump experiment has been conducted for a cavitating

(Fig. 75) and non-cavitating sample (chloroform-soaked polypropylene) (Fig. 76) with a simultaneous recording of the temperature of the sample. To minimize the desorption of a modifier, after removal of the sample from a conditioning vessel, sufficiently high deformation rates were applied, $3.33\times10^{-3}s^{-1}$ and $3.33\times10^{-2}s^{-1}$, so that the time required for deformation of the sample was short as compared to the time at which the desorption takes place.

With the cavitating material (reference polypropylene) an increase in the deformation rate of the sample from $3.33\times10^{-3}s^{-1}$ to $3.33\times10^{-2}s^{-1}$ is accompanied by a decrease in the flow stress of the material, as a result of an intensive temperature increase in the deformation zone by approx. 24°C. A reverse effect has been observed after decreasing the deformation rate of the sample (from $3.33\times10^{-2}s^{-1}$ to $3.33\times10^{-3}s^{-1}$). As a result of a decrease in the deformation rate of the sample, a sudden temperature decrease (by approx. 24°C) occurs in the deformation zone, whose effect is an increase in the flow stress of the material. Further changes in the deformation rate of the sample lead to identical observations.

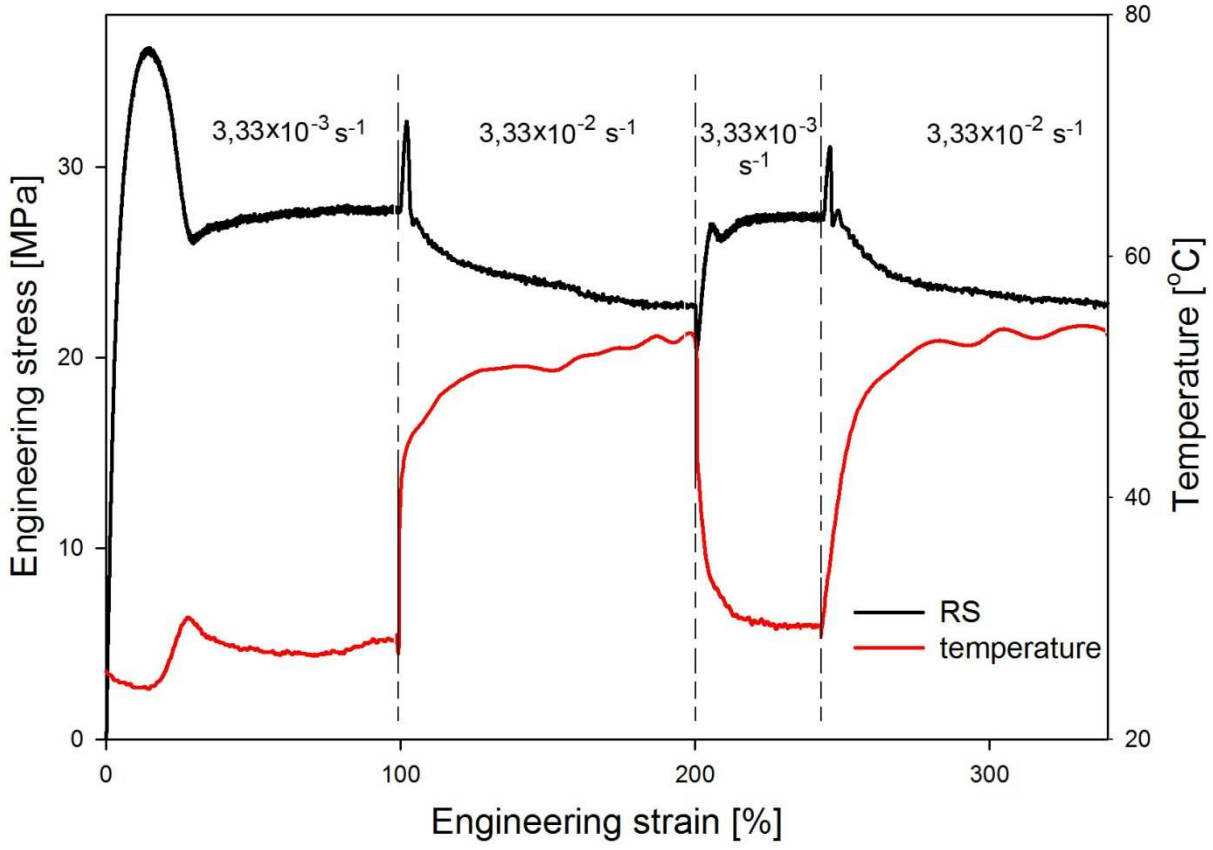

Fig. 75. Strain rate jump experiment for polypropylene sample. The red curve represents the maximum temperature in the deformation zone during deformation of the sample.

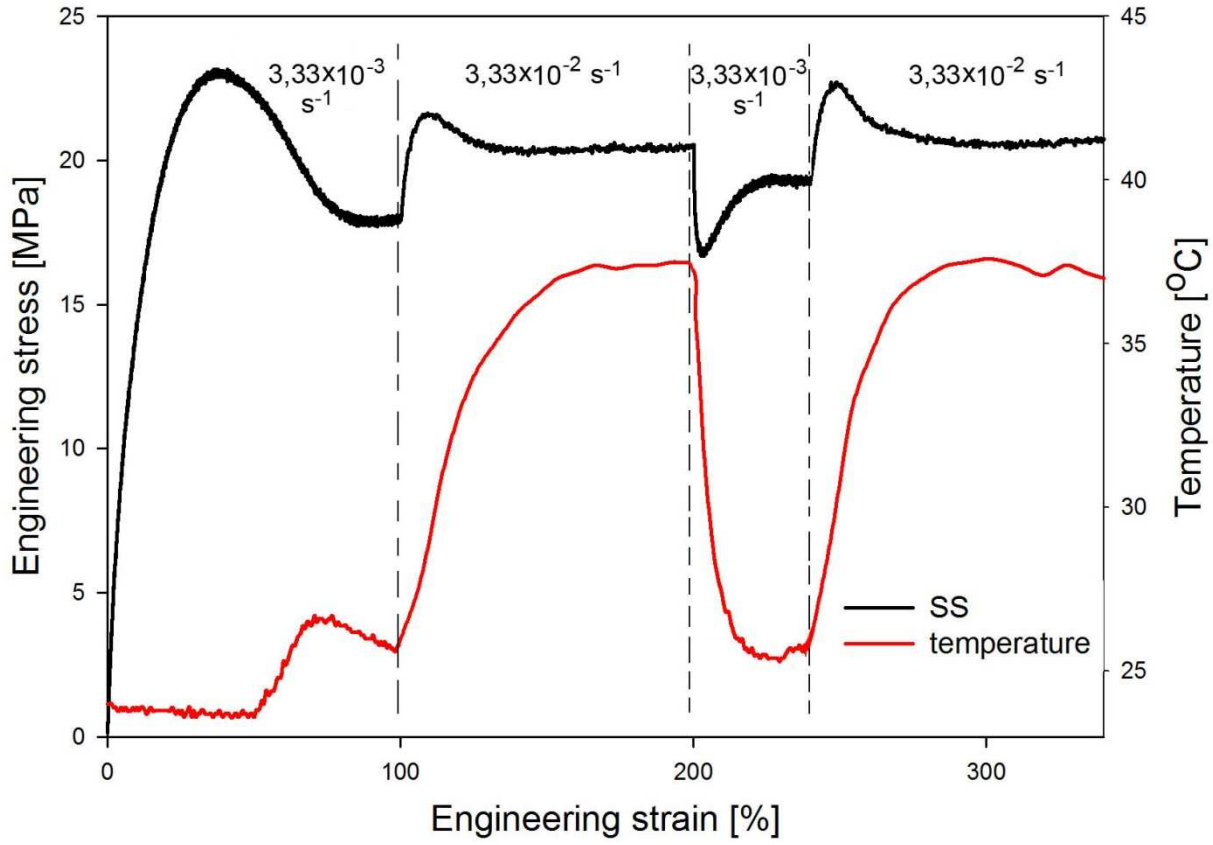

Fig. 76. Strain rate jump experiment for chloroform-soaked polypropylene sample. The red curve represents the maximum temperature in the deformation zone during deformation of the sample.

Change in the deformation rate from $3.33\times10^{-3}s^{-1}$ to $3.33\times10^{-2}s^{-1}$ during tensile drawing of the modified material, therefore non-cavitating, is accompanied by an increase in the value of plastic flow stress. Temperature change in the deformation zone is approx. $12^{o}C$ and is not sufficient to compensate the effect caused by an increase in the deformation rate of the sample. A reverse effect is observed after decreasing the deformation rate of the sample (from $3.33\times10^{-2}s^{-1}$ to $3.33\times10^{-3}s^{-1}$), which results in a temperature decrease in the deformation zone by approx. $12^{o}C$, however the deformation rate of the sample is a deciding parameter. Hence, after a change in the deformation rate of the material, a decrease in the flow stress value is recorded. Further changes in the deformation rate of the sample lead to identical changes in stress and temperature.

Cavitation accompanying deformation of polypropylene influences macroscopic properties of the material. Temperature increase in the deformation zone is intensified by the appearance and presence of cavities in the deformed material. Deformation of the non-cavitating material is also accompanied by a thermal effect, but it is significantly smaller. In such a case, the influence of temperature increase is minor and it is the change in the deformation rate of the sample that plays a dominant role. The presence or absence of cavitation during deformation of polypropylene intensifies the influence of one of the above mentioned factors.

5.6. Conclusions

Modification of the properties of amorphous phase of a series of crystalline polymers, whose tensile drawing is accompanied by formation of discontinuities, by removing stabilizers and low molecular weight fractions or introduction of a penetrant, allowed to determine the role of the free volume of unordered regions in the process of initiating of cavitation pores. Increase in the size of pores of the free volume of amorphous phase, obtained as a result of extraction of stabilizers and low molecular weight fractions with a mixture of non-solvents, or a decrease in the average size of "empty" spaces, as a result of introduction of molecules of a low molecular weight penetrant, leads to an increase or decrease in the intensity of cavitation**.** The packing of the amorphous phase of the material, which is a consequence of the chemical structure of macromolecules and organization of the supermolecular structure, naturally generates the free volume pores, whose size and dynamics of reorganization caused by thermal movements of polymer chains has a direct influence on initiation of cavitation during deformation of the material. The dominant role of the free volume of amorphous phase, which is an integral part of unordered regions of all crystalline polymers, in formation of cavitation pores proves that initiation of the phenomenon is of a homogeneous nature.

Modification of the amorphous phase of polypropylene, as a result of introduction of chloroform or hexane molecules, leads to complete elimination of cavity formation in the deformed material. Using two liquids of distinctly different physicochemical properties results in a similar change of deformation of the material – elimination of cavitation. Therefore, it turns out that it is not the type of substance used to fill the unordered regions, but rather the degree of filling, total or partial, causing a decrease in the size of the "empty" spaces, of the free volume pores of the material's amorphous phase, which is important in eliminating the process of formation of discontinuities, both cavities and dilatation microcracks, during deformation of polymer material.

Introduction of a low-molecular weight liquid, penetrating amorphous phase of the material and at the same time deprived of the possibility of penetration into the crystalline regions, results in a decrease in deformation stress (macroscopic yield point and flow) of such modified material. The observed reduction in yield stress as an effect of introduction of molecules of penetrant is the result of swelling of the unordered phase. Macroscopic change in size of the sample, as a result of swelling of unordered regions, induces tensile stress, whose values are insufficient to initiate plastic deformation of crystals, however efficient enough to decrease the measured values of stress at yield point. Clearly,

deformed amorphous phase acts on the adjacent, physically "connected" crystalline regions with a force equal to the value of the observed stress difference, at which deformation of the material takes place. The stress values were experimentally determined. The observed dependence seems particularly useful for materials which exhibit a natural tendency to sorption of low molecular weight substances in the conditions of their normal use, e.g. polyamide 6 absorbs water. A strong correlation between the mechanical properties of polyamide 6 and the content of water absorbed by the material so far has not been explained in detail [23]. The presented results, obtained for polyamide 6 and polyolefins, demonstrate the dominant role of the degree of swelling of amorphous phase with regard to changes of mechanical properties of the material saturated with a low molecular weight penetrant.

Cavities generated during tensile drawing of polymer materials can significantly affect plastic deformation, especially at higher deformation rates. The heat emitted during deformation of the cavitating sample, as a result of activation of plastic deformation mechanisms at subsequent stages of plastic deformation of the material, is significantly higher than in the case of the non-cavitating sample. The observed difference in heat emission between the cavitating and non-cavitating sample results in a decrease in stress at which deformation of the material capable of generation of cavitation pores takes place. Smaller thermal effect accompanying deformation of the sample with no ability to generate discontinuities allows to achieve higher stresses at which deformation of such material takes place.

To summarize, the dissertation allowed to formulate the following important conclusions:

1. It has been concluded that cavitation is initiated in the amorphous phase from homogeneous nuclei, which are fluctuations of the free volume. Nucleation is therefore of a homogeneous nature and is inextricably linked with the packing of macromolecules in the amorphous phase.

2. Blocking cavitation in crystallizing polymers is possible by removing homogeneous cavitation nuclei by filling the free volume of amorphous phase of the material with low molecular weight liquids. The type of liquid is not relevant, except that it should not dissolve polymer crystals.

3. The above observation is valid for polyethylene, polypropylene and polyamide. It seems that other crystallizing polymers should also reflect similar dependencies.

4. Mechanism of stress reduction at yield point in crystalline polymers, whose amorphous phase is swollen has been explained. The explanation does not require modification of the commonly

accepted plasticity of polymer crystals and leaves their basic attributes unchanged, i.e. crystallographic slips and critical shear stress, for their activation.

5. Special attention has been paid to the above mechanism for polyamide 6, which exhibits a natural tendency to absorb water and decrease stress at yield point, which so far has not been explained with regard to the plasticity of polymer crystals.

6. Significant temperature increase of the deformed polypropylene samples has been noted if the material is cavitating during deformation. Temperature of the samples exceeded 50^{o}C for high deformation rates. Similar temperature increases can be expected for other polymers cavitating during deformation.

5.7. References

[1] G'Sell, C.; Hiver, J.-M.; Dahoun, A. *Int. J. Solids Struct.,* **2002**, 39, 3857.
[2] Samuels, R. J. *J. Polym. Sci., Part C,* **1967**, 20, 253.

[3] Kryszewski, M.; Galeski, A.; Pakula, T.; Szylhabel, R. *Polimery(Polish),* **1971**, 16, 8.
[4] Brandrup, J.; Immergut, E.H.; Grulke, E.A. "Polymer Handbook", John Wiley&Sons, Inc., New York, **1999**.

[5] Jean, Y.C.; Mallon, P.E.; Schrader, D.M. "Principles & Applications of Positron & Positronium Chemistry", World Scientific, New Jersey, **2003**.

[6] Kansy, J. *J. Nuclear Instruments and Methods of Physics Research* **1996,** A374, 235.

[7] Olley, R. H.; Hodge, A. M.; Bassett, D. C. *J. Polym. Sci. Polym. Phys. Ed.*, **1979**, 17, 627.

[8] Rabiej, M. *Polimery(Polish)*, **2003**, 48, 288.

[9] Audouin, L.; Girois, S.; Achimsky, L.; Verdu, J. *Polym. Degrad. Stab.,* **1998**, 60, 137.

[10] Khelidj, N.; Colin, X.; Audouin, L.; Verdu, J.; Monchy-Leroy, C.; Prunier, V. *Polym. Degrad. Stab.,* **2006**, 91, 1598.

[11] Tao, S.J. *J. Chem. Phys*., **1972**, 56, 5499.

[12] Eldrup, M.; Lightbody, D.; Sherwood, J.N. *J. Chem. Phys.,* **1981,** 63, 51.

[13] Morosoff, N.; Peterlin, A.; *J Polym Sci Part A-2 Polym Phys*, **1972,** 10, 1237.

[14] Zuo, F.; Keum, J.K.; Chen, X.; Hsiao, B.S.; Chen, H.; Lai, S-Y.; Wevers, R.; Li, J. , *Polymer* **2007,** 48, 6867.
[15] Lezak E.; Bartczak, Z.; Galeski, A.; *Macromolecules* **2006,** *39,* 4811.
[16] Boukal, I. *J Appl Polym Sci* **1967**,11, 1483.
[17] Galeski, A.; Argon, A.S.; Cohen, R.E. *Macromolecules*,**1988**, 21, 2761.

[18] Viana, J.C. *Polymer,* **2005**, 46, 11773.

[19] Stern, C.; Frick, A.; Weickert, G. *J.Appl.Polym.Sci.,* **2007**, 103, 519.

[20] Hobeika, S.; Men, Y.; Strobl, G. *Macromolecules*, **2000**, 33, 1827.

[21] Pawlak, A. *Polymer* **2007,** 48, 1397.

[22] Pawlak, A.; Galeski A, *Macromolecules*, **2008**, 41, 2839.

[23] Miri, V.; Persyn, O.; Lefebvre, J.-M.; Seguela, R. *European Polym J,* **2009**, 45, 757.

[24] Murthy, N. S.; Stamm, M.; Sibilia, J. P.; Krimm, S. *Macromolecules* **1989**, 22, 1261.
[25] Park, J. B.; Devries, K. L.; Statton, W. O. *J. Macromol. Sci., Part B: Phys.* **1978**, 15, 229.
[26] Murthy, N. S.; Minor, H.; Latif, R. A. *J. Macromol. Sci., Part B: Phys.* **1987**, 26, 425.
[27] Seguela, R. Eur.Polym.J.,

Papers at various stages of publication that resulted from PhD thesis investigations:

1. A.Galeski, A.Rozanski
Cavitation during Drawing of Crystalline Polymers
Macromol Symp.

2. A.Rozanski, A.Galeski, M.Debowska
Initiation of cavitation of polypropylene during tensile drawing.
Macromolecules

3. A.Rozanski, A.Galeski
Cavitation supression in polypropylene, polyethylene and polyamide 6
Eur.Polym.J.

4. A.Rozanski, A.Galeski,
Effect of amorphous phase modification on plastic yielding of crystalline polymers: cases of polypropylene, polyamide 6 and polyethylene.
Macromolecules

5. A.Rozanski, A.Galeski,
The role of additives on the cavitation phenomenon in polypropylene.
J.Polym.Sci.Part B: Polym.Phys.Ed

6. A.Rozanski, A.Galeski,
Plastic deformation of polypropylene: effect of cavitation on the lamella fragmentation.
Polymer

7. A.Rozanski, A.Pawlak, A.Galeski
Thermal effects connected with cavitation during tensile drawing of polypropylene
Polymer